

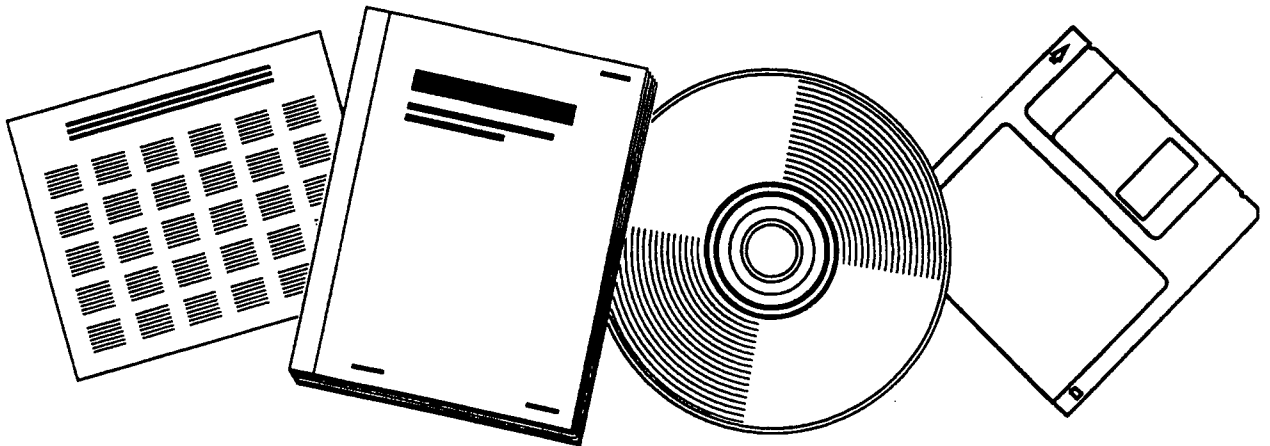


PB98-116023

NTIS[®]
Information is our business.

COASTAL HYDROLOGY AND HYDRAULICS

DEC 97



U.S. DEPARTMENT OF COMMERCE
National Technical Information Service



PB98-116023

FINAL REPORT

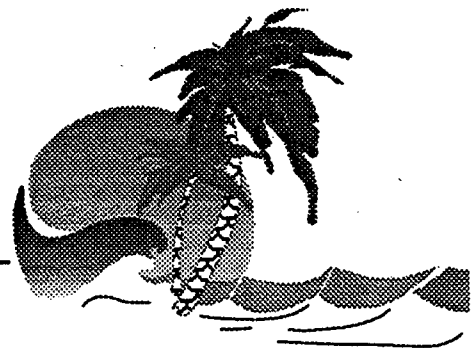
COASTAL HYDROLOGY AND HYDRAULICS

PRINCIPAL RESEARCHER

D. MAX SHEPPARD

**COASTAL AND OCEANOGRAPHIC ENGINEERING DEPARTMENT
UNIVERSITY OF FLORIDA
GAINESVILLE, FLORIDA**

December 1997



Coastal & Oceanographic Engineering Department
433 Weil Hall • P.O. Box 116590 • Gainesville, Florida 32611-6590



**UNIVERSITY OF
FLORIDA**

FINAL REPORT

COASTAL HYDROLOGY AND HYDRAULICS

HPR STUDY No. 0679
WPI No. 0510679
STATE JOB No. 99700-3524-119
CONTRACT No. B-8357
UPN No. 93030119
ACCOUNT No. 451127712
CONTRACT PERIOD 08/20/93 – 10/31/97

PRINCIPAL RESEARCHER

D. MAX SHEPPARD
COASTAL AND OCEANOGRAPHIC ENGINEERING DEPARTMENT
UNIVERSITY OF FLORIDA
GAINESVILLE, FLORIDA

December 1997

1. Report No. WPI 0510679		2. Government Accession No.		3. Recipient's Catalog No.	
4. Title and Subtitle Coastal Hydrology and Hydraulics		5. Report Date 12/97		6. Performing Organization Code 4910451127712	
		7. Author(s) D.M. Sheppard		8. Performing Organization Report No. UFL/COEL-97/006	
9. Performing Organization Name and Address Coastal and Oceanographic Engineering Department University of Florida 336 Weil Hall Gainesville FL 32611-6590		10. Work Unit No. (TRAIS) 99700-3524-119		11. Contract or Grant No. B8357	
		12. Sponsoring Agency Name and Address Florida Department of Transportation 605 Suwannee Street Tallahassee FL 32399-0450		13. Type of Report and Period Covered Final Report 8/20/93 - 10/31/97	
		14. Sponsoring Agency Code			
15. Supplementary Notes Prepared in cooperation with the U.S. Department of Transportation and the Federal Highway Administration					
16. Abstract <p>This report covers two related but separate topics. The first reports on a sensitivity study regarding hurricane storm surge generated hydraulics in tidal waters. That is, the hydraulics in tidally influenced coastal water bodies such as bays, estuaries, rivers, coastal waterways, etc. More specifically, the study examines the sensitivity of flow velocity and water elevation at various points in a tidal system to variations in an open coast storm surge hydrograph. A depth averaged, finite element flow model is used to perform numerical experiments where certain hydrograph parameters (rate of water rise, duration of peak water elevation, and rate of water elevation) are varied and the hydraulics monitored at points within the system. The results are presented in a variety of plots of non-dimensional quantities. Some general conclusions are made that should be of interest to those modeling hurricane induced flows in tidal waters.</p> <p>The second part of the report describes an unsuccessful attempt to measure currents and waves at a site near the Bonner Bridge over Oregon Inlet, North Carolina. Sediment scour at the ends of eight bridge piers on the Bonner Bridge were being monitored by the North Carolina Department of Transportation (NCDOT) and the U.S. Geological Survey (USGS) for operational purposes. The objective of this project was to measure current velocities and waves near two of the piers so that local scour prediction equations could be tested for larger structures. Problems were encountered due to the extreme dynamic nature of the sediment transport in the vicinity of the inlet. This resulted in the deposition of large quantities of sand at the location of the instruments which buried one of the instruments and severely damaged the other two.</p>					
17. Key Words Bridge scour, Pier scour, Maximum scour			18. Distribution Statement No restrictions. This document is available to the public through the National Technical Information Service, Springfield, VA, 22161		
19. Security Classif. (of this report) Unclassified		20. Security Classif. (of this page) Unclassified		21. No. of Pages 89	22. Price

DISCLAIMER

“The opinions, findings and conclusions expressed in this publication are those of the authors and not necessarily those of the Florida Department of Transportation or the U.S. Department of Transportation.”

“Prepared in cooperation with the State of Florida Department of Transportation and the U.S. Department of Transportation.”

SI* (MODERN METRIC) CONVERSION FACTORS

APPROXIMATE CONVERSIONS TO SI UNITS				APPROXIMATE CONVERSIONS FROM SI UNITS																																											
Symbol	When You Know	Multiply By	To Find	Symbol	When You Know	Multiply By	To Find																																								
<p>LENGTH</p> <table style="width: 100%; border-collapse: collapse;"> <tr> <td style="width: 25%;">inches</td> <td style="width: 25%;">millimeters</td> <td style="width: 25%;">25.4</td> <td style="width: 25%;">millimeters</td> </tr> <tr> <td>feet</td> <td>meters</td> <td>0.305</td> <td>meters</td> </tr> <tr> <td>yards</td> <td>meters</td> <td>0.914</td> <td>m</td> </tr> <tr> <td>miles</td> <td>kilometers</td> <td>1.61</td> <td>km</td> </tr> </table>				inches	millimeters	25.4	millimeters	feet	meters	0.305	meters	yards	meters	0.914	m	miles	kilometers	1.61	km	<p>LENGTH</p> <table style="width: 100%; border-collapse: collapse;"> <tr> <td style="width: 25%;">mm</td> <td style="width: 25%;">inches</td> <td style="width: 25%;">0.039</td> <td style="width: 25%;">inches</td> </tr> <tr> <td>m</td> <td>feet</td> <td>3.28</td> <td>feet</td> </tr> <tr> <td>m</td> <td>yards</td> <td>1.09</td> <td>yards</td> </tr> <tr> <td>km</td> <td>miles</td> <td>0.621</td> <td>miles</td> </tr> </table>				mm	inches	0.039	inches	m	feet	3.28	feet	m	yards	1.09	yards	km	miles	0.621	miles								
inches	millimeters	25.4	millimeters																																												
feet	meters	0.305	meters																																												
yards	meters	0.914	m																																												
miles	kilometers	1.61	km																																												
mm	inches	0.039	inches																																												
m	feet	3.28	feet																																												
m	yards	1.09	yards																																												
km	miles	0.621	miles																																												
<p>AREA</p> <table style="width: 100%; border-collapse: collapse;"> <tr> <td style="width: 25%;">square inches</td> <td style="width: 25%;">square millimeters</td> <td style="width: 25%;">645.2</td> <td style="width: 25%;">square inches</td> </tr> <tr> <td>square feet</td> <td>square meters</td> <td>0.093</td> <td>square feet</td> </tr> <tr> <td>square yards</td> <td>square meters</td> <td>0.836</td> <td>square yards</td> </tr> <tr> <td>acres</td> <td>hectares</td> <td>0.405</td> <td>acres</td> </tr> <tr> <td>square miles</td> <td>square kilometres</td> <td>2.59</td> <td>square miles</td> </tr> </table>				square inches	square millimeters	645.2	square inches	square feet	square meters	0.093	square feet	square yards	square meters	0.836	square yards	acres	hectares	0.405	acres	square miles	square kilometres	2.59	square miles	<p>AREA</p> <table style="width: 100%; border-collapse: collapse;"> <tr> <td style="width: 25%;">mm²</td> <td style="width: 25%;">square millimeters</td> <td style="width: 25%;">0.0016</td> <td style="width: 25%;">square inches</td> </tr> <tr> <td>m²</td> <td>square meters</td> <td>10.764</td> <td>square feet</td> </tr> <tr> <td>ha</td> <td>square meters</td> <td>1.195</td> <td>square yards</td> </tr> <tr> <td>ac</td> <td>hectares</td> <td>2.47</td> <td>acres</td> </tr> <tr> <td>mi²</td> <td>square kilometers</td> <td>0.386</td> <td>square miles</td> </tr> </table>				mm ²	square millimeters	0.0016	square inches	m ²	square meters	10.764	square feet	ha	square meters	1.195	square yards	ac	hectares	2.47	acres	mi ²	square kilometers	0.386	square miles
square inches	square millimeters	645.2	square inches																																												
square feet	square meters	0.093	square feet																																												
square yards	square meters	0.836	square yards																																												
acres	hectares	0.405	acres																																												
square miles	square kilometres	2.59	square miles																																												
mm ²	square millimeters	0.0016	square inches																																												
m ²	square meters	10.764	square feet																																												
ha	square meters	1.195	square yards																																												
ac	hectares	2.47	acres																																												
mi ²	square kilometers	0.386	square miles																																												
<p>VOLUME</p> <table style="width: 100%; border-collapse: collapse;"> <tr> <td style="width: 25%;">fl oz</td> <td style="width: 25%;">milliliters</td> <td style="width: 25%;">29.57</td> <td style="width: 25%;">fluid ounces</td> </tr> <tr> <td>gal</td> <td>liters</td> <td>3.785</td> <td>gallons</td> </tr> <tr> <td>ft³</td> <td>cubic meters</td> <td>0.028</td> <td>cubic feet</td> </tr> <tr> <td>yd³</td> <td>cubic meters</td> <td>0.765</td> <td>cubic yards</td> </tr> </table>				fl oz	milliliters	29.57	fluid ounces	gal	liters	3.785	gallons	ft ³	cubic meters	0.028	cubic feet	yd ³	cubic meters	0.765	cubic yards	<p>VOLUME</p> <table style="width: 100%; border-collapse: collapse;"> <tr> <td style="width: 25%;">ml</td> <td style="width: 25%;">milliliters</td> <td style="width: 25%;">0.034</td> <td style="width: 25%;">fluid ounces</td> </tr> <tr> <td>l</td> <td>liters</td> <td>0.264</td> <td>gallons</td> </tr> <tr> <td>m³</td> <td>cubic meters</td> <td>35.71</td> <td>cubic feet</td> </tr> <tr> <td>m³</td> <td>cubic meters</td> <td>1.307</td> <td>cubic yards</td> </tr> </table>				ml	milliliters	0.034	fluid ounces	l	liters	0.264	gallons	m ³	cubic meters	35.71	cubic feet	m ³	cubic meters	1.307	cubic yards								
fl oz	milliliters	29.57	fluid ounces																																												
gal	liters	3.785	gallons																																												
ft ³	cubic meters	0.028	cubic feet																																												
yd ³	cubic meters	0.765	cubic yards																																												
ml	milliliters	0.034	fluid ounces																																												
l	liters	0.264	gallons																																												
m ³	cubic meters	35.71	cubic feet																																												
m ³	cubic meters	1.307	cubic yards																																												
<p>MASS</p> <table style="width: 100%; border-collapse: collapse;"> <tr> <td style="width: 25%;">oz</td> <td style="width: 25%;">grams</td> <td style="width: 25%;">28.35</td> <td style="width: 25%;">ounces</td> </tr> <tr> <td>lb</td> <td>kilograms</td> <td>0.454</td> <td>pounds</td> </tr> <tr> <td>T</td> <td>megagrams</td> <td>0.907</td> <td>short tons (2000 lb)</td> </tr> </table>				oz	grams	28.35	ounces	lb	kilograms	0.454	pounds	T	megagrams	0.907	short tons (2000 lb)	<p>MASS</p> <table style="width: 100%; border-collapse: collapse;"> <tr> <td style="width: 25%;">g</td> <td style="width: 25%;">grams</td> <td style="width: 25%;">0.035</td> <td style="width: 25%;">ounces</td> </tr> <tr> <td>kg</td> <td>kilograms</td> <td>2.202</td> <td>pounds</td> </tr> <tr> <td>Mg</td> <td>megagrams</td> <td>1.103</td> <td>short tons (2000 lb)</td> </tr> </table>				g	grams	0.035	ounces	kg	kilograms	2.202	pounds	Mg	megagrams	1.103	short tons (2000 lb)																
oz	grams	28.35	ounces																																												
lb	kilograms	0.454	pounds																																												
T	megagrams	0.907	short tons (2000 lb)																																												
g	grams	0.035	ounces																																												
kg	kilograms	2.202	pounds																																												
Mg	megagrams	1.103	short tons (2000 lb)																																												
<p>TEMPERATURE (exact)</p> <table style="width: 100%; border-collapse: collapse;"> <tr> <td style="width: 25%;">°F</td> <td style="width: 25%;">Fahrenheit temperature</td> <td style="width: 25%;">5(F-32)/9 or (F-32)/1.8</td> <td style="width: 25%;">Celcius temperature</td> </tr> </table>				°F	Fahrenheit temperature	5(F-32)/9 or (F-32)/1.8	Celcius temperature	<p>TEMPERATURE (exact)</p> <table style="width: 100%; border-collapse: collapse;"> <tr> <td style="width: 25%;">°C</td> <td style="width: 25%;">Celcius temperature</td> <td style="width: 25%;">1.8C + 32</td> <td style="width: 25%;">Fahrenheit temperature</td> </tr> </table>				°C	Celcius temperature	1.8C + 32	Fahrenheit temperature																																
°F	Fahrenheit temperature	5(F-32)/9 or (F-32)/1.8	Celcius temperature																																												
°C	Celcius temperature	1.8C + 32	Fahrenheit temperature																																												
<p>ILLUMINATION</p> <table style="width: 100%; border-collapse: collapse;"> <tr> <td style="width: 25%;">fc</td> <td style="width: 25%;">foot-candles</td> <td style="width: 25%;">10.76</td> <td style="width: 25%;">lux</td> </tr> <tr> <td>fl</td> <td>foot-Lamberts</td> <td>3.426</td> <td>candela/m²</td> </tr> </table>				fc	foot-candles	10.76	lux	fl	foot-Lamberts	3.426	candela/m ²	<p>ILLUMINATION</p> <table style="width: 100%; border-collapse: collapse;"> <tr> <td style="width: 25%;">lx</td> <td style="width: 25%;">lux</td> <td style="width: 25%;">0.0929</td> <td style="width: 25%;">foot-candles</td> </tr> <tr> <td>cd/m²</td> <td>candela/m²</td> <td>0.2919</td> <td>foot-Lamberts</td> </tr> </table>				lx	lux	0.0929	foot-candles	cd/m ²	candela/m ²	0.2919	foot-Lamberts																								
fc	foot-candles	10.76	lux																																												
fl	foot-Lamberts	3.426	candela/m ²																																												
lx	lux	0.0929	foot-candles																																												
cd/m ²	candela/m ²	0.2919	foot-Lamberts																																												
<p>FORCE and PRESSURE or STRESS</p> <table style="width: 100%; border-collapse: collapse;"> <tr> <td style="width: 25%;">lbf</td> <td style="width: 25%;">poundforce</td> <td style="width: 25%;">4.45</td> <td style="width: 25%;">newtons</td> </tr> <tr> <td>psi</td> <td>poundforce per square inch</td> <td>6.89</td> <td>kilopascals</td> </tr> </table>				lbf	poundforce	4.45	newtons	psi	poundforce per square inch	6.89	kilopascals	<p>FORCE and PRESSURE or STRESS</p> <table style="width: 100%; border-collapse: collapse;"> <tr> <td style="width: 25%;">N</td> <td style="width: 25%;">newtons</td> <td style="width: 25%;">0.225</td> <td style="width: 25%;">poundforce</td> </tr> <tr> <td>kPa</td> <td>kilopascals</td> <td>0.145</td> <td>poundforce per square inch</td> </tr> </table>				N	newtons	0.225	poundforce	kPa	kilopascals	0.145	poundforce per square inch																								
lbf	poundforce	4.45	newtons																																												
psi	poundforce per square inch	6.89	kilopascals																																												
N	newtons	0.225	poundforce																																												
kPa	kilopascals	0.145	poundforce per square inch																																												

* SI is the symbol for the International System of Units. Appropriate rounding should be made to comply with Section 4 of ASTM E380. (Revised August 1992)

Table of Contents

List of Figures	ii
List of Symbols	vi
1. Introduction.....	1
2. Storm Surge Hydrograph Study.....	3
2.1 Procedures	3
2.2 Model Test Results.....	5
2.2.1 St. Lucie study area.....	6
2.2.2 St. Johns River study area.....	8
2.3 Conclusions	9
3. Field Measurement Program.....	11
3.1 Background	11
3.2 Scour-Depth Monitoring System.....	11
3.3 Conclusions	12
4. References.....	14
Appendix A Sensitivity of Bridge Scour Producing Currents to Storm Surge Parameters	
Appendix B Field Performance of an Acoustic Scour-Depth Monitoring System	

List of Figures

Figure 1.	General location of study areas.....	15
Figure 2.	St. Lucie Estuary study area	16
Figure 3.	St. Johns River study area.....	17
Figure 4.	St. Lucie Estuary finite element mesh	18
Figure 5.	St. Johns River finite element mesh	19
Figure 6.	St. Lucie & St. Johns River storm surge variation	20
Figure 7.	St. Lucie study area locations	21
Figure 8.	St. Johns River study area locations	22
Figure 9.	Maximum elevation comparisons – Indian River Lagoon.....	23
Figure 10.	Maximum water elevation and elevation at maximum velocity magnitude comparisons– Indian River Lagoon	24
Figure 11.	Maximum velocity magnitude comparisons – Indian River Lagoon	25
Figure 12.	Maximum velocity magnitude vs. distance – Indian River Lagoon	26
Figure 13.	Velocity magnitude vs. time at Gage 2 – rate of rise variation – Indian River Lagoon.....	27
Figure 14.	Velocity magnitude vs. time at Gage 2 – rate of fall variation – Indian River Lagoon.....	28
Figure 15.	Velocity magnitude vs. time at Gage 2 – duration of peak variation – Indian River Lagoon.....	29
Figure 16.	Velocity magnitude vs. time at Gage 1 – rate of rise variation – Indian River Lagoon.....	30
Figure 17.	Velocity magnitude vs. time at Gage 1 – rate of fall variation – Indian River Lagoon.....	31
Figure 18.	Velocity magnitude vs. time at Gage 1 – duration of peak variation – Indian River Lagoon.....	32

Figure 19. Maximum elevation comparisons – Intracoastal Waterway	33
Figure 20. Maximum water elevation and elevation at maximum velocity magnitude comparisons – Intracoastal Waterway	34
Figure 21. Maximum velocity magnitude comparisons – Intracoastal Waterway	35
Figure 22. Maximum velocity magnitude vs. distance – Intracoastal Waterway	36
Figure 23. Velocity magnitude vs. time at Gage 3 – rate of rise variation – Intracoastal Waterway	37
Figure 24. Velocity magnitude vs. time at Gage 3 – rate of fall variation – Intracoastal Waterway	38
Figure 25. Velocity magnitude vs. time at Gage 3 – duration of peak variation – Intracoastal Waterway	39
Figure 26. Velocity magnitude vs. time at Gage 4 – rate of rise variation – Intracoastal Waterway	40
Figure 27. Velocity magnitude vs. time at Gage 4 – rate of fall variation – Intracoastal Waterway	41
Figure 28. Velocity magnitude vs. time at Gage 4 – duration of peak variation – Intracoastal Waterway	42
Figure 29. Maximum elevation comparisons – St. Lucie Estuary	43
Figure 30. Maximum water elevation and elevation at maximum velocity magnitude comparisons – St. Lucie Estuary	44
Figure 31. Maximum velocity magnitude comparisons – St. Lucie Estuary	45
Figure 32. Maximum velocity magnitude vs. distance – St. Lucie Estuary	46
Figure 33. Velocity magnitude vs. time at Gage 5 – rate of rise variation – St. Lucie Estuary	47
Figure 34. Velocity magnitude vs. time at Gage 5 – rate of fall variation – St. Lucie Estuary	48

Figure 35. Velocity magnitude vs. time at Gage 5 – duration of peak variation – St. Lucie Estuary	49
Figure 36. Velocity magnitude vs. time at Gage 6 – rate of rise variation – St. Lucie Estuary	50
Figure 37. Velocity magnitude vs. time at Gage 6 – rate of fall variation – St. Lucie Estuary	51
Figure 38. Velocity magnitude vs. time at Gage 6 – duration of peak variation – St. Lucie Estuary	52
Figure 39. Maximum elevation comparisons – St. Johns River	53
Figure 40. Maximum water elevation and elevation at maximum velocity magnitude comparisons – St. Johns River	54
Figure 41. Maximum velocity magnitude comparisons – St. Johns River	55
Figure 42. Maximum velocity magnitude vs. distance – St. Johns River	56
Figure 43. Velocity magnitude vs. time at Gage 1 – rate of rise variation – St. Johns River.....	57
Figure 44. Velocity magnitude vs. time at Gage 1 – rate of fall variation – St. Johns River.....	58
Figure 45. Velocity magnitude vs. time at Gage 1 – duration of peak variation – St. Johns River.....	59
Figure 46. Velocity magnitude vs. time at Gage 2 – rate of rise variation – St. Johns River.....	60
Figure 47. Velocity magnitude vs. time at Gage 2 – rate of fall variation – St. Johns River.....	61
Figure 48. Velocity magnitude vs. time at Gage 2 – duration of peak variation – St. Johns River.....	62
Figure 49. Velocity magnitude and baseline elevation vs. time – St. Johns River	63
Figure 50. Vicinity map for Oregon Inlet	64
Figure 51. Drawing of Herbert C. Bonner Bridge over Oregon Inlet	65

Figure 52. Tethered current meter installation	66
Figure 53. Electromagnetic current meter, pressure transducer, data acquisition (puv) installation	67

List of Symbols

- H_i = peak water elevation at a given point,
 H_b = peak baseline water elevation at the same point,
 V_i = maximum velocity at a given point,
 V_b = maximum baseline velocity at the same point,
 H_{pv} = peak water elevation at maximum velocity magnitude,
 H_{im} = peak water elevation at inlet or entrance.

Coastal Hydrology and Hydraulics

1. INTRODUCTION

Two important parameters needed in the design of structures that will be subjected to forces from flowing water are water depth and flow velocity. If the bed material where the structure is to be located is erodible, (i.e. if for the range of bed shear stresses anticipated exceed that needed to move the sediment) then these two parameters are also needed to estimate the sediment scour depths near the structure. In tidal inlets, bays and coastal waterways in Florida as well as many other coastal states in the United States on the Gulf of Mexico and Atlantic Ocean the event that produces the most extreme flow conditions is hurricane generated meteorological tide or storm surge. One-in-one-hundred and one-in-five-hundred year return interval storm surges are used in the design of bridges over waterways in the United States. The open coast hydrographs (water elevation versus time plots) for these design surges are usually obtained with the use of computer models that solve for the flow induced by the wind and pressure in the hurricane. Numerous (hypothetical or real) hurricanes must be hindcast in order to generate the database for the extremal analysis needed to produce the one in one and five hundred year surges. Comparisons of predicted and measured storm surges on the open coast indicate that the predicted peak water elevation is often close to measured values, but other features of the hydrograph such as rate of rise or fall can differ greatly.

The propagation of storm surges through tidal inlets and/or river mouths into bay-estuary-river systems is a complex process due to the highly irregular boundaries and in some cases the flooding of barrier islands and other subaerial lands. It is therefore not usually obvious how the difference in predicted and actual open coast hydrographs affect the currents and water elevations at various locations in the bay-estuary-river system. Variations in design currents and water elevation can have a major impact on design scour depth predictions and therefore it is important to know how sensitive these quantities are to variations in the storm surge parameters. To address these issues, a study was conducted to examine the sensitivity of design scour producing currents in a tidal system to certain variations in the open coast storm surge parameters.

The research conducted under this contract is divided into two related but separate categories. The objective of the first category (Storm Surge Hydrograph Study) was to examine the sensitivity of bridge scour producing currents in a tidal environment to variations in certain parameters associated with open coast storm surges. The objective of the second category (Field Measurement Program) was to measure the scour producing water currents and waves near the Bonner Bridge over Oregon Inlet, North Carolina, where bridge pier scour was already being monitored. The two projects are related in that they both are directed at obtaining a better understanding of the processes that cause sediment scour near bridges.

The specific objectives of the Storm Surge Hydrograph Study were to:

1. Pick two locations on the Florida coast to be representative of the types of conditions found in Florida for the purposes of the sensitivity study,
2. Configure a two-dimensional, depth averaged circulation model for the two locations,
3. Calibrate the models using data,
4. Conduct numerical experiments where certain storm surge parameters are varied and the current velocities and water elevations at different locations throughout the inlet, bay, estuary, and river system are monitored,
5. Establish a means of quantifying the sensitivity of the currents and water elevations to variations in the storm surge parameters, and
6. Using the methodology developed in Item 5 above, quantify the sensitivity of currents to storm surge parameters.

A description of the procedures used in this study, a discussion of the hydrograph parameters examined and ranges tested, the model test results, and the conclusions from the study are presented in Section 2 of this report. Two technical papers on the results of this study have been presented, one at the Florida Department of Transportation (FDOT) Design Conference on August 10, 1994 [Sheppard et al. (1994)] and one at the ASCE Water Resources Engineering Conference in San Antonio Texas from August 14-18, 1995 [Sheppard et al. (1995)]. A copy of the ASCE paper is included as Appendix A.

The objective of the Field Measurement Program was to work with the North Carolina Department of Transportation (NCDOT) and the U.S. Geologic Survey (USGS) to obtain environmental data in Oregon Inlet near the area where bridge pier scour was being monitored. The environmental data to be measured/obtained was wave magnitude, direction and frequency, water temperature, current magnitude and direction, and surface sediment samples.

A summary of the Field Measurement Program is presented in Section 3 of this report. Two technical papers were presented on the results of this work. The first paper was presented at the FDOT Design Conference in Orlando, Florida in August 1994 and the second at the ASCE Hydraulics Engineering Conference in Buffalo, New York in August 1994 [Robert R. Mason, Jr. and D. Max Sheppard]. A copy of the ASCE paper is included in this report as Appendix B.

2. STORM SURGE HYDROGRAPH STUDY

Included in this section are 1) the procedures used in the Storm Surge Hydrograph Study, 2) the rationale for selecting the two coastal system scenarios, 3) the hydrograph parameters and ranges tested, and 4) the model test results and conclusions of this part of the study.

2.1 Procedures

The first step was to select two locations in Florida's coastal waters that would be representative of the types of coastal conditions found in Florida. The two sites selected were:

- The St. Lucie Estuary and portions of Indian River Lagoon (more specifically, the area between Ft. Pierce and Jupiter Inlets) and
- The lower St. Johns River (from the mouth of the river at Mayport to Palatka, over 50 miles up river).

The St. Lucie Estuary was selected for two reasons. First, it is somewhat representative of the inlet/bay/estuary systems found in Florida. Secondly, data suitable for calibration of the hydrodynamic model was available from previous field monitoring programs. The lower St. Johns River was selected as a representative riverine coastal system in Florida and, in addition, the St. Johns River is an area of immediate interest for bridge construction by the FDOT. A general location map for the two sites is presented in Figure 1. A more detailed map of the St. Lucie Estuary study area is given in Figure 2 and one for the St. Johns River study area in Figure 3.

There were a number of two-dimensional, depth averaged flow models available for use in this study, but the one selected was RMA2 (Norton and McAnally, 1973, Thomas and McAnally, 1991) with the BOSS International pre and post processor. When the project was initiated, the BOSS software was called "FASTTABS". Later, (improved) versions of this software are called "SMS". RMA2 is a depth-averaged two-dimensional model employing a finite element solution procedure to solve the shallow water wave equations. The pre and post processors provide a graphical interface for efficient mesh generation, boundary condition specification and presentation of the results. Additionally, pre-processing software developed by Reed and Sheppard to expedite mesh generation was also used in this study.

As stated above, there were several hydrodynamic models available that could have been used in this study. RMA2 was selected as it was specifically developed for coastal hydraulics and has been used extensively by the U.S. Army Corps of Engineers and the consulting engineering community for coastal hydraulics problems.

Meshes for the two study areas were generated for RMA2. The St. Lucie Estuary mesh is shown in Figure 4 and the St. Johns River mesh in Figure 5.

Since only the changes in the flow parameters (and not their specific values) were of interest in this study, it was not necessary to have a precise calibration of the models. It was, however, necessary for the model parameters (mean water depths, bottom roughness, turbulence exchange coefficients) to be approximately correct; thus calibrations were performed using (primarily) existing data. The St. Lucie Estuary study area model was calibrated using data from a number of previous modeling studies (Williams, 1985; Morris, 1987; Sheng, et al., 1990; Smith, 1990) as well as information from the NOAA Tide Tables. There was less existing data for the St. Johns River suitable for calibration purposes. This model was calibrated using stage and discharge data obtained as part of another FDOT District 2 sponsored study. The ranges of Manning's n and turbulence exchange coefficients used in the analysis were 0.018-0.028 lbs/ft² and 141-1450 lbs/ft², respectively.

On completion of the calibrations, numerical experiments were performed using first a "baseline" hydrograph as an input followed by hydrographs where specific parameters (rate of rise, rate of fall and duration of the peak) were varied. The baseline hydrograph was similar to those computed by NOAA (National Oceanic and Atmospheric Administration) for the east coast of Florida.

For each storm surge hydrograph variation considered, water elevations and depth averaged velocities were monitored at various points along the river or within the bay/estuary system. The flow parameters that are important to bridge scour prediction include: water depth and elevation, local depth average velocity, channel average velocity, and the duration of these quantities. The bay, river, estuary, or tributary system was divided into regions according to how the above quantities were anticipated to respond to a storm surge at the inlet or mouth. The response was believed to depend primarily on the:

1. distance from the inlet or mouth (or in some cases from the open bay),
2. width or depth of the channel connecting the point of interest to the inlet or mouth, and
3. channel bottom roughness.

The relative importance of these factors was examined as part of the sensitivity analysis. Two different approaches were taken to the sensitivity analysis. The first approach was that of constant storm surge energy. In this approach, the storm surge hydrographs were varied (rate of rise, rate of fall, and duration of peak) from the baseline hydrograph while holding the energy in the hydrograph approximately constant. Using this approach, a sensitivity analysis was performed on the St. Lucie study area. The results of this analysis were presented at the FDOT Design Conference in August 1994 and at ASCE Water Resources Engineering Conference in San Antonio, Texas in August 1995 [Sheppard et al. (1995)]. As stated previously, a copy of this paper is included as Appendix A in this report.

The second approach taken was that of a constant storm surge peak height. The surge parameter variations were made while holding the maximum height of the hydrograph constant. Even though the constant energy approach is thought to be more scientifically correct, the constant maximum height method is perhaps more useful for this particular problem. Users of the results of this study will most likely have accurate (1 in 100 and 1 in 500 year) storm surge maximum elevation predictions and less accurate storm surge hydrograph shapes. As with the constant energy method, the surge parameters such as rate of rise, rate of fall and duration of peak were varied and the flow monitored at points throughout the tidal system. To vary the rate of rise, the maximum slope of the rise was decreased from the baseline. To vary the rate of fall, the maximum slope of the fall was decreased from the baseline. Both of these variations increased the area under the hydrograph by approximately 20%. Therefore, for uniformity, the duration of peak was extended so as to produce a 20% increase in the area under hydrograph. It is important to note that while the area under the hydrographs were increased from that of the baseline hydrograph, the amount of increase was the same in all three cases. Figure 6 shows the storm surge hydrograph variations used for both study areas. The model test results and conclusions for the constant peak height hydrograph approach are presented in Sections 2.2 and 2.3 of this report, respectively.

2.2 Model Test Results

The points monitored in the St. Lucie study area are within three distinct areas – the Indian River Lagoon, the Intracoastal Waterway, and St. Lucie Estuary. These areas are shown in Figure 7. The monitoring areas for the St. Johns River study are shown in Figure 8.

For each location monitored the model output was analyzed and the results presented in a series of graphs. Some of the quantities in the graphs were nondimensionized so as to extend their range of application. A discussion of the quantities used in the graphs are given below:

Maximum Water Elevation and Water Elevation at the time of Maximum Velocity

For some situations there are major differences between the maximum water elevation at a point and the water elevation at the time of maximum velocity at that point. Since both quantities are of interest to the design engineer, both are examined in this study. The maximum (or peak) water elevation at a given point in the coastal system during a storm surge event is denoted by H_i . The peak water elevation at that point due to the baseline storm surge is denoted by H_b . The ratio of the difference between the peak water elevation, H_i , (for a particular hydrograph variation) and the baseline peak water elevation, H_b , to the peak baseline water elevation, [i.e. $(H_i - H_b)/H_b$] is used to illustrate the sensitivity of the water elevation at a point to the variation in the hydrograph.

Note that the maximum water elevation may occur at a different time during the surge for the baseline hydrograph than the hydrograph with the modified parameter.

To illustrate the difference in the range of values for the maximum water elevation and the water elevation at the time of maximum velocity magnitude (for the hydrograph variations in this study) comparisons between the two quantities are made in Figures 10, 20, 30 and 40. The maximum (or peak) elevation at the time of maximum velocity magnitude is denoted by H_{pv} . The peak water elevation at the inlet or entrance is denoted by H_{im} . The ratio of the difference between peak water elevation, H_i , and the peak elevation at the time of maximum velocity magnitude, H_{pv} , to the peak water elevation at the inlet, [i.e. $(H_i - H_{pv})/H_{im}$] is used to illustrate the difference in the elevations.

Maximum Velocity

The maximum depth averaged velocity that occurs at a point during the course of a storm surge event is denoted by V_i . The maximum velocity that occurs at that point during the baseline storm surge is denoted by V_b . The ratio of the difference between the maximum depth averaged velocity, V_i , for a particular hydrograph variation and the baseline maximum velocity, V_b , at the same point to the maximum baseline velocity [i.e. $(V_i - V_b)/V_b$] is used to show the sensitivity of the maximum velocity to the hydrograph variation. The dependence of maximum velocity on the distance from the inlet or river mouth is illustrated in plots of dimensional velocity versus distance. Time variation of depth averaged velocities are presented for selected locations. The locations of the points (denoted as gages) for the St. Lucie study are shown in Figure 7 and those for the St. Johns River study in Figure 8.

2.2.1 St. Lucie study area

The St. Lucie study area was evaluated in three areas: Indian River Lagoon, Intracoastal Waterway, and St. Lucie Estuary. The model results are described below.

Indian River Lagoon

Figure 9 presents the Maximum Elevation Comparisons for the Indian River Lagoon area. As shown in the graph, the largest percentage differences occur within the lagoon, not near St. Lucie and Fort Piece Inlets. The peak height was most sensitive to variations in the duration of peak and least sensitive to rate of rate of fall.

Figure 10 shows a comparison between the maximum water elevation and the water elevation at the maximum velocity magnitude within the Indian River Lagoon area. As seen in the graph, the elevation differs by less than 15%.

Figure 11 presents the Maximum Velocity Magnitude Comparisons. As with the peak height comparisons, the largest differences occur within the lagoon, not at the inlets. Variations in the rate of rise and rate of fall have maximum depth averaged velocity magnitudes less than the baseline within the center of the lagoon. The variation in the duration of peak produces a greater maximum depth averaged velocity magnitude throughout the lagoon. It is important to note that the largest velocity magnitude

differences occur near the two causeways within the lagoon. This implies that the sensitivity of the velocity magnitude is dependent on the geometry and the constriction of the flow at these locations. Figure 12 presents the magnitudes of the velocities throughout the lagoon. While Figure 11 shows large variations within the lagoon, the magnitude of these velocities are small at these locations (less than 1 foot per second). Therefore, a small increase or decrease in velocity at these points will cause a significant percentage difference.

The velocity magnitude time series at two points within Indian River Lagoon (Gages 1 and 2) for the storm surge variations are presented in Figures 13 through 18. The locations of the two gages are shown in Figure 7. These graphs show where the maximum velocity magnitude occurs in relation to the baseline velocity magnitude at the same location. Note that these graphs only show magnitude of the flow, not direction. These figures show the effect of the variation of the hydrograph parameters on velocity at two distinct points within the system.

Intracoastal Waterway

The comparisons of maximum water elevations within the Intracoastal Waterway are shown of Figure 19. Similar to the Indian River Lagoon, the largest percentage differences occur within the Intracoastal Waterway, and the percentage difference decreases toward the St. Lucie and Jupiter Inlets. It also appears that the peak elevation is most sensitive to variations in the duration of peak and least sensitive to rate of fall.

As shown in Figure 20, the largest differences between the maximum water elevation and the water elevation at maximum velocity magnitude is 20% for the variation in the duration of peak parameter near the inlet. The remaining parameters have differences within 10 – 15%.

There does not seem to be a consistent trend regarding the sensitivity of the maximum velocity to the hydrograph parameters (Figure 21). In a manner similar to that for the Indian River Lagoon, the percentage differences are small near the inlets (less than 15%) and greatest within the Intracoastal Waterway. The rationale as to the variation may be explained as it relates to the geometry of the waterway. However, as shown in Figure 22, the magnitudes of the velocities are small (less than 1 foot per second) within part of the Intracoastal Waterway, which may explain the variation of the maximum velocities.

Figures 23 through 28 show the effect of the hydrograph parameter variations in velocity at two locations within the Intracoastal Waterway. The locations are shown in Figure 7.

St. Lucie Estuary

The Maximum Elevation Comparisons are shown in Figure 29 for the St. Lucie Estuary. As with the Indian River Lagoon, the percentage differences are relatively small

(less than 10%) near the inlet, but reach an approximately constant value as one moves in the upstream direction of the estuary. Again the peak height appears to be more sensitive to variations in the duration of peak and least sensitive to the rate of fall.

As shown in Figure 30, the largest differences between maximum water elevation and the water elevation at maximum velocity magnitudes is less than 15%.

The maximum velocity does not appear to be very sensitive to any of the variations in the storm surge hydrograph in the St. Lucie Estuary. The maximum variation was about 10% and only had a 5% change with the duration of peak and rate of fall changes. Figure 31 shows the Maximum Velocity Comparisons and Figure 32 shows the magnitude of the velocities in St. Lucie Estuary.

Figures 33 through 38 show the effect of the hydrograph parameter variations on velocity at two locations within the estuary. The locations of these gages are shown in Figure 7.

2.2.2. St. Johns River study area

Due to the St. Johns River's large drainage basin, the net discharge is quite large. The value used in this study was 35,000 m³/sec. A discharge was not included in the hydrodynamic model of the St. Lucie Estuary. Thus, the discharges used are close to those that occur under average conditions.

As shown in Figure 39, the nondimensional peak water elevation difference increased with distance from the mouth of the river, but the values did not exceed 15%. The peak water elevation appears to be most sensitive to variations in the duration of peak and least sensitive to variations in the rate of fall.

The difference between the peak water elevation and the water elevation at maximum velocity magnitude was less than 12%. There does not appear to be a correlation between distance from the river mouth and these differences.

As shown in Figure 41, it appears that variations to the duration of peak and rate of fall have virtually no effect near the mouth of the river, but do have a slight effect (less than 10%) upstream. However, variations to the rate of rise are most influential at the mouth and decrease upstream. The maximum velocity magnitudes were found during the flood stage. The magnitudes of these velocities are shown in Figure 42.

Figures 43 through 48 show the effect of the hydrograph parameter variations on velocity at two locations within the estuary. The locations of these gages are shown in Figure 8.

Figure 49 is a graph of the velocity and water elevation for the baseline hydrograph at the gages in the St. Johns River. This shows the time lag between the peak water elevation and peak velocity at Gages 1 and 2 for the baseline hydrograph.

2.3 CONCLUSIONS

In drawing conclusions from the results of this study the assumptions made and the limitations of the procedures and computer models used in the analysis must be kept in mind. For example, all real flows are three dimensional in nature and thus are only approximated with a two dimensional flow model. Even if water density stratification (due to, for example, temperature and/or salinity differences) does not exist, the secondary flows that occur in the sharp bends of rivers and streams cannot be accounted for with a two dimensional model. In spite of these shortcomings many of the important processes can be simulated with the procedures and models used in this study. Thus, a number of important conclusions can be derived from the results of such an analysis. Some of the conclusions are summarized below:

- The peak water elevation at a point in the coastal system appears to be most sensitive to the duration of the peak and least sensitive to the rate of fall of the open coast storm surge hydrograph. This is most likely due to the flow at the point having a longer time to respond to the surge (i.e. the “effective frequency” at the peak of the surge is lower resulting in a greater response). Varying the rate of fall of the open coast storm surge increases the duration of the flow at lower water elevations, but not at the peak elevation, thus the lesser sensitivity to this parameter. Therefore for design high water elevation calculations the open coast hydrograph with the longest duration peak anticipated should be used for the analysis.
- The peak height is not as sensitive to variations in the hydrograph parameters near the inlet locations as it is away from the inlets in the bodies of water such as estuaries, rivers, or lagoons.
- There does not appear to be a correlation between maximum elevation and peak elevation at maximum velocity magnitude, and distance from the inlets or river mouth. There is considerable variation of values along the study areas. For design variation purposes, the peak elevation (rather than the elevation at maximum velocity magnitude) could be used for sediment scour and structure loading calculations. While this is conservative, the differences between peak elevation and elevation at maximum velocity are relatively small (usually less than 15%).
- In general, increases in the duration of the storm surge peak results in higher velocities than those produced by the baseline surge. An increase in peak duration that produces a 20% increase in area under the hydrograph results in maximum velocity increases up to 20%. The variation with distance from the inlet/river mouth can be seen in Figures 11, 21, 31, and 41. As would be expected, the maximum velocity magnitude and their sensitivities are functions of the geometry of the water body being evaluated. It is believed that the variations in maximum velocity and sensitivity to the hydrograph parameters in Indian River Lagoon can be attributed in part to the presence of causeways in that body of water. Flow separation and eddy formation on the down flow side of the causeway were observed in the model output. Again, as anticipated, the large flow discharge in St. Johns River impacted the

maximum values of the velocity in the river. It should be noted that the maximum velocity magnitude occurred during the flood stage of the surge propagation in the St. Johns River.

- It is important to remember that for most numerical models, such as that used in this study, the results are less accurate near the boundaries. This is particularly true for the water boundaries such as those at the north and south boundaries of the St. Lucie Model. The model imposes an artificial vertical wall at these points and, thus, both the absolute flow values and the sensitivities will be inaccurate in the immediate neighborhood of these boundaries and should not be used.

3. FIELD MEASUREMENT PROGRAM

This section presents a brief summary of the Field Measurement Program, the scour-depth monitoring system, and conclusions. Details of this work can be found in the paper titled "Field Performance of an Acoustic Scour-Depth Monitoring System" by Robert R. Mason, Jr. and D. Max Sheppard. This paper was presented at the FDOT Design Conference in Orlando, Florida from August 12-14, 1994. A copy of this paper is included with this report as Appendix B.

3.1 Background

Since completion of the Bonner Bridge in 1962, the North Carolina Department of Transportation (NCDOT) has made periodic soundings of Oregon Inlet to monitor channel migration, deposition, and local scour. The vicinity map for Oregon Inlet is shown in Figure 50 and the study area is shown in Figure 51. These data indicate that some sections of Oregon Inlet have scoured and filled through an 11 m range. In 1978, NCDOT discovered that, as a result of scour, several pilings were penetrating only 2.1 m into the channel bottom. In response to this history of channel instability, the USGS and NCDOT joined in a cooperative effort to develop and install a data-collection system to permit continuous remote monitoring of scour depth at 16 bridge pilings. The system was installed in September 1992.

A second data-collection program began in November 1993 and ended in January 1994. This effort consisted of deployment and operation of three instrument packages that measure and record current magnitude and direction, wave frequency and direction, water-surface elevation, and water temperature near Bonner Bridge. This program was a cooperative effort between the FDOT, the University of Florida Coastal and Oceanographic Engineering Department (UFCOE), the NCDOT and USGS.

The objective of this study was to obtain information about the flow that was producing the scour and deposition at the piers on Bonner Bridge. Scour depths were already being measured at both ends of the nine consecutive piers by the NCDOT and USGS.

3.2 Scour-Depth Monitoring System

Instrumentation to measure flow and wave parameters were installed approximately 30 meters seaward of two of the piers being monitored for scour.

The main component of the Bonner Bridge scour-depth monitoring system is a Datasonics PSA 902 digitally-recording, acoustic fathometer operating 16 transducers, each generating a 200-kHz acoustic beam with a conical 10-degree spread. At the time of deployment in 1992, each transducer was mounted at least 1.5 m above the channel bottom and between 1.8 m and 4 m below the water surface.

The fathometer is configured as two separate channels, each controlling eight transducers. A time-varying gain circuit, one for each channel, can be adjusted to calibrate the transducers on that channel to an overall (group) optimal setting.

On November 4, 1993, three additional hydrographic instruments were installed near the Bonner Bridge. Two of these instruments were Endeco current meters (type 174SSM) that measure and record water temperature as well as current magnitude and direction. The third instrument was a Seadata wave-tide recorder that measures and records current magnitude and direction, wave frequency and direction, and water-surface elevation. The current meter and puv installations are shown in Figures 52 and 53, respectively.

The water depth at the instrumentation at the time of deployment was approximately 5 m. The *insitu* recording instrumentation was deployed for approximately 3 months. Even though there were no major storms during the deployment of the flow and wave instruments, there was a significant deposition of sediment in the study area. This completely buried one of the flow meters and the wave instrumentation and damaged the other two flow meters. The damaged flow meters contained approximately one months flow velocity data.

3.3 Conclusions

Approximately one and one-half months of current data were recovered from the two current gauges that survived. This data was reduced analyzed and attempts were made to correlate the measured scour depths with the flow velocities from the current meters. The measured scour depths are a combination of aggradation and degradation, contraction scour and local scour. The component that would correlate with the flow velocity immediately upstream from the pier is local scour. The primary objective of this measurement program was to obtain more information about local scour for larger scale structures. The problem with any field experiment is, of course, the lack of control of the quantities influencing the phenomena being studied and this is a text book example of the problems that can be encountered. The global movement of sediment in this tidal inlet was such that it completely overshadowed the local scour. Thus, the “noise” was much greater than the “signal” and little or no correlation between scour depth and flow velocity was observed. This illustrates the importance and need for controlled laboratory experiments when trying to isolate a single component of a complex process, such as local bridge pier scour. Since the ultimate goal this and similar research is to understand and predict bridge scour under field conditions, field data are equally important but the measurements must be sufficient to allow the prediction of all of the primary processes affecting the phenomena. Lessons learned from this experience can be summarized as follows:

- If the objective of a study is to isolate a single component of a complex process in a field measurement program then a site where the other components are negligible or at least small should be located. In this case, by far the most expensive part of the

measurement program (the scour measurement instrumentation) was already in place for operational monitoring purposes. Therefore, for a small investment there was potentially much to be gained.

- The global movement of sediment in this inlet under “normal” ambient conditions was under estimated. Perhaps a closer examination of historical surveys and more discussions with local workers in the area would have revealed the extreme dynamic nature of the study site.
- When deploying instrumentation at a location somewhat unfamiliar to the researcher, more frequent site visits should be planned, budgeted and conducted. Had this been done the instrument fixed to the bottom would not have been lost.
- Controlled laboratory experiments for investigating a single component of a complex process with many input parameters are the most cost effective way to obtain high quality data.

4. REFERENCES

- Sheppard, D.M., C.W. Reed, and S. Harr, (1994) "Sensitivity of Bridge Scour Producing Currents to Storm Surge Parameters Progress Report," FDOT Design Conference, Orlando, Florida, August 10, 1994.
- Mason, R.R., Jr. and D.M. Sheppard, (1994) "Field Performance of an Acoustic Scour-Depth Monitoring System," FDOT Design Conference, Orlando, Florida, August, 12-14, 1994.
- Morris, F.W. (1987) "Modeling of Hydrodynamics and Salinity in the St. Lucie Estuary," SFWMD Technical Publication 87-1, January.
- Norton, W.A. and W.H. McAnally, (1973) "A Finite Element Model for Lower Granite Reservoir," Water Resources Engineers, Inc., Walnut Creek California.
- Thomas and McAnally, (1991) "User's Manual for the Generalized Computer Program System: Open-Channel Flow and Sedimentation, TABS-2', U.S. Army Engineer Waterways Experiment Station, Vicksburg, Mississippi.
- Fasstabs User's Manual, (1992) Boss Corporation and Brigham Young University.
- Sheng, Y.P., S. Peene and Y.M. Liu, (1990) "Numerical Modeling of Tidal Hydrodynamics and Salinity Transport in the Indian River Lagoon," Florida Scientist, vol.53, No.3, p.147.
- Smith, N.P., (1990) "Longitudinal Transport in a Coastal Lagoon," Estuarine, Coastal and Shelf Science, Vol.31, 835-849.
- SMS User's Manual, (1995) Boss Corporation and Brigham Young University.
- Williams, J.L., (1985) "Computer Simulation of the Hydrodynamics of the Indian River Lagoon," MS Thesis, Florida Institute of Technology, Melbourne.

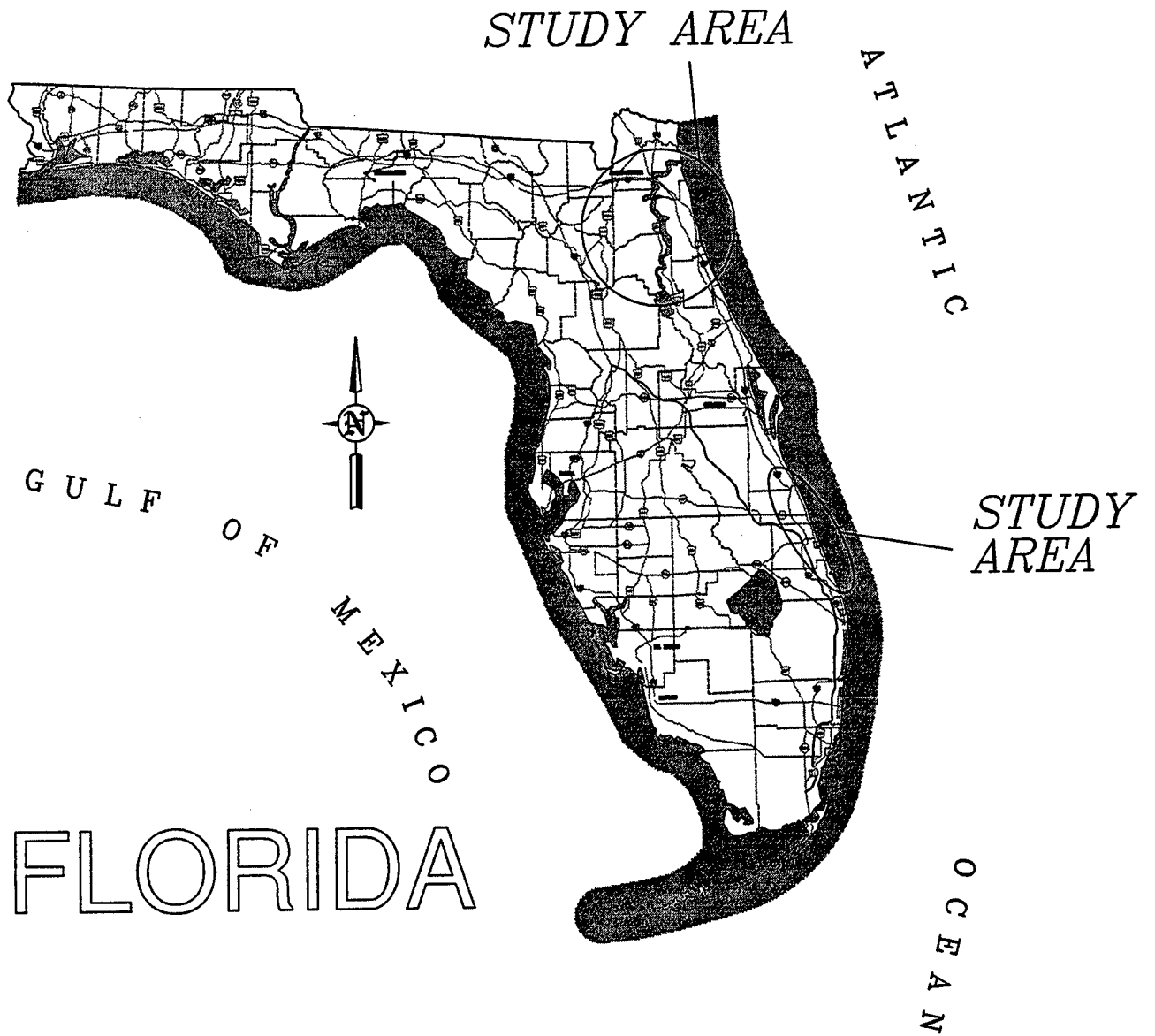


Figure 1. General location of study areas.

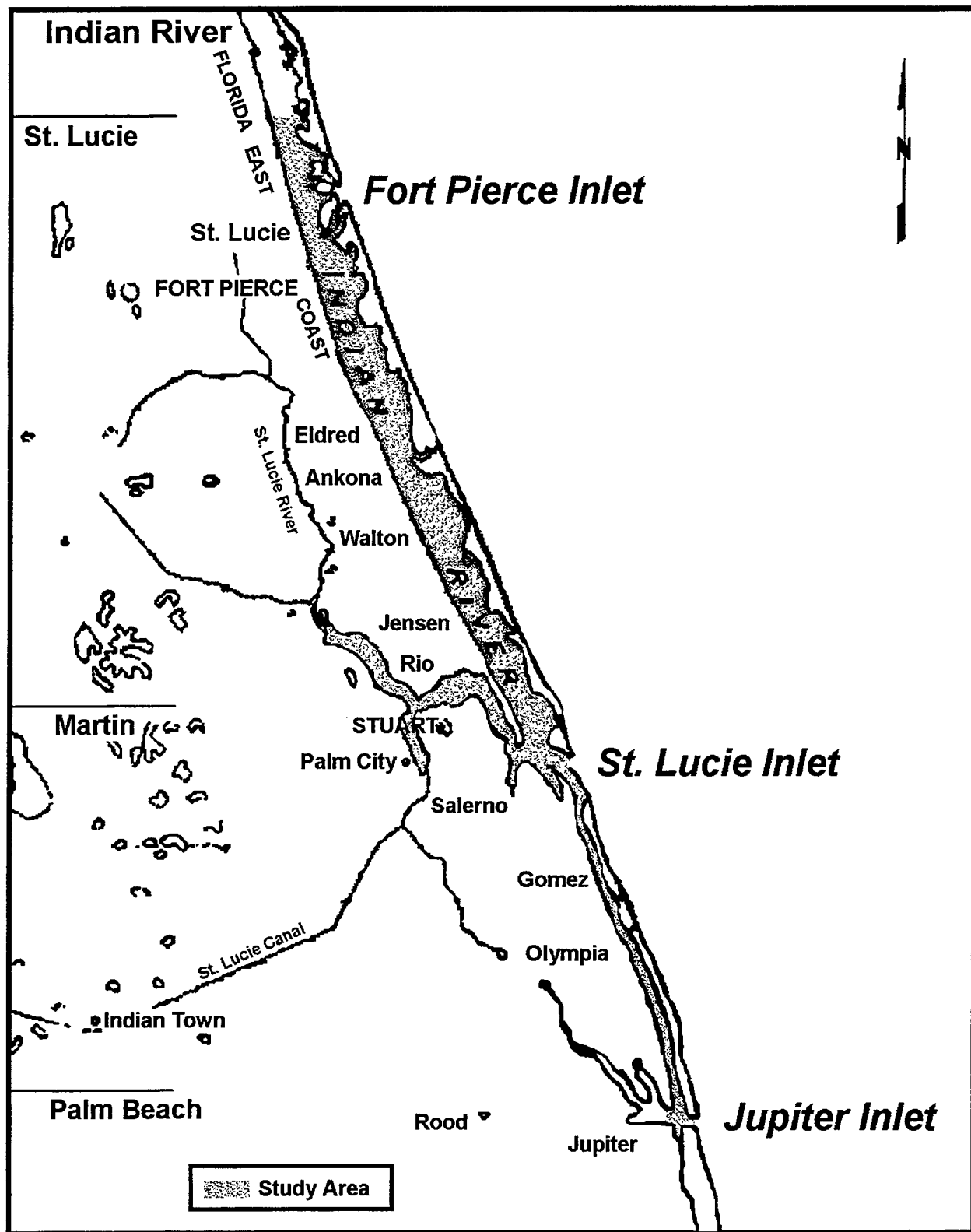


Figure 2. St. Lucie Estuary study area.

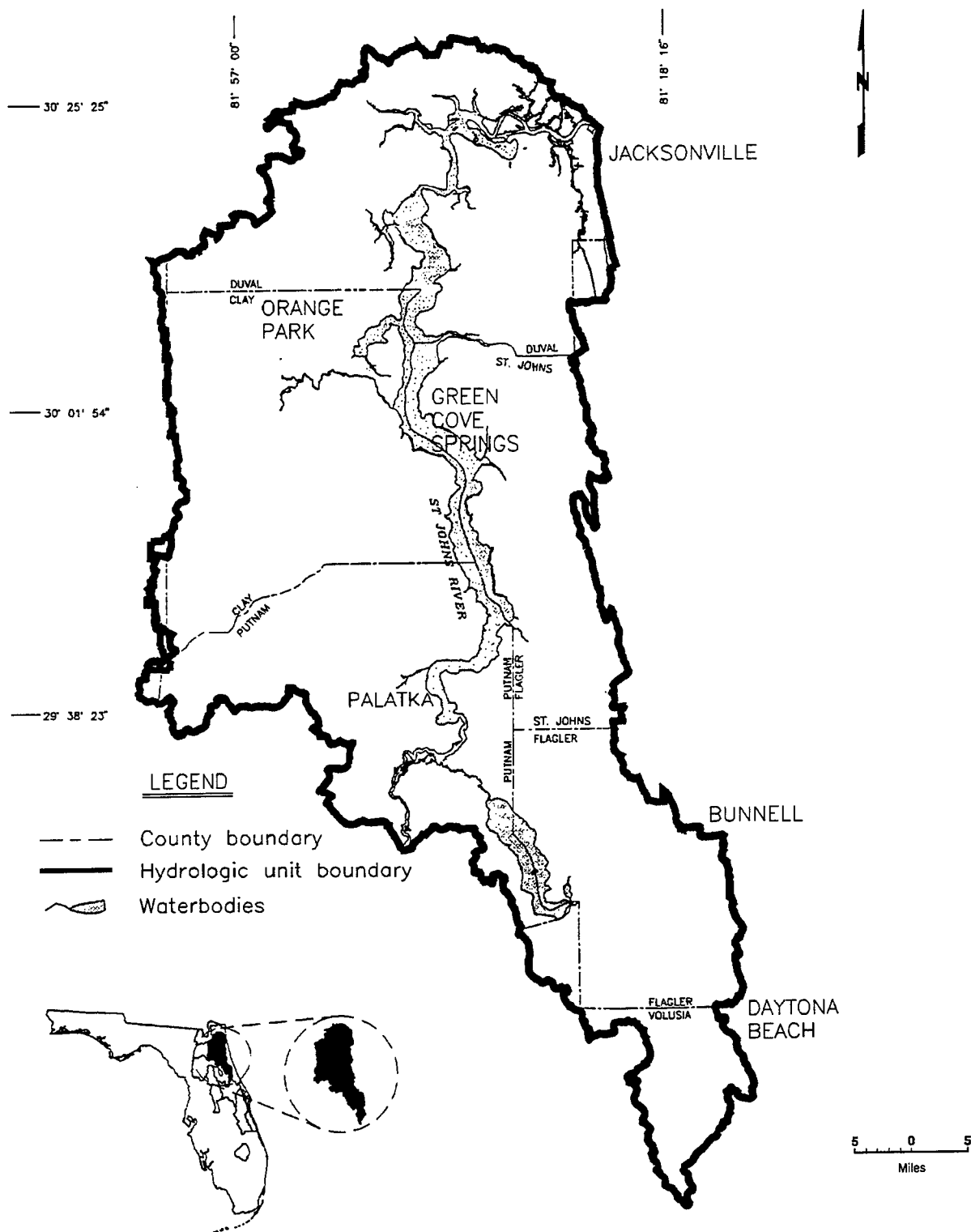


Figure 3. St. Johns River study area.

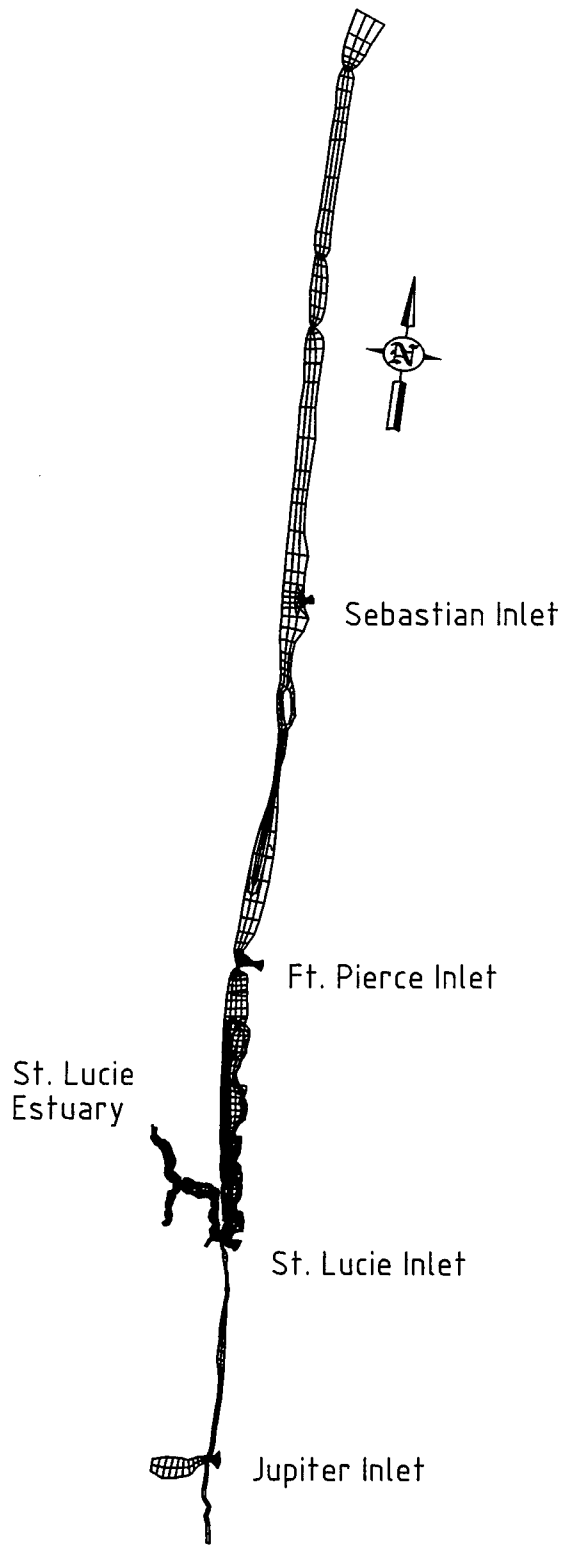


Figure 4. St. Lucie Estuary finite element mesh.

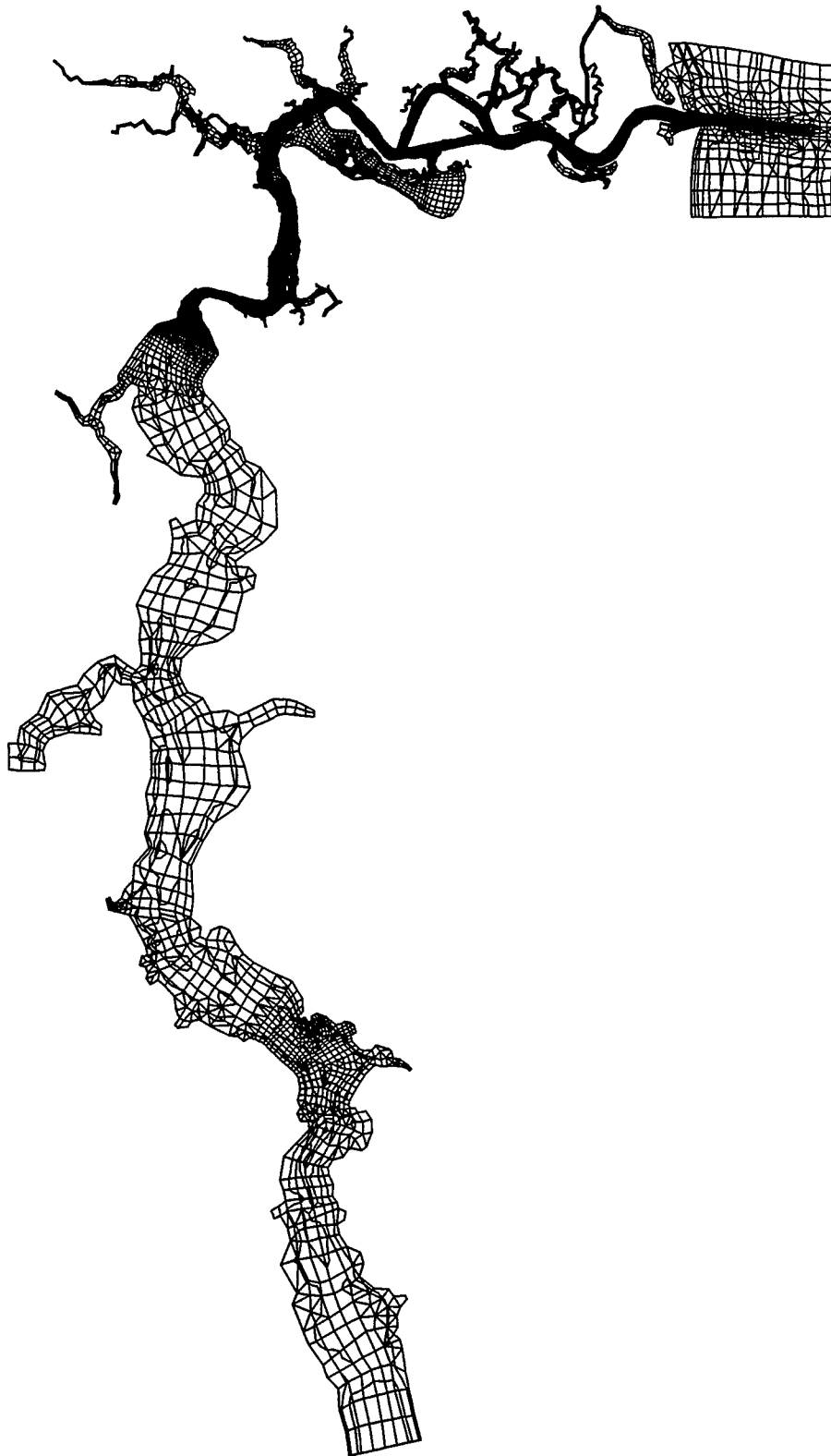


Figure 5. St. Johns River finite element mesh.

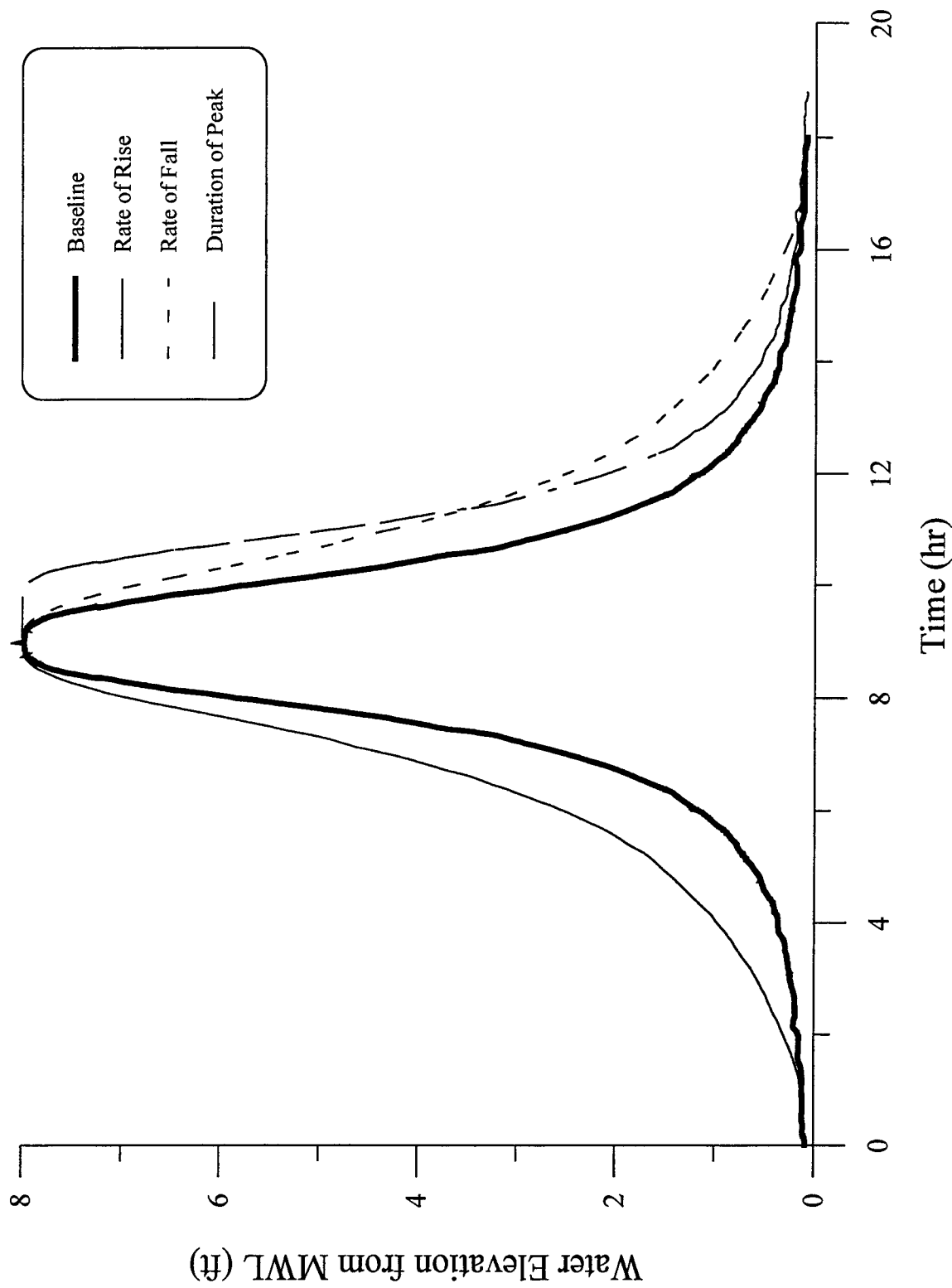


Figure 6. St. Lucie & St. Johns River storm surge variation.

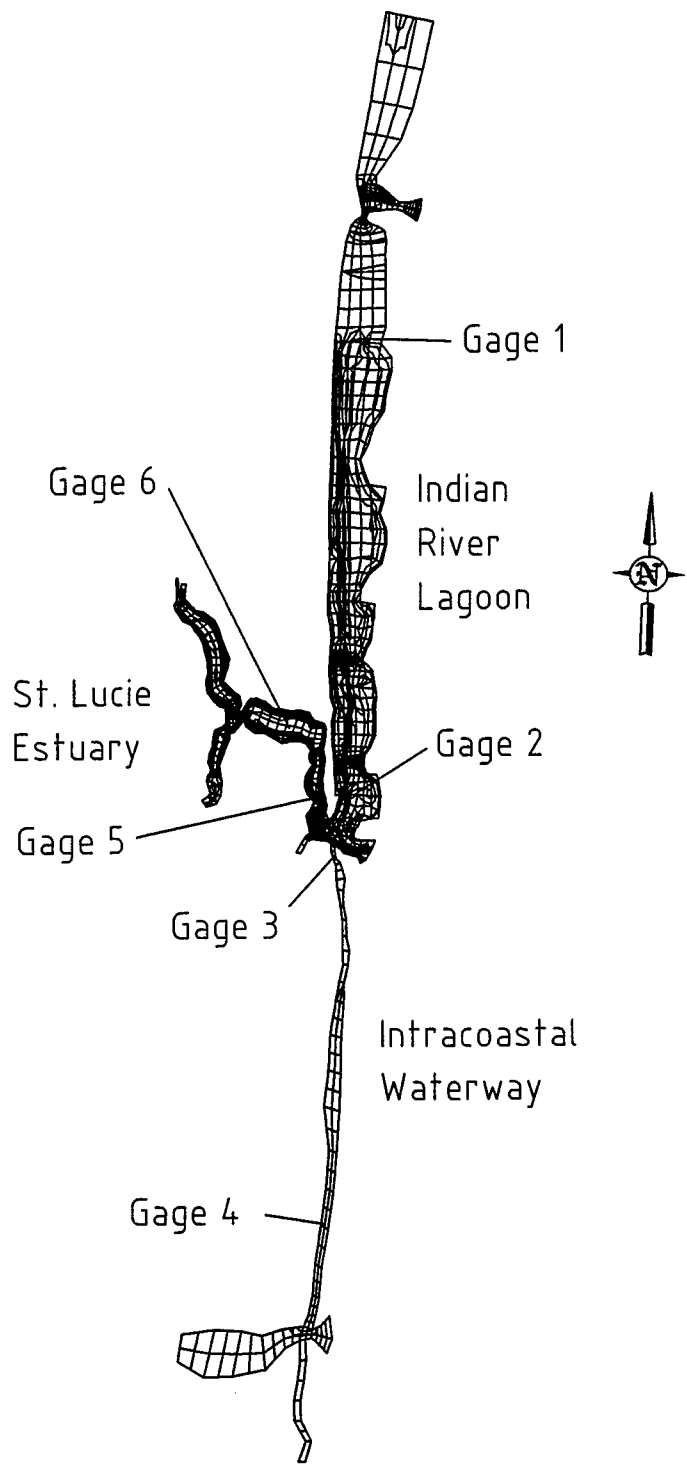


Figure 7. St. Lucie study area locations.

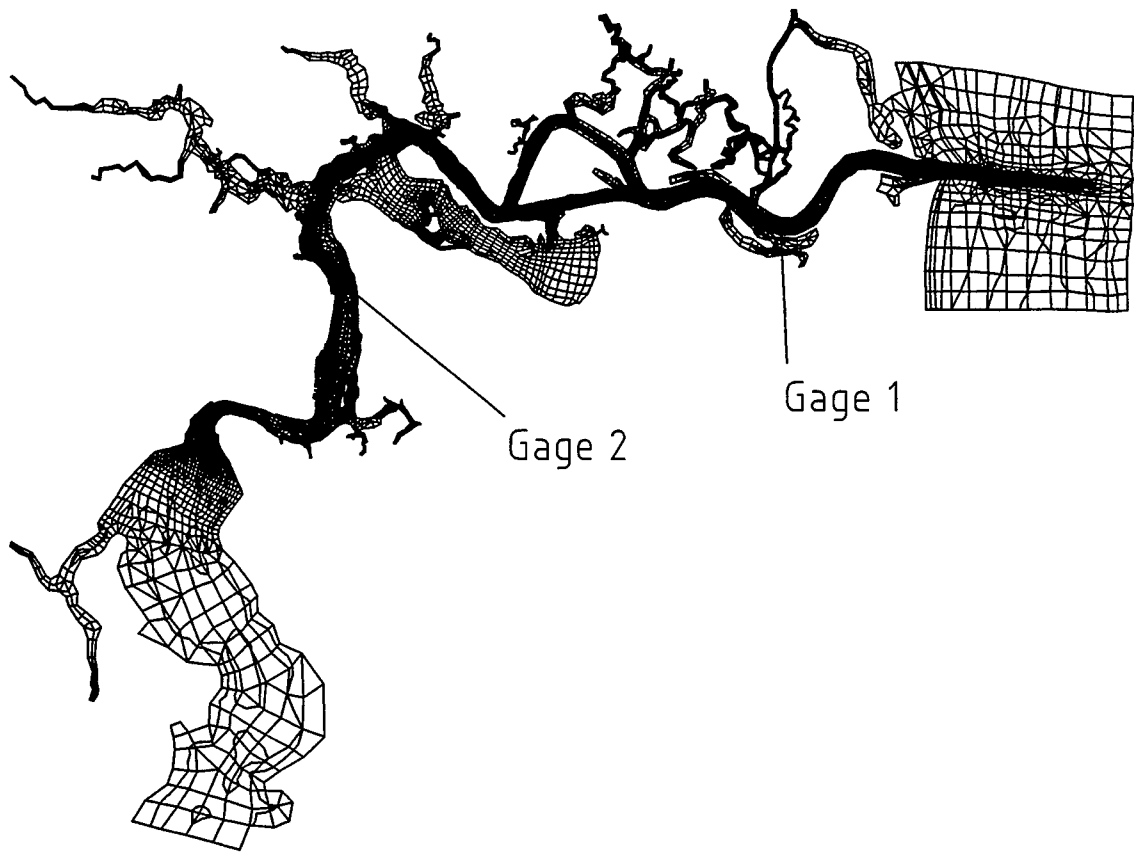


Figure 8. St. Johns River study area locations.

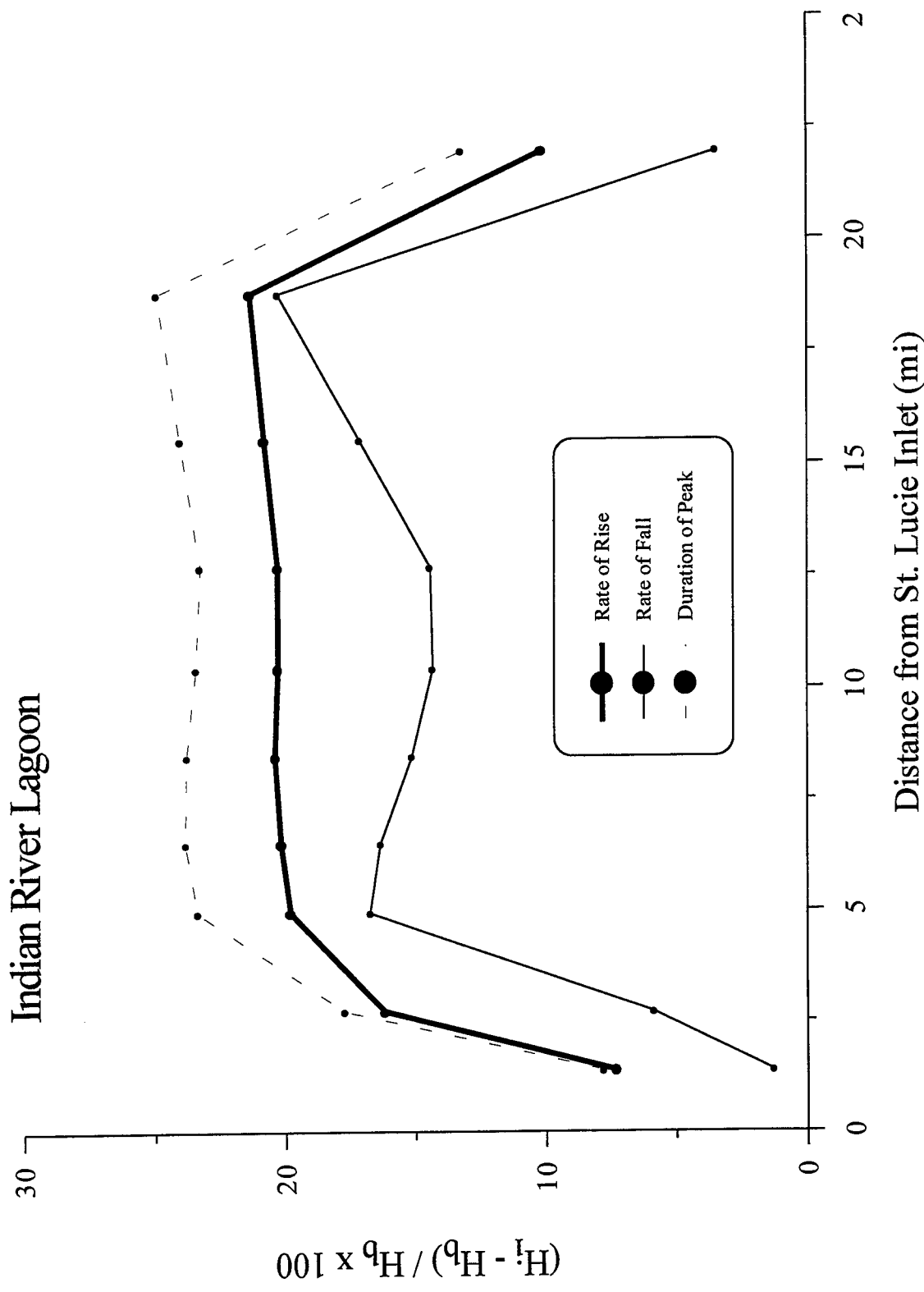


Figure 9. Maximum elevation comparisons – Indian River Lagoon.

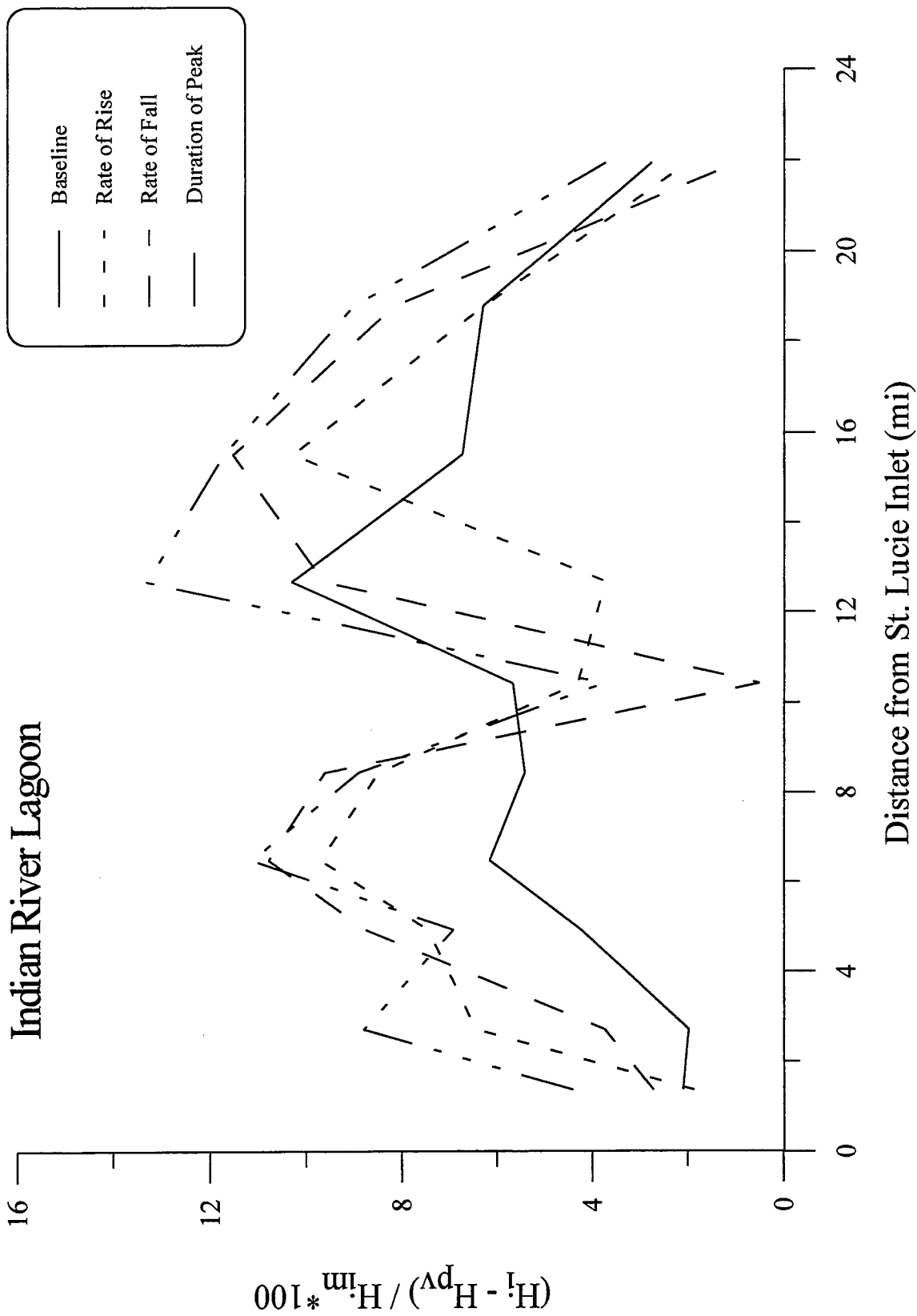


Figure 10. Maximum water elevation and elevation at maximum velocity magnitude comparisons – Indian River Lagoon.

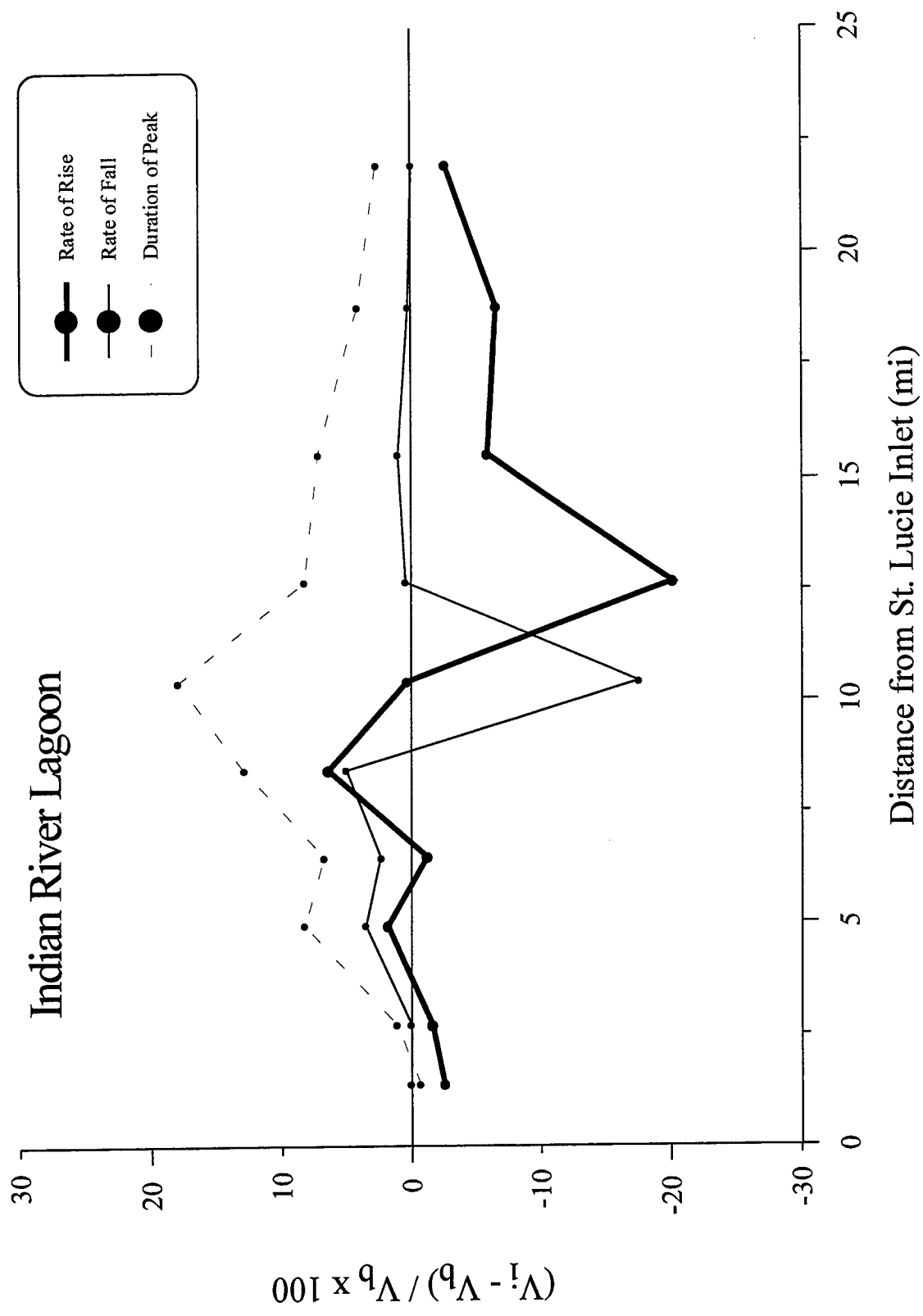


Figure 11. Maximum velocity magnitude comparisons – Indian River Lagoon.

Indian River Lagoon

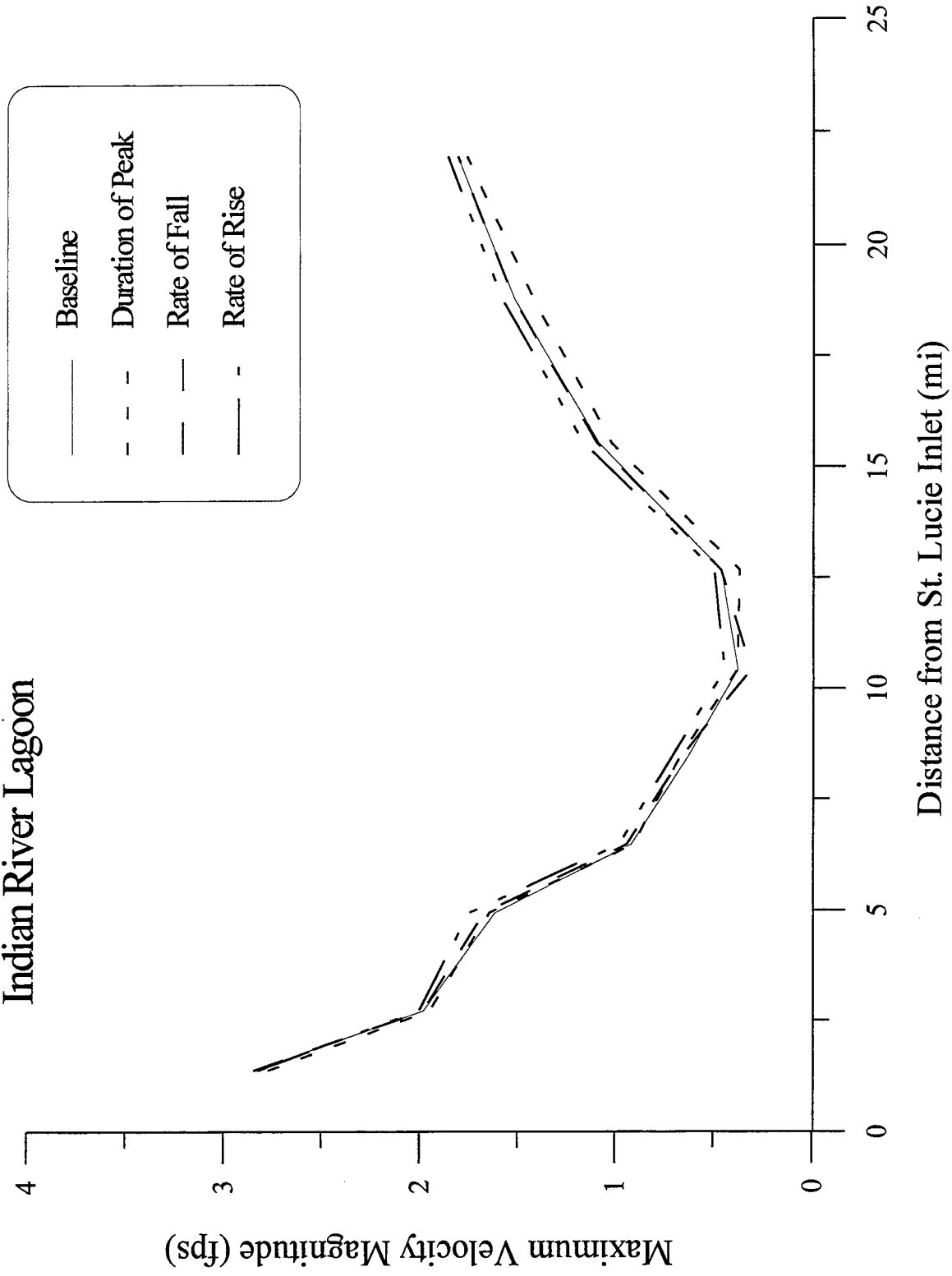


Figure 12. Maximum velocity magnitude vs. distance – Indian River Lagoon.

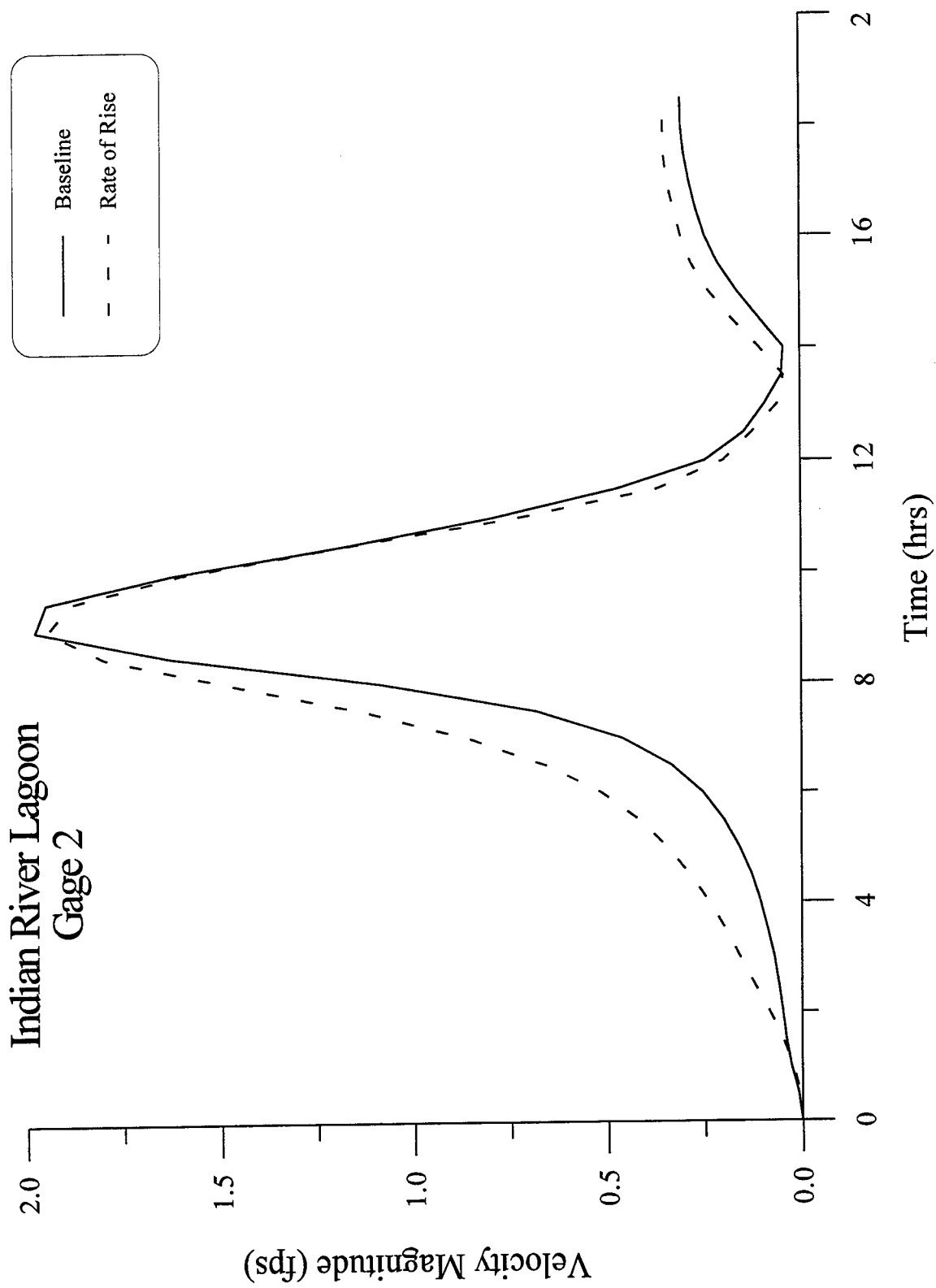


Figure 13. Velocity magnitude vs. time at Gage 2 – rate of rise variation – Indian River Lagoon.

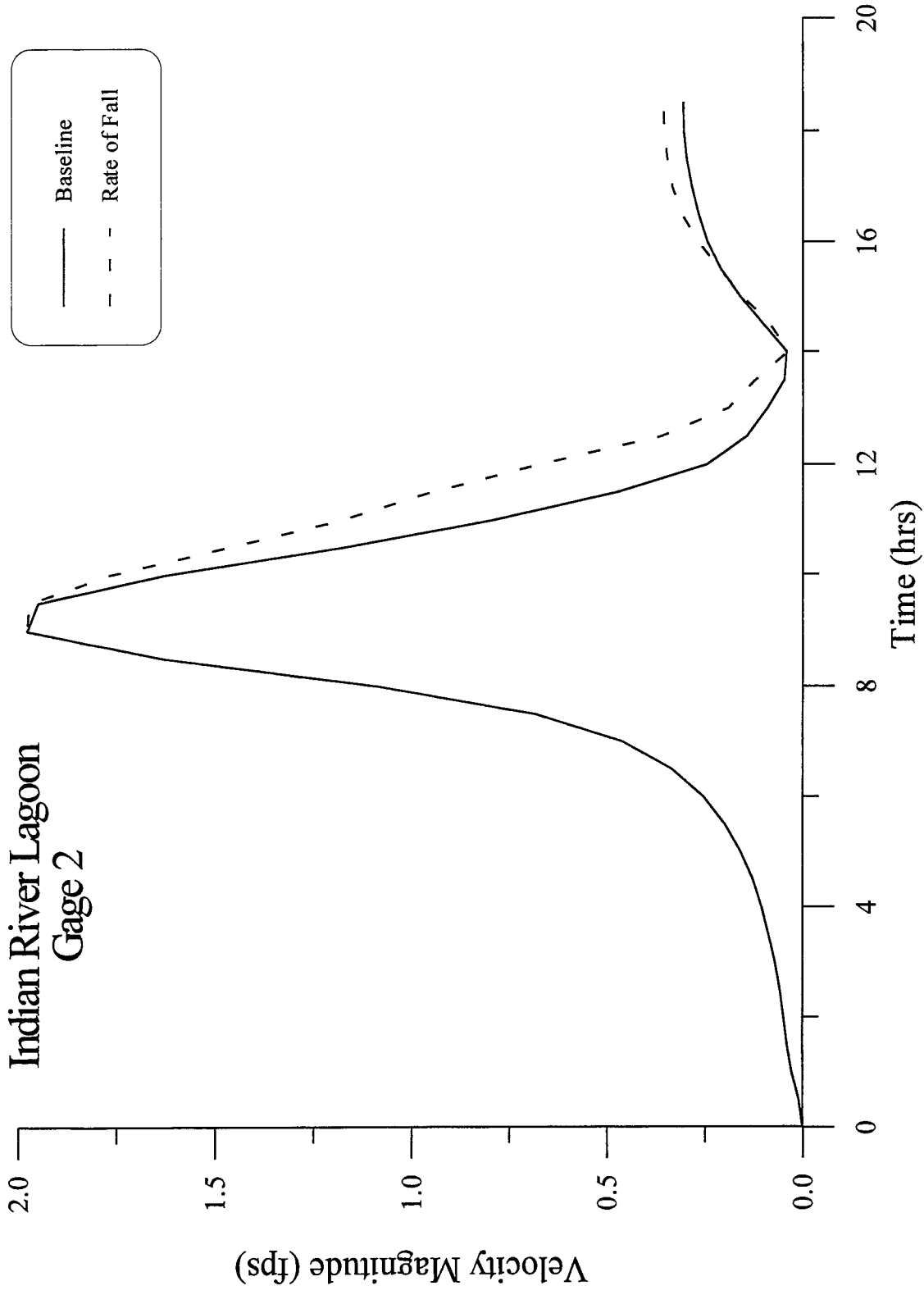


Figure 14. Velocity magnitude vs. time at Gage 2 – rate of fall variation – Indian River Lagoon.

Indian River Lagoon Gage 2

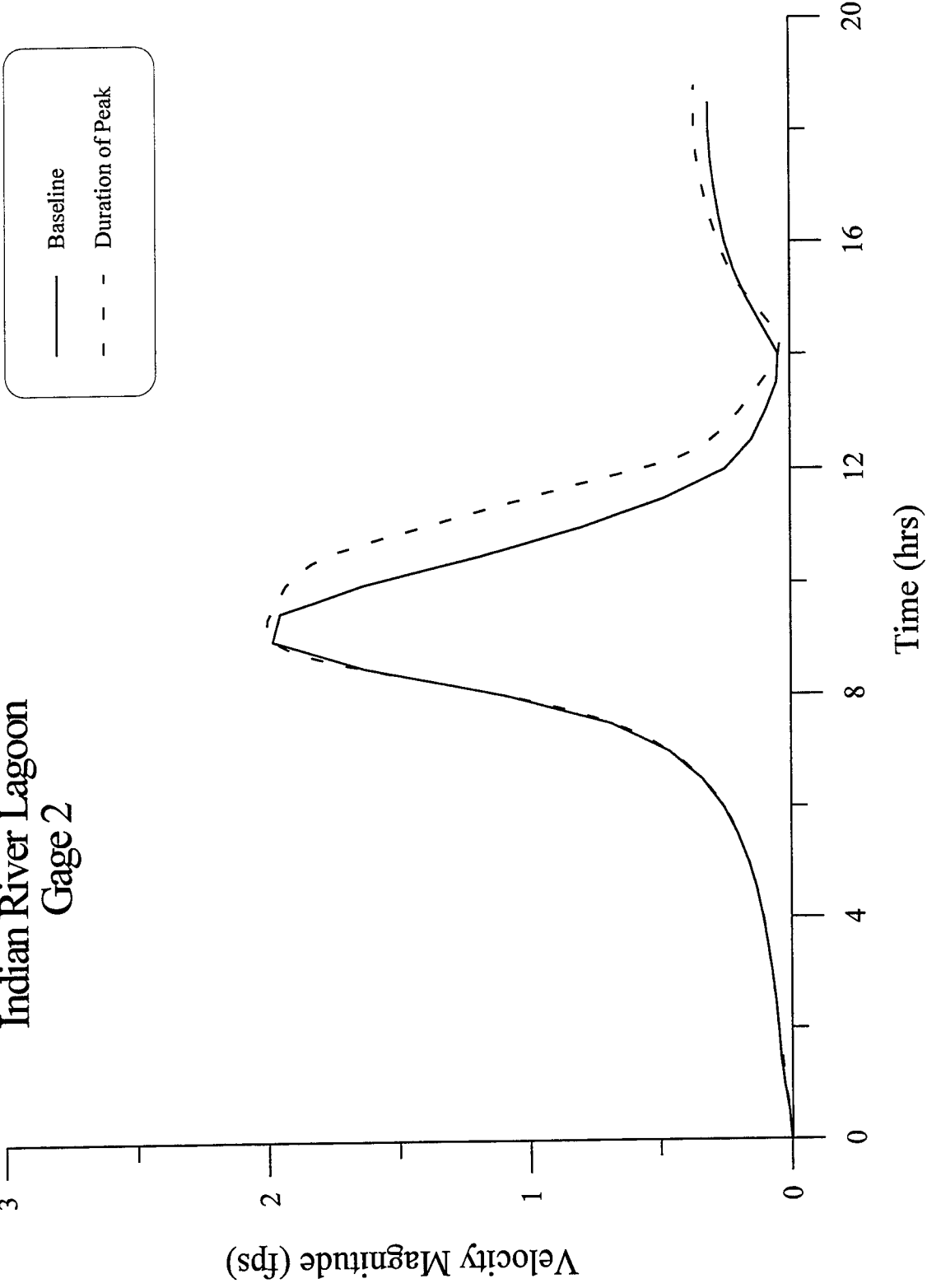


Figure 15. Velocity magnitude vs. time at Gage 2 – duration of peak variation – Indian River Lagoon.

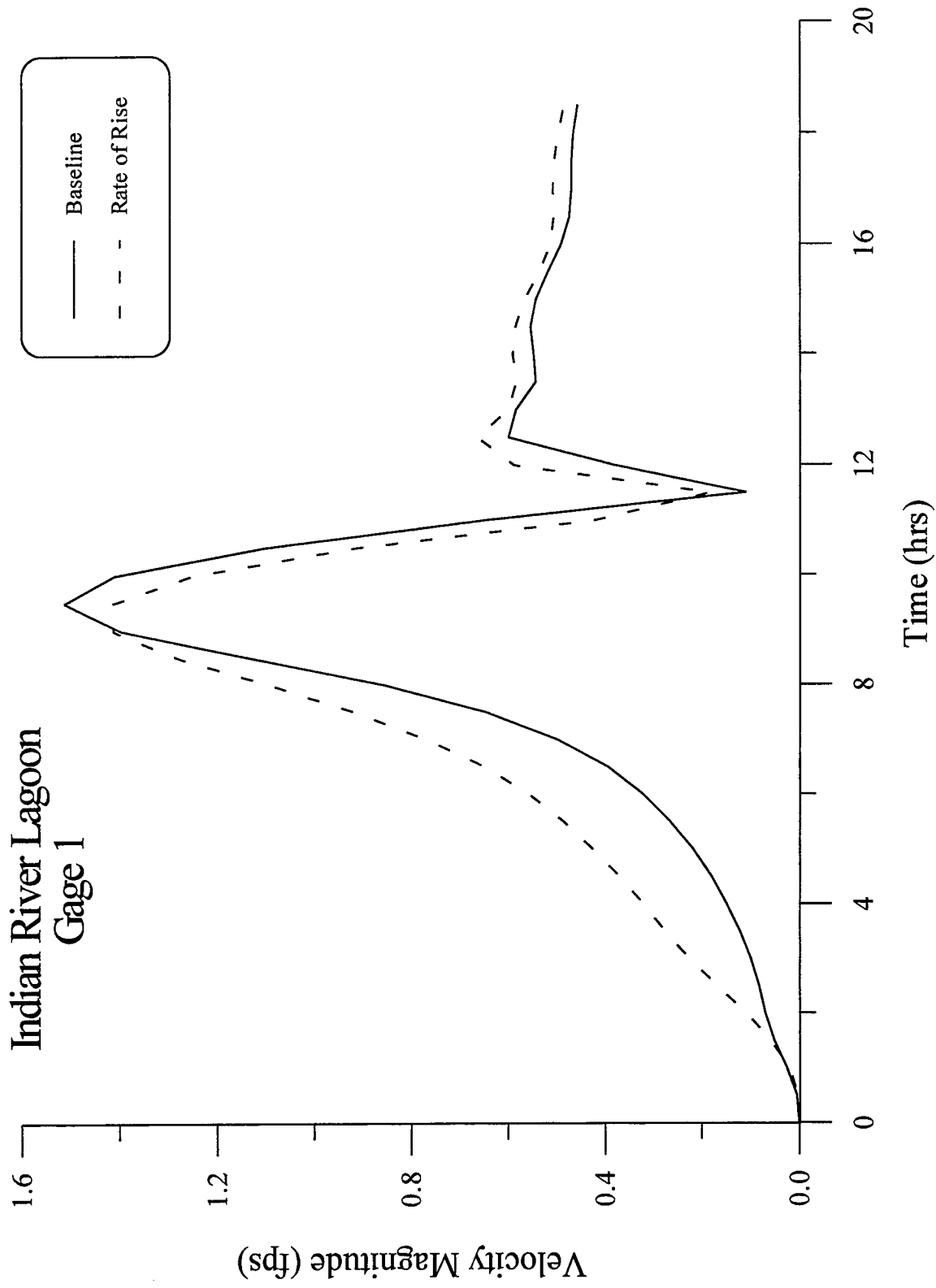


Figure 16. Velocity magnitude vs. time at Gage 1 – rate of rise variation – Indian River Lagoon.

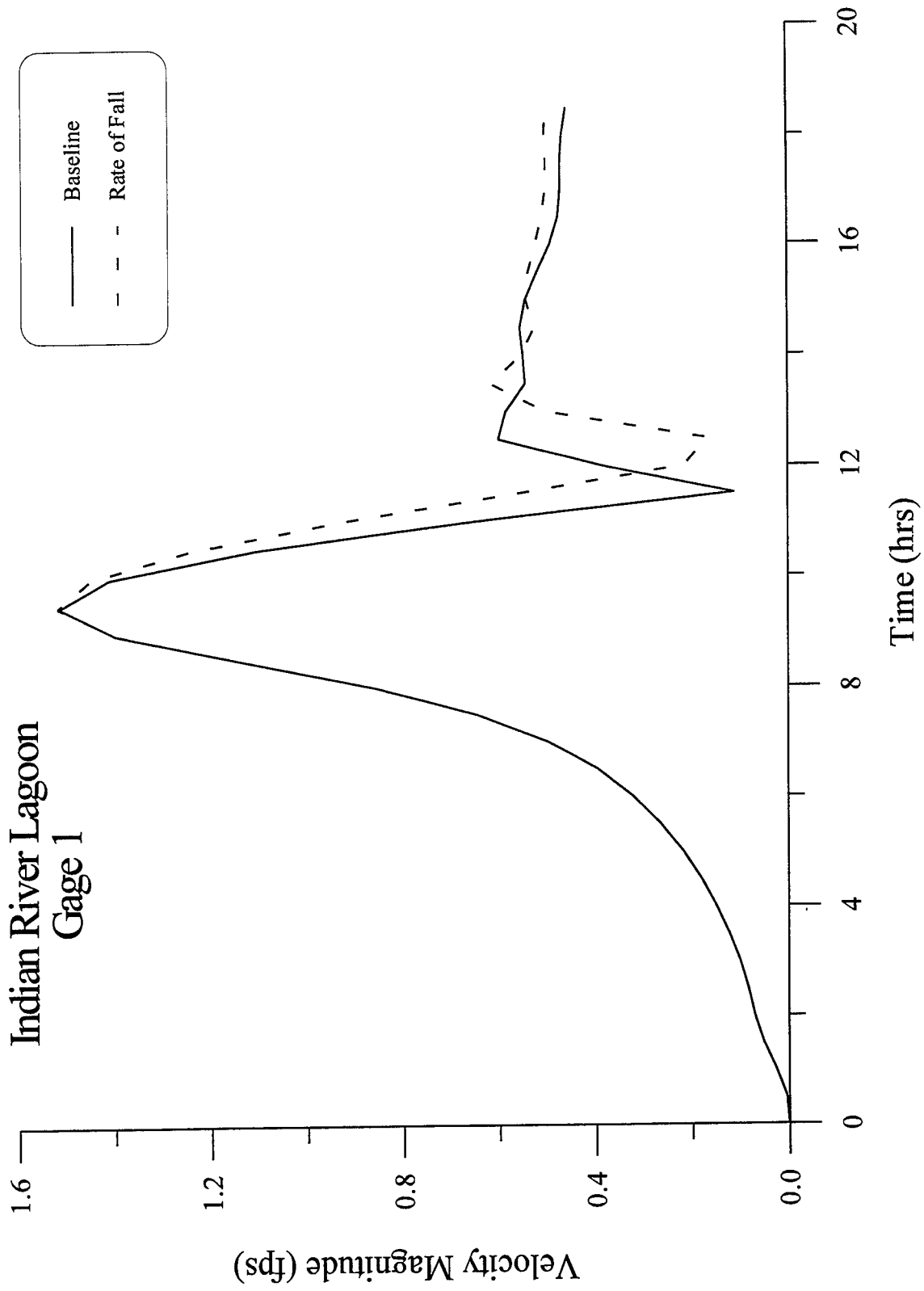


Figure 17. Velocity magnitude vs. time at Gage 1 – rate of fall variation – Indian River Lagoon.

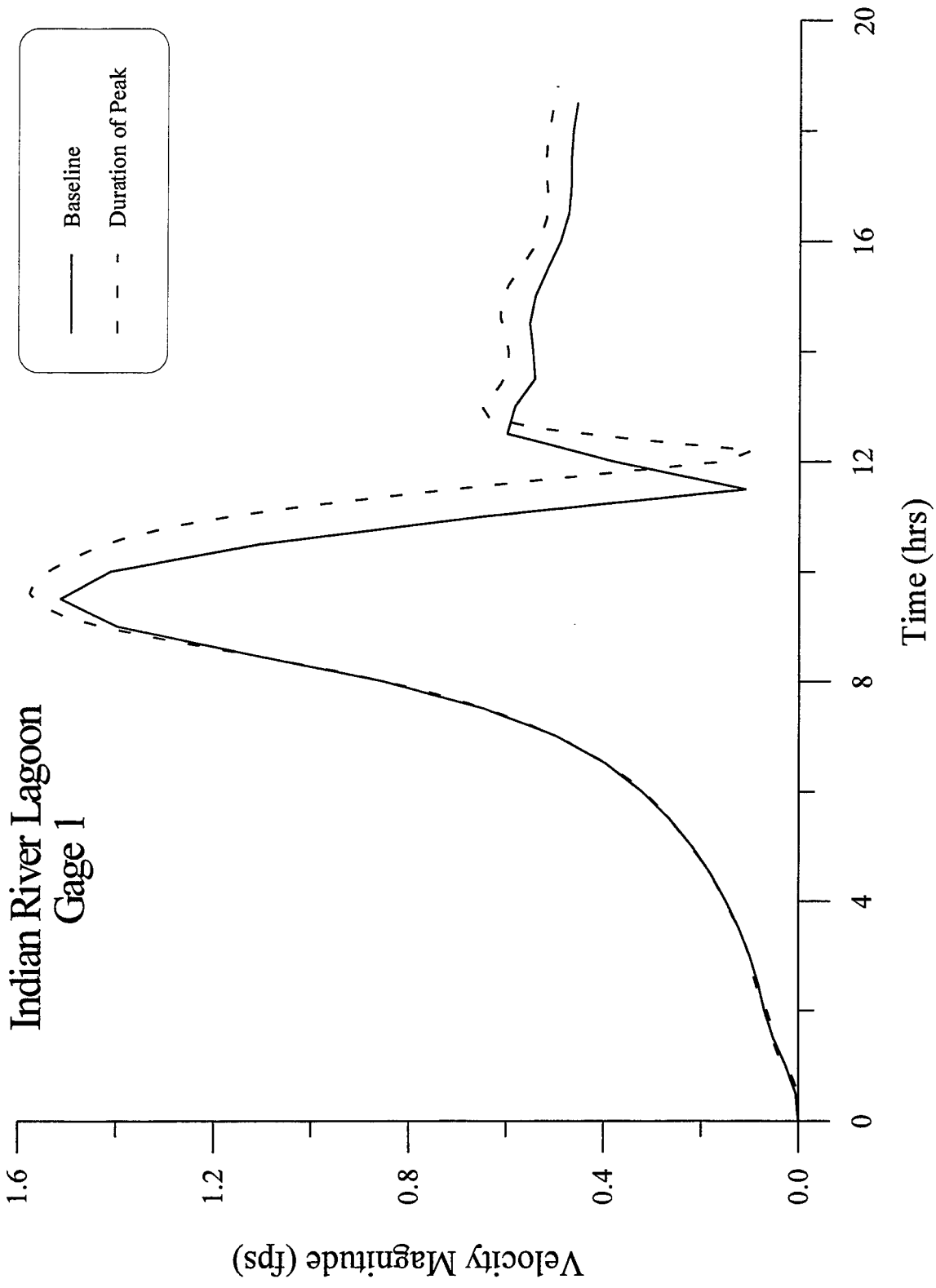


Figure 18. Velocity magnitude vs. time at Gage 1 – duration of peak variation – Indian River Lagoon.

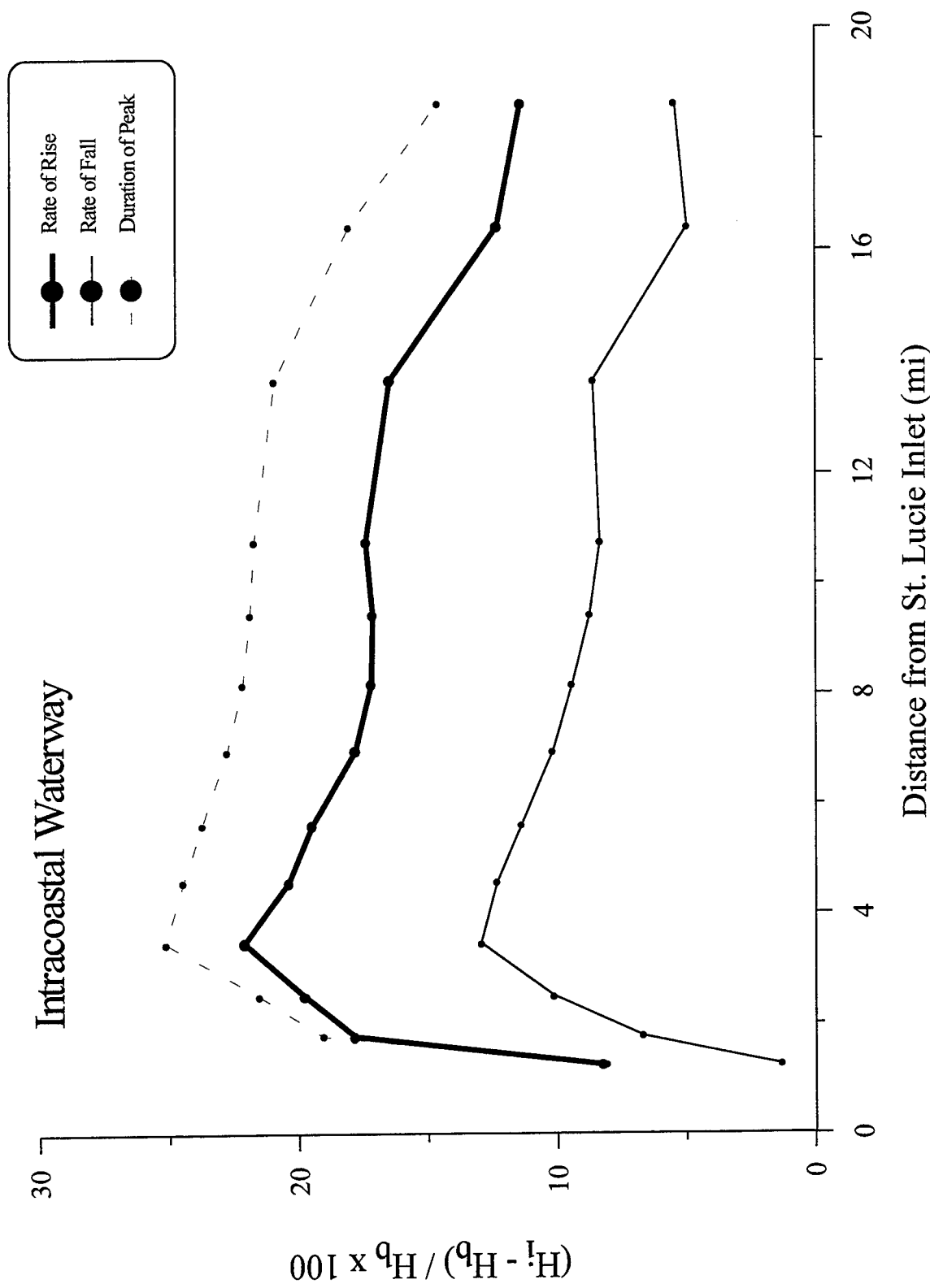


Figure 19. Maximum elevation comparisons – Intracoastal Waterway.

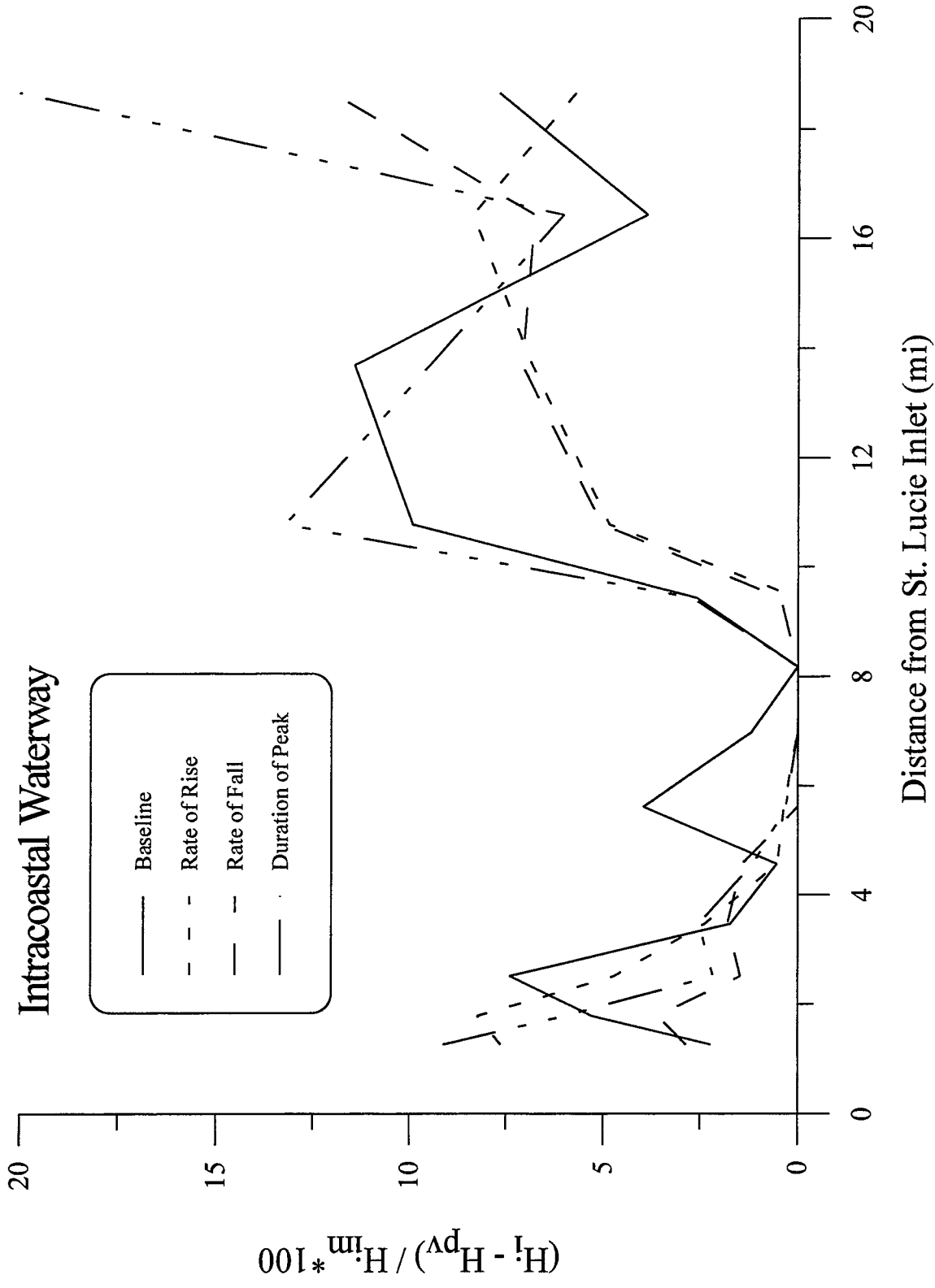


Figure 20. Maximum water elevation and elevation at maximum velocity magnitude comparisons – Intracoastal Waterway.

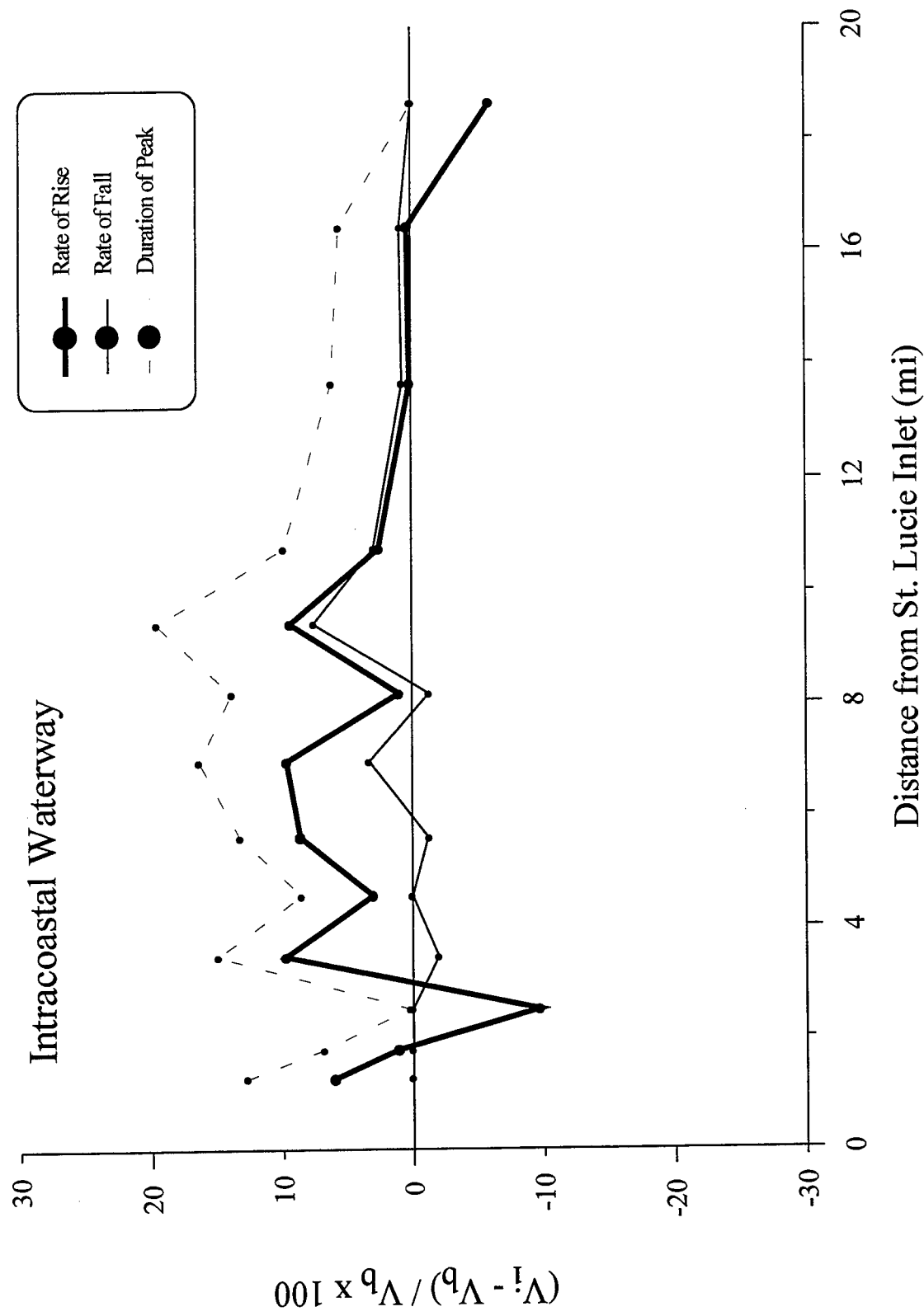


Figure 21. Maximum velocity magnitude comparisons – Intracoastal Waterway.

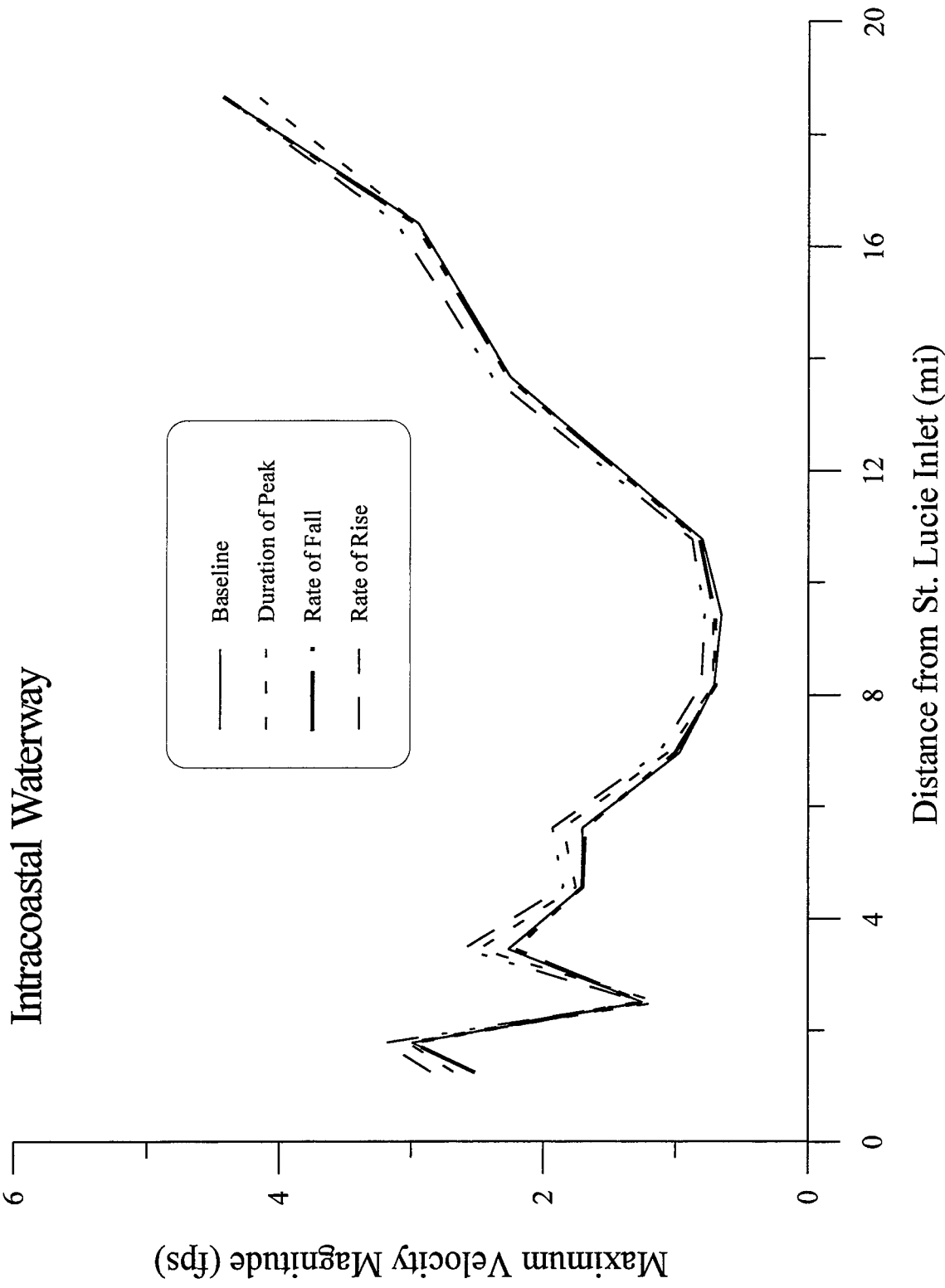


Figure 22. Maximum velocity magnitude vs. distance – Intracoastal Waterway.

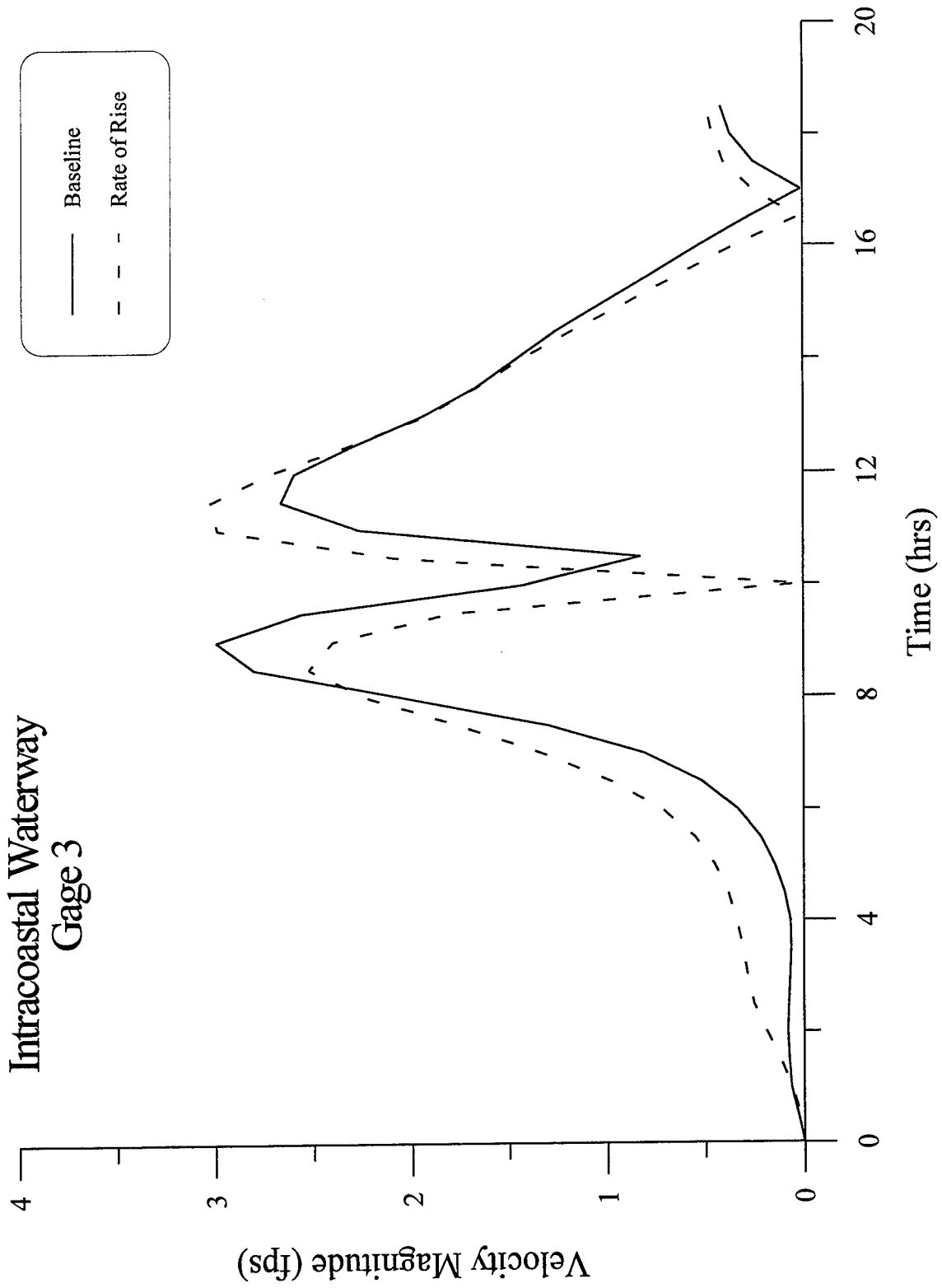


Figure 23. Velocity magnitude vs. time at Gage 3 – rate of rise variation – Intracoastal Waterway.

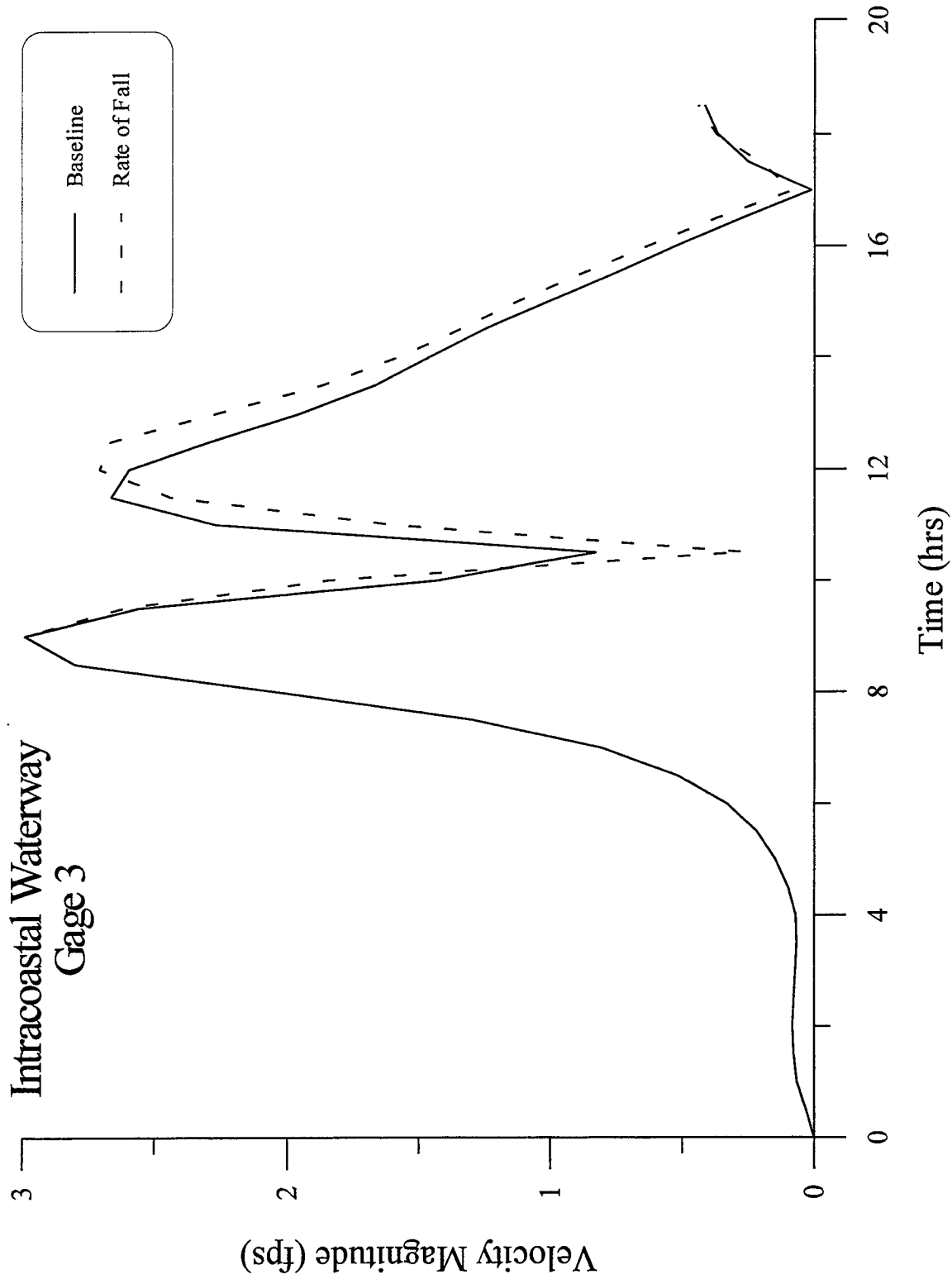


Figure 24. Velocity magnitude vs. time at Gage 3 – rate of fall variation – Intracoastal Waterway.

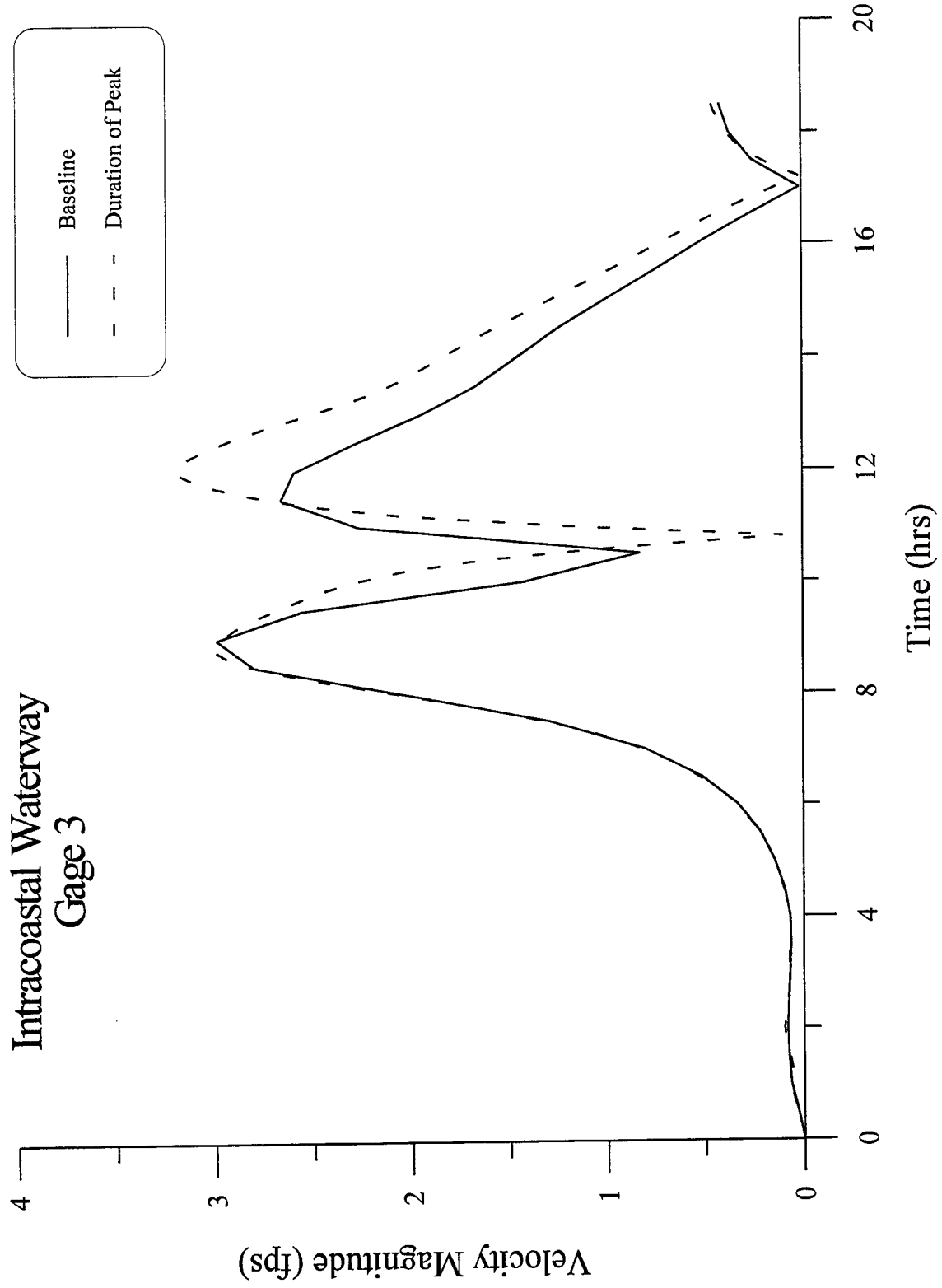


Figure 25. Velocity magnitude vs. time at Gage 3 – duration of peak variation – Intracoastal Waterway.

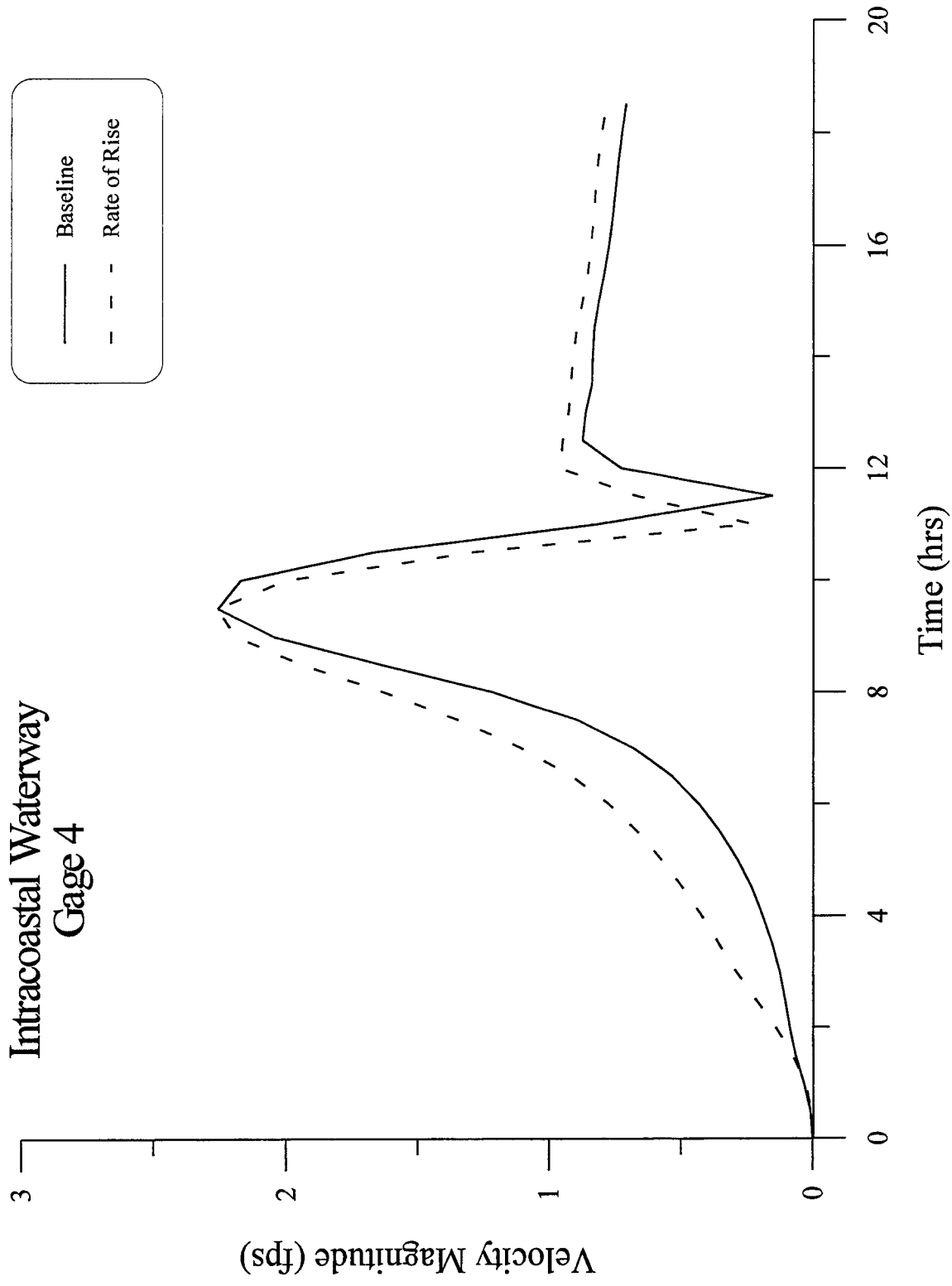


Figure 26. Velocity magnitude vs. time at Gage 4 – rate of rise variation – Intracoastal Waterway.

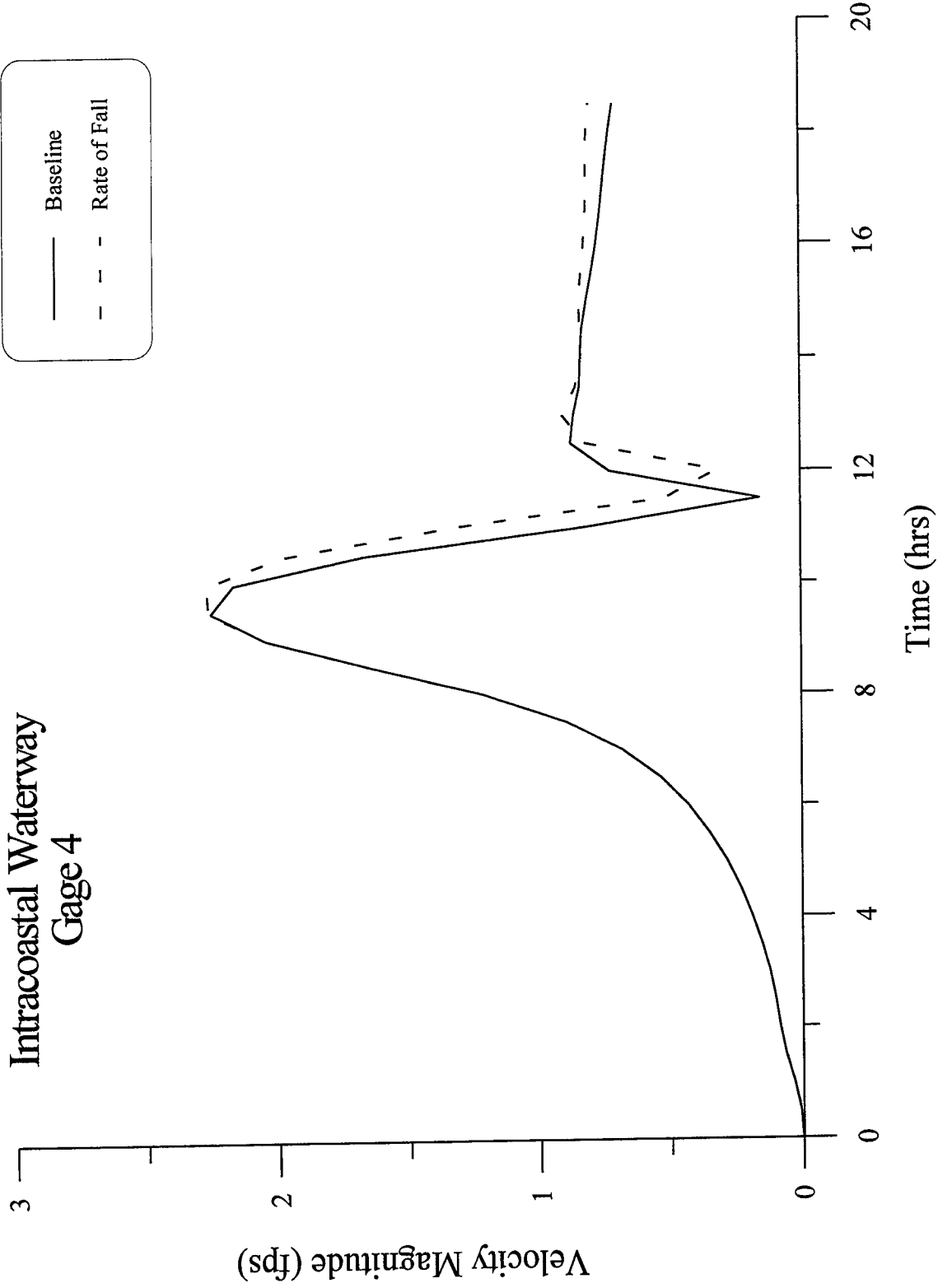


Figure 27. Velocity magnitude vs. time at Gage 4 – rate of fall variation – Intracoastal Waterway.

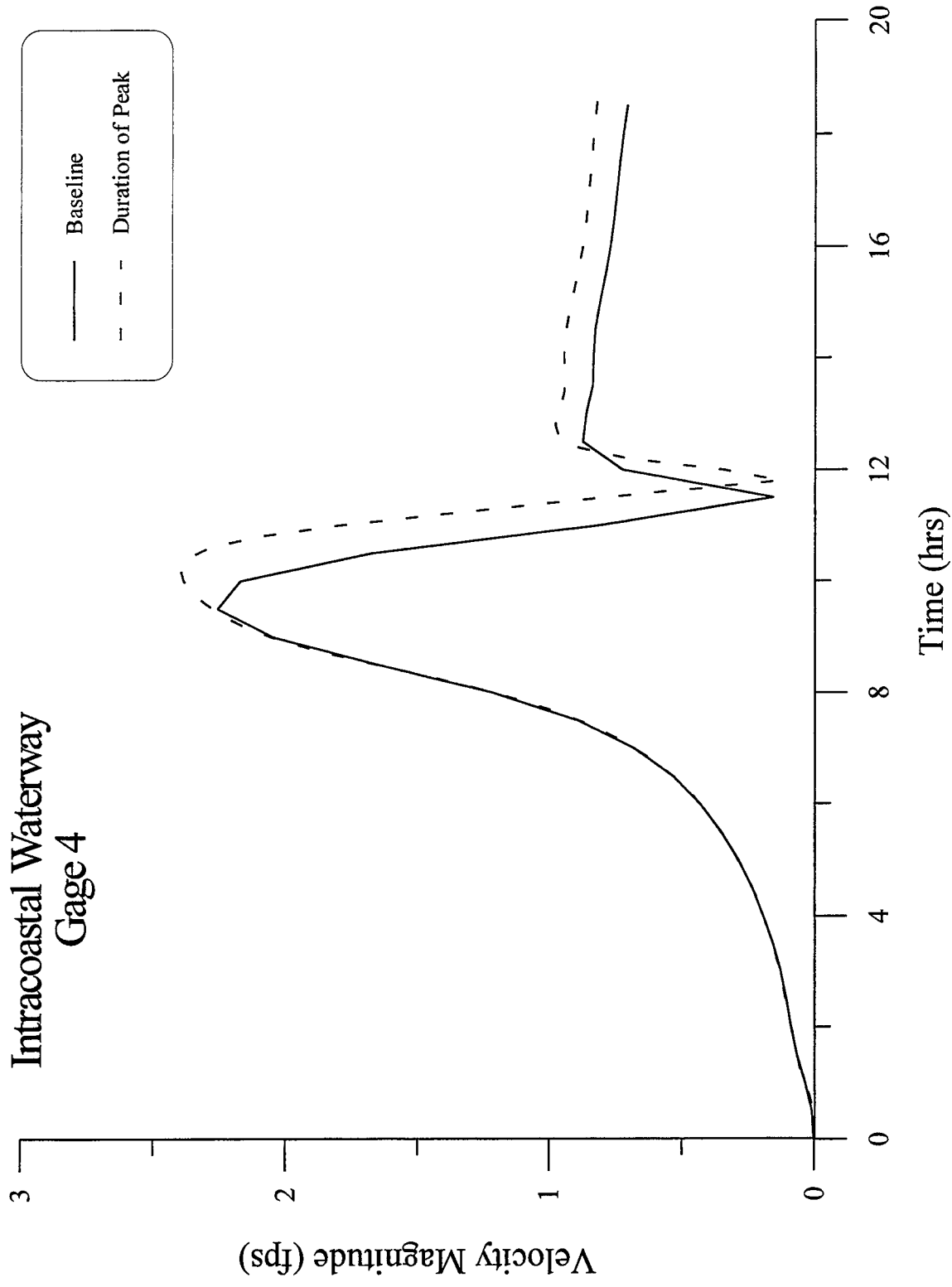


Figure 28. Velocity magnitude vs. time at Gage 4 – duration of peak variation – Intracoastal Waterway.

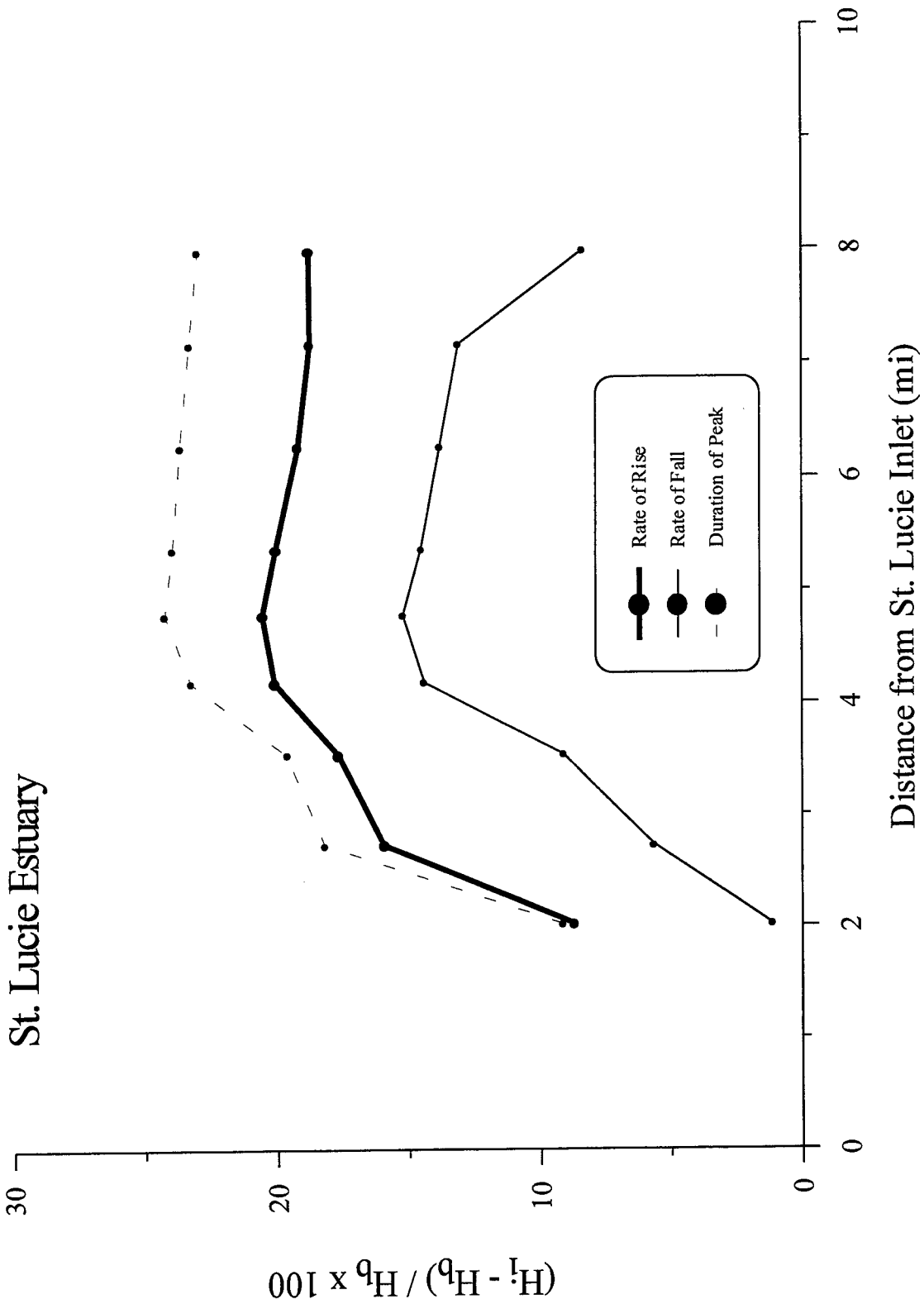


Figure 29. Maximum elevation comparisons – St. Lucie Estuary.

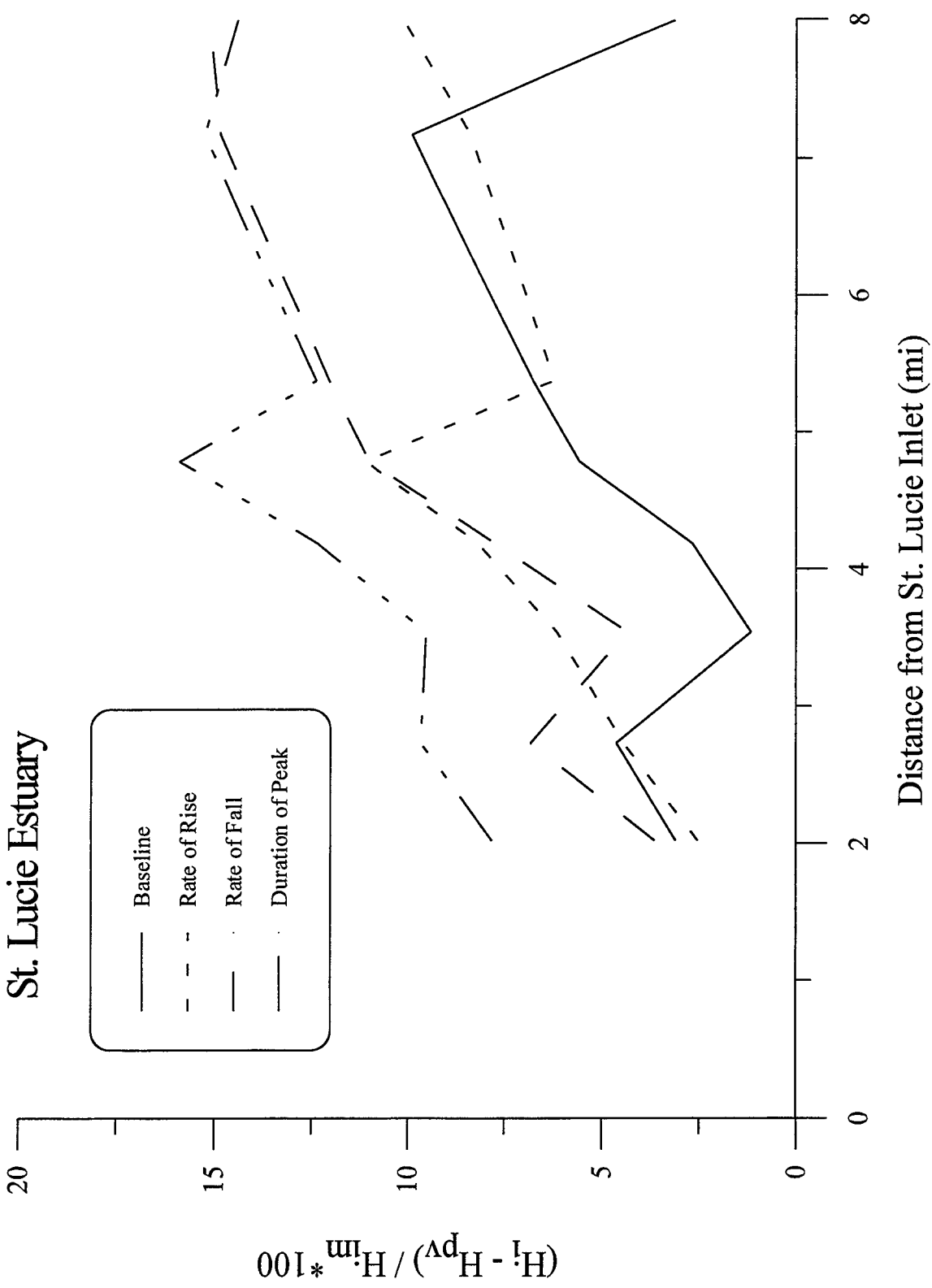


Figure 30. Maximum water elevation and elevation at maximum velocity magnitude comparisons – St. Lucie Estuary.

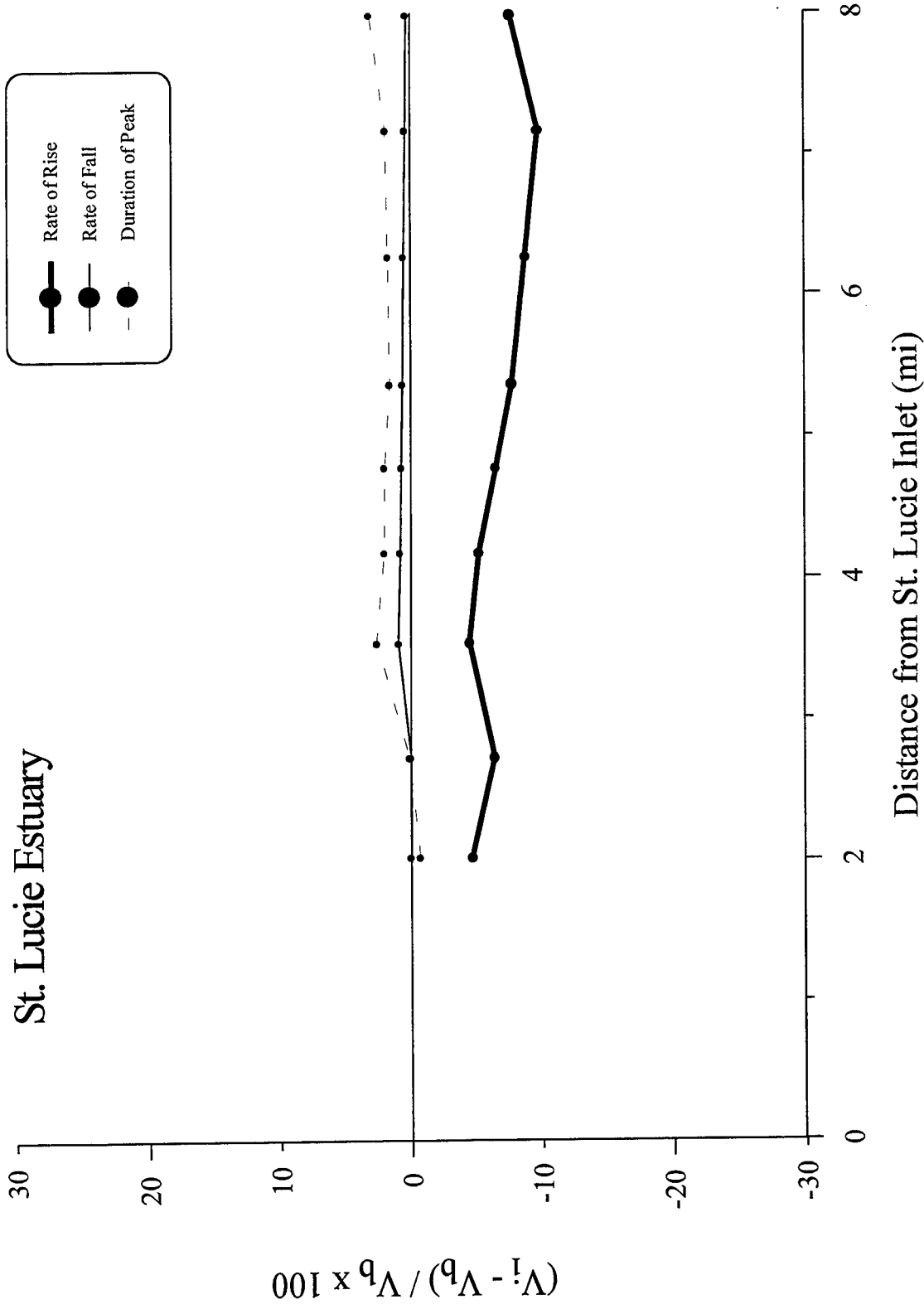


Figure 31. Maximum velocity magnitude comparisons – St. Lucie Estuary.

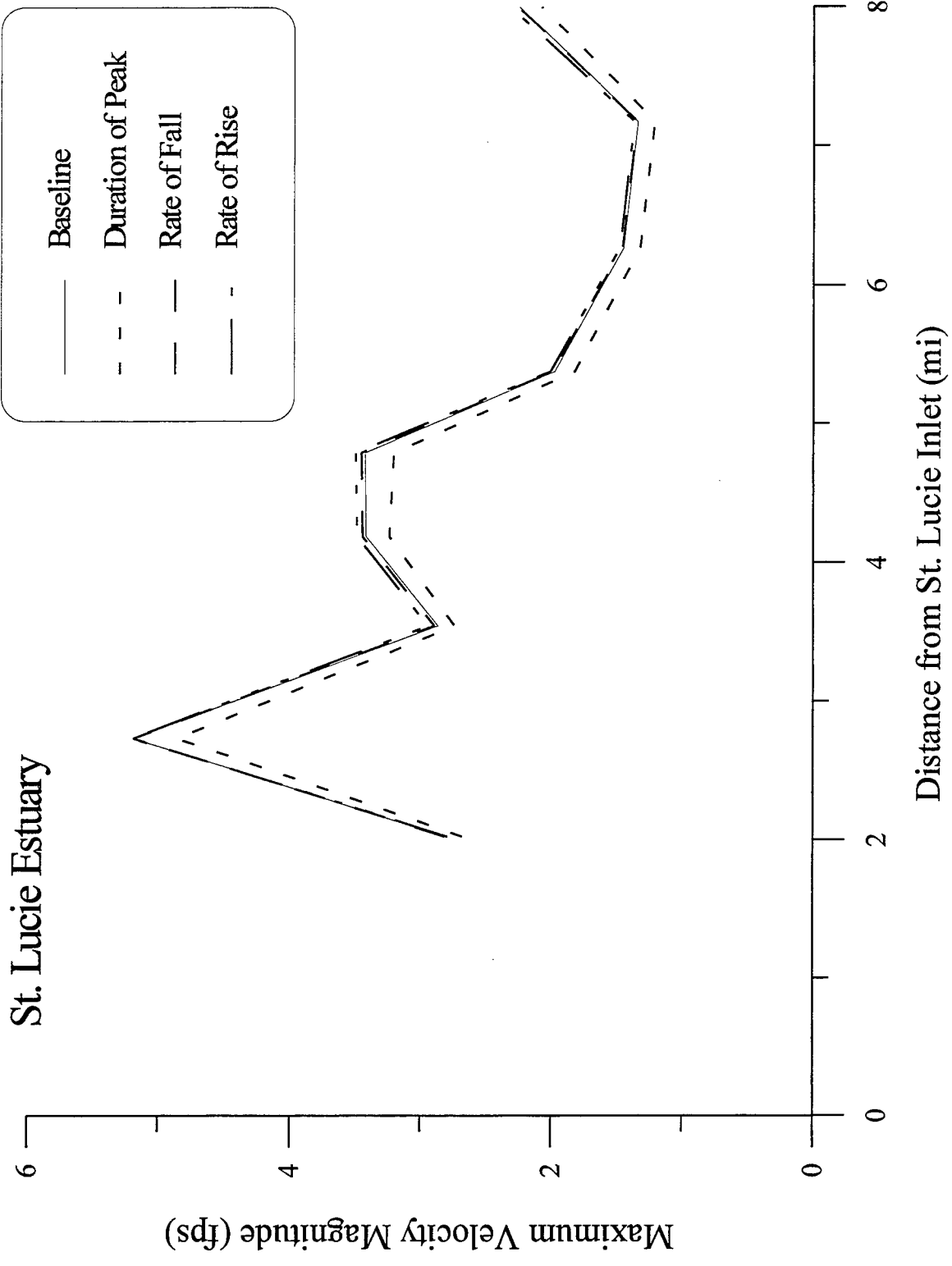


Figure 32. Maximum velocity magnitude vs. distance – St. Lucie Estuary.

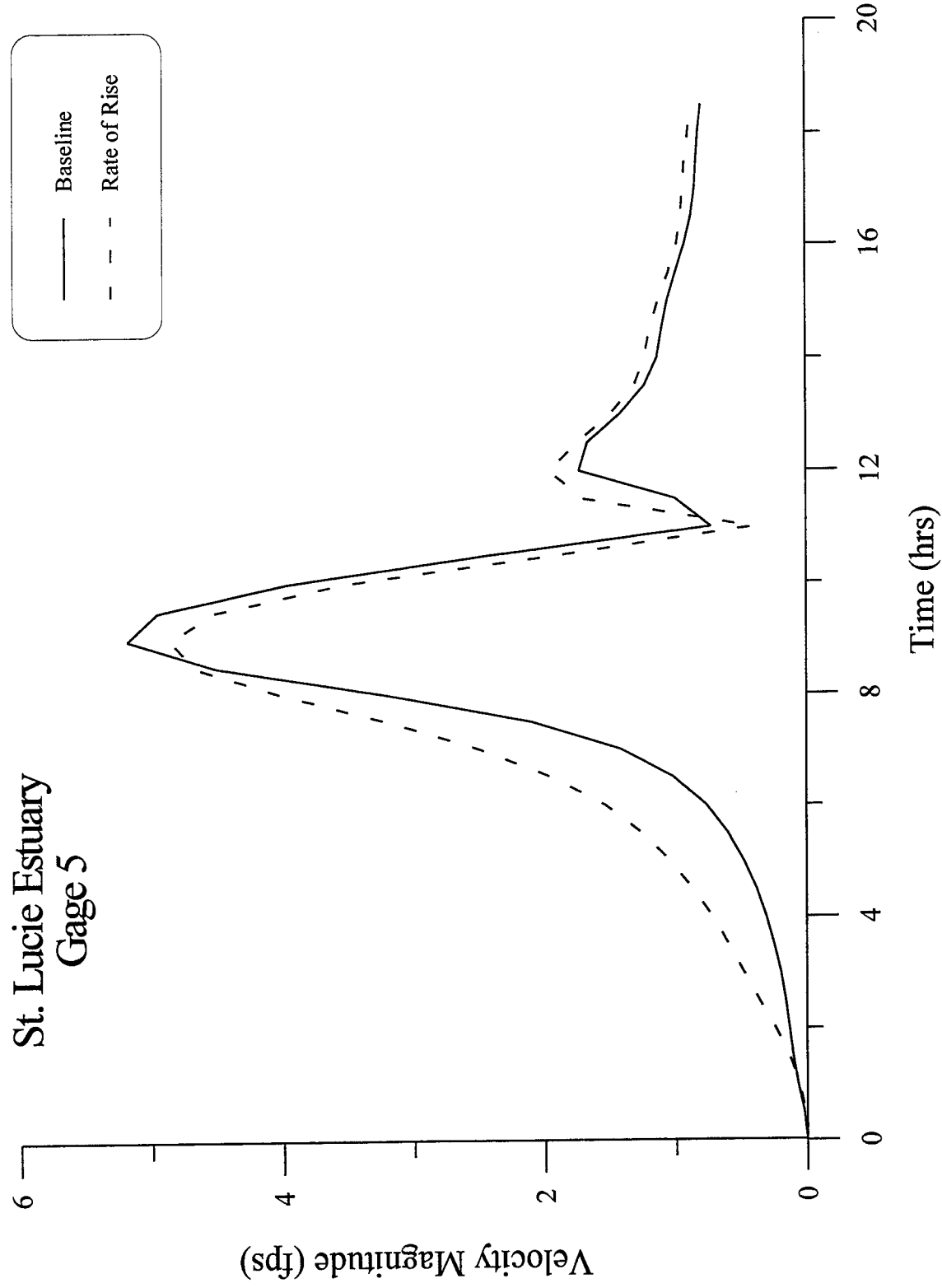


Figure 33. Velocity magnitude vs. time at Gage 5 -- rate of rise variation -- St. Lucie Estuary.

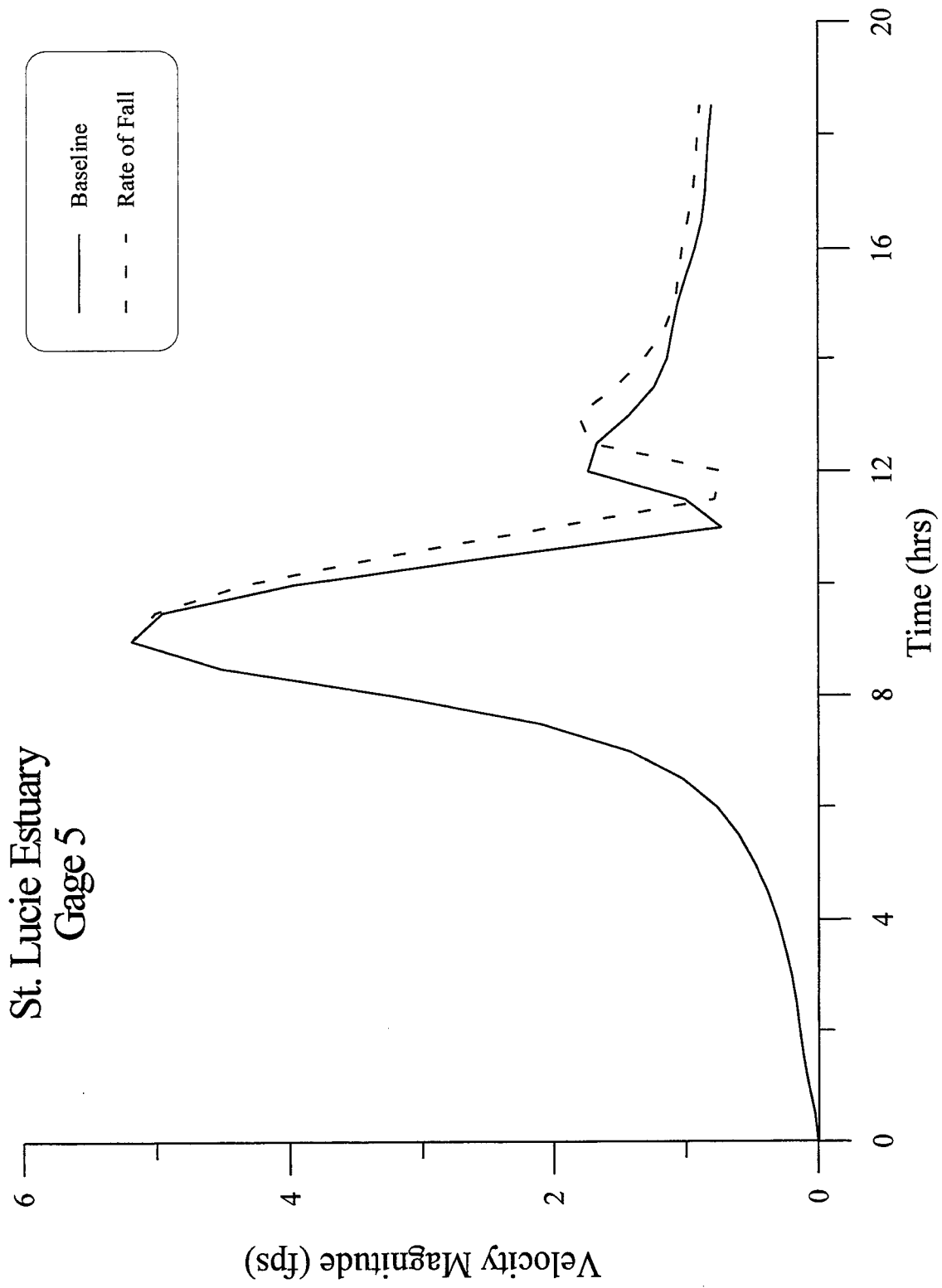


Figure 34. Velocity magnitude vs. time at Gage 5 – rate of fall variation – St. Lucie Estuary.

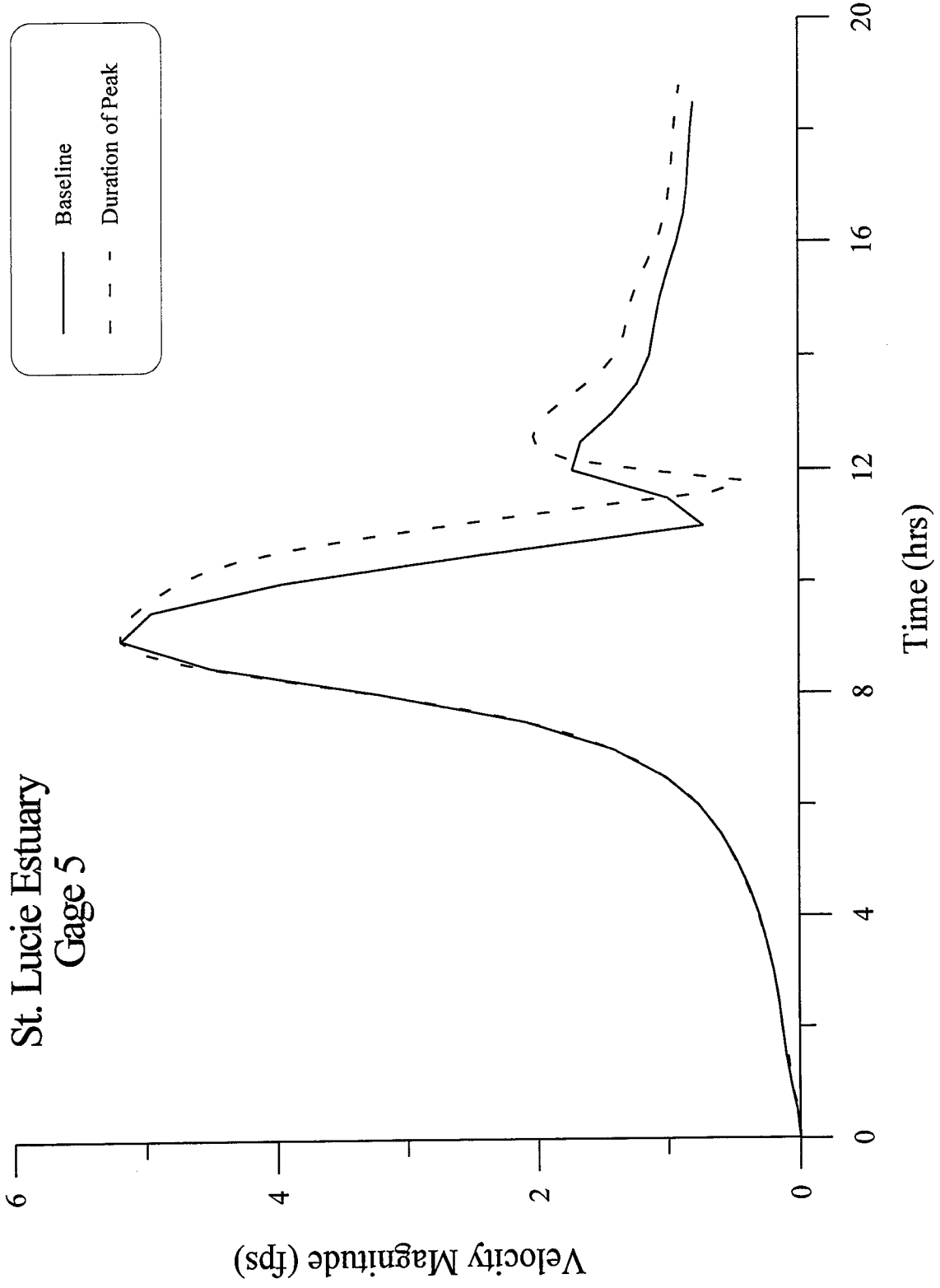


Figure 35. Velocity magnitude vs. time at Gage 5 – duration of peak variation – St. Lucie Estuary.

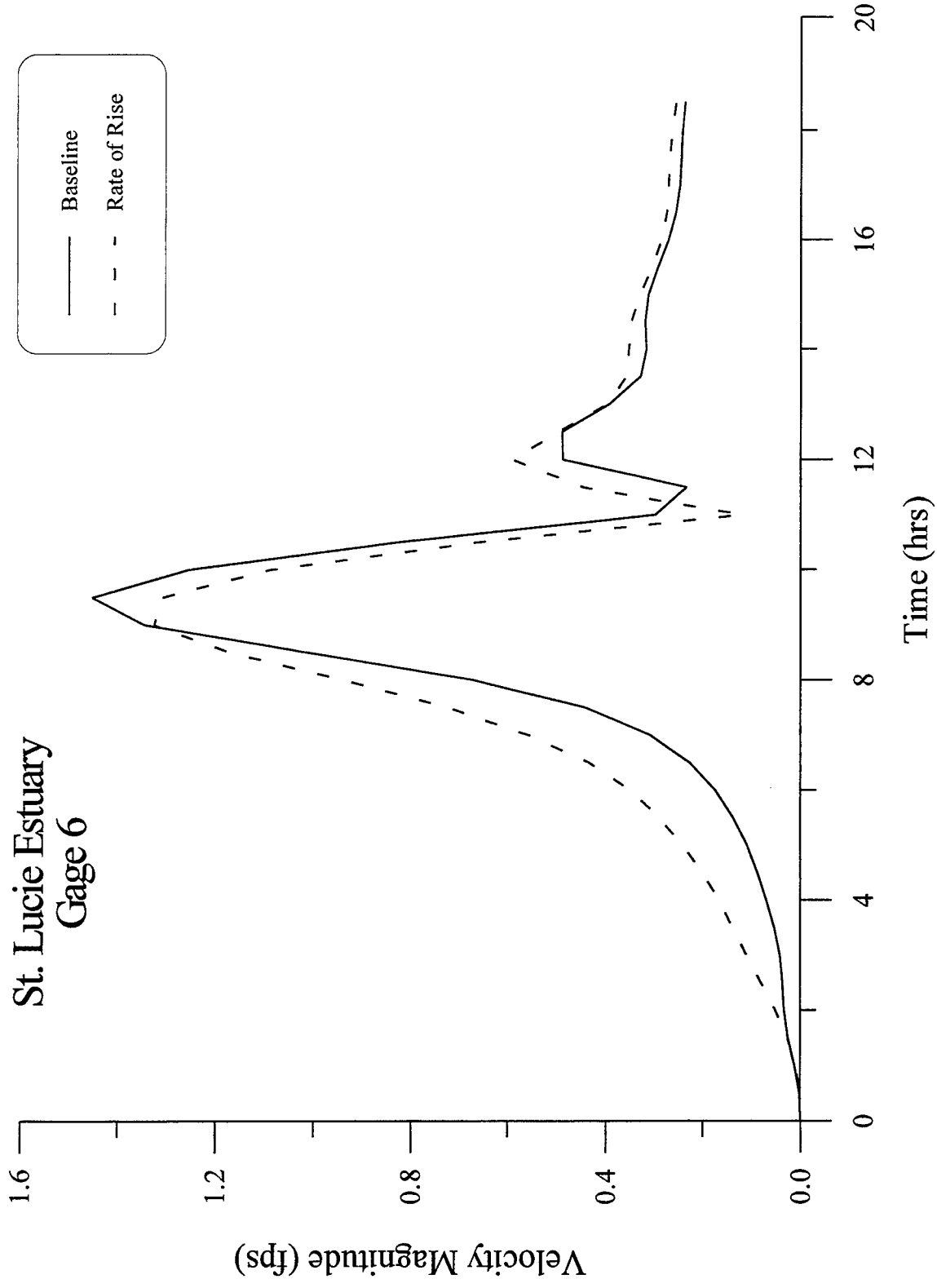


Figure 36. Velocity magnitude vs. time at Gage 6 – rate of rise variation – St. Lucie Estuary.

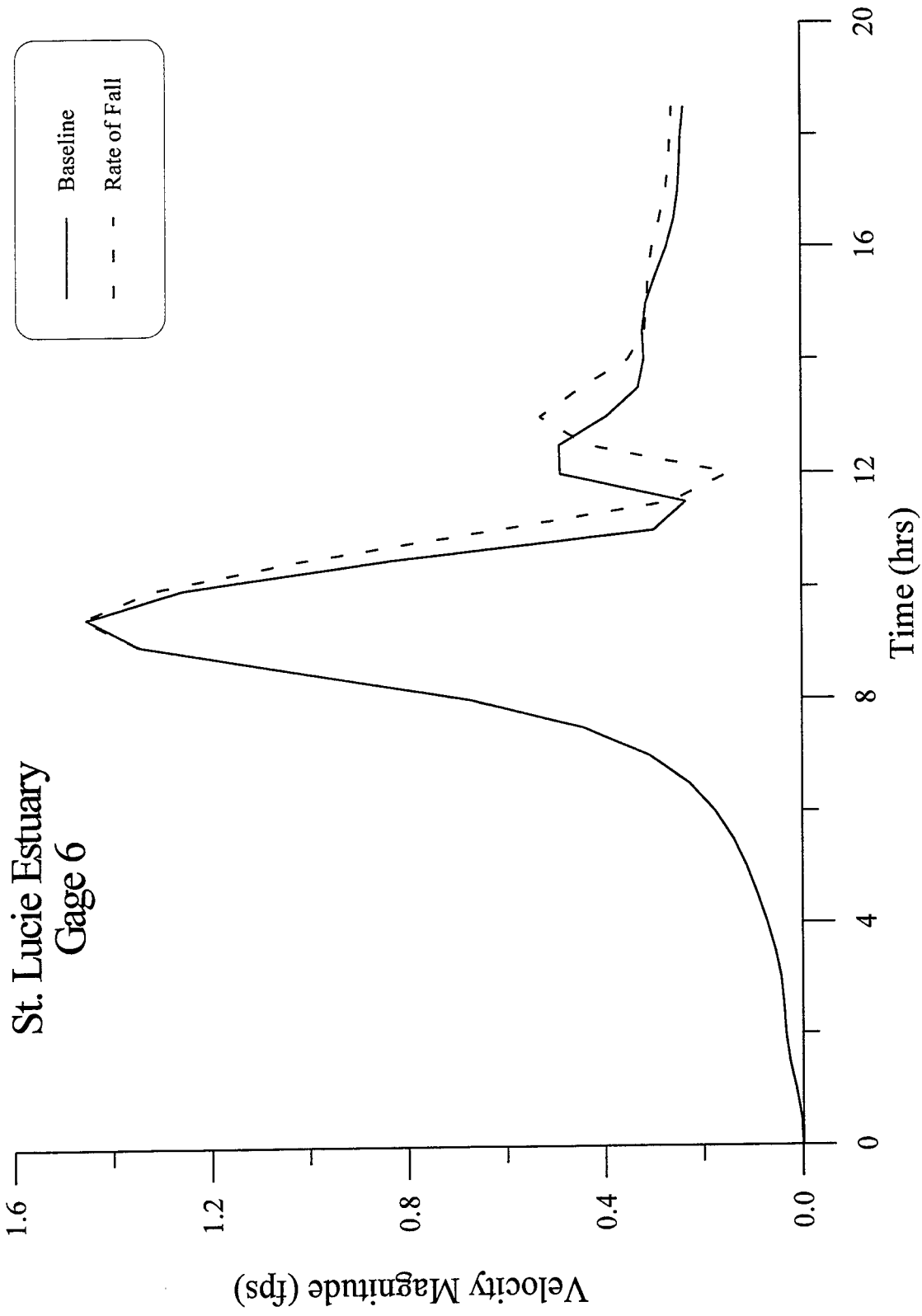


Figure 37. Velocity magnitude vs. time at Gage 6 – rate of fall variation – St. Lucie Estuary.

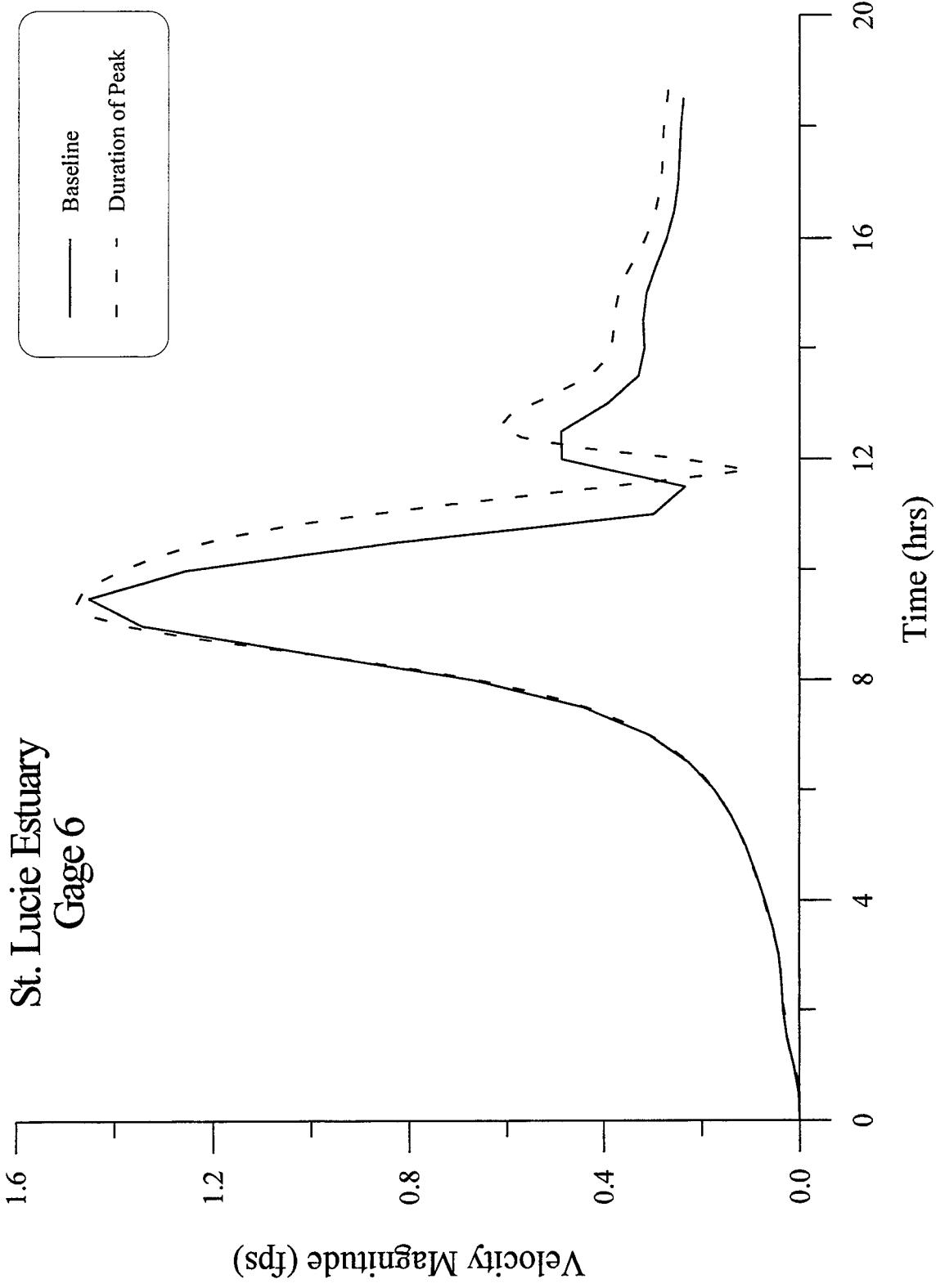


Figure 38. Velocity magnitude vs. time at Gage 6 – duration of peak variation – St. Lucie Estuary.

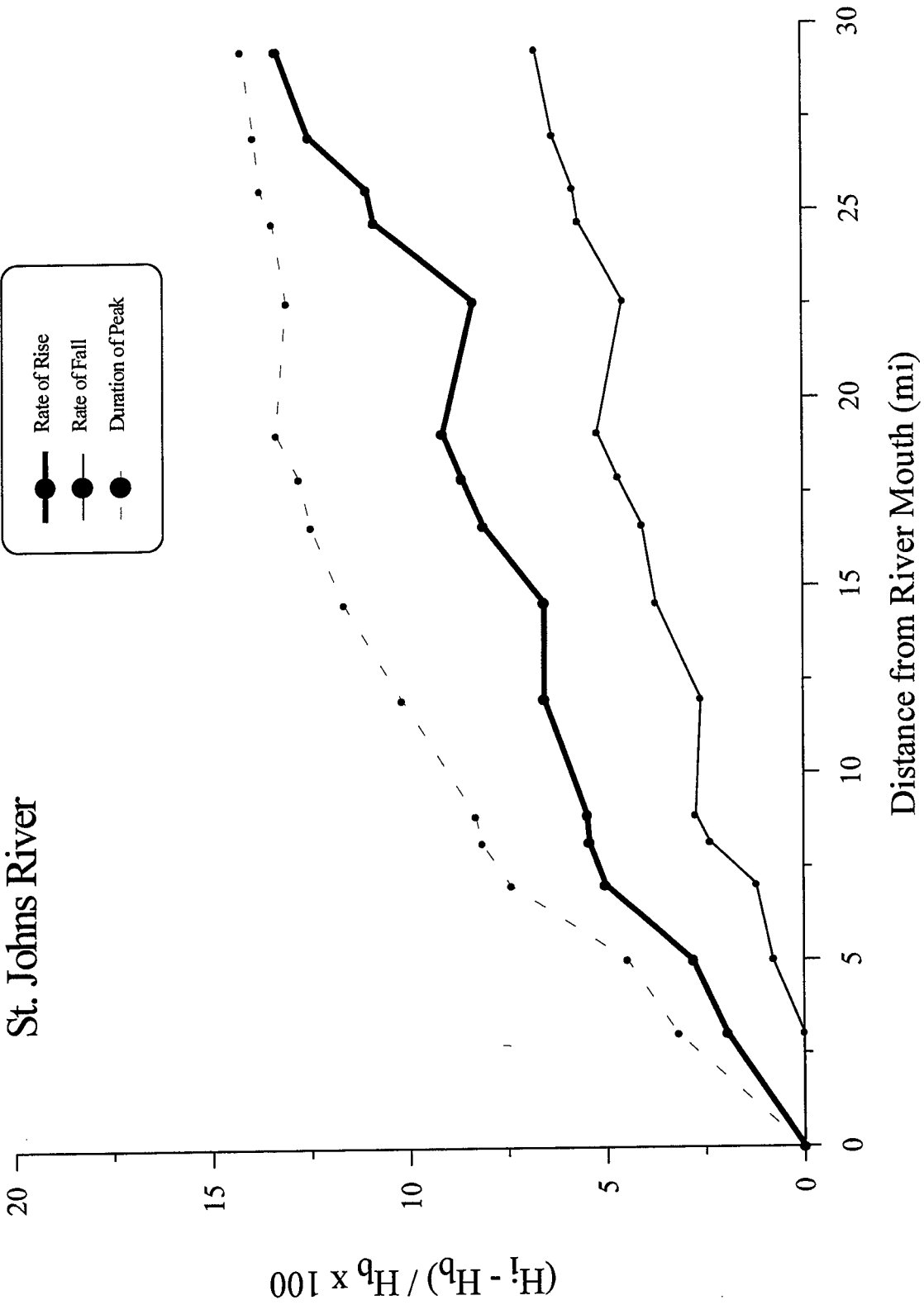


Figure 39. Maximum elevation comparisons – St. Johns River.

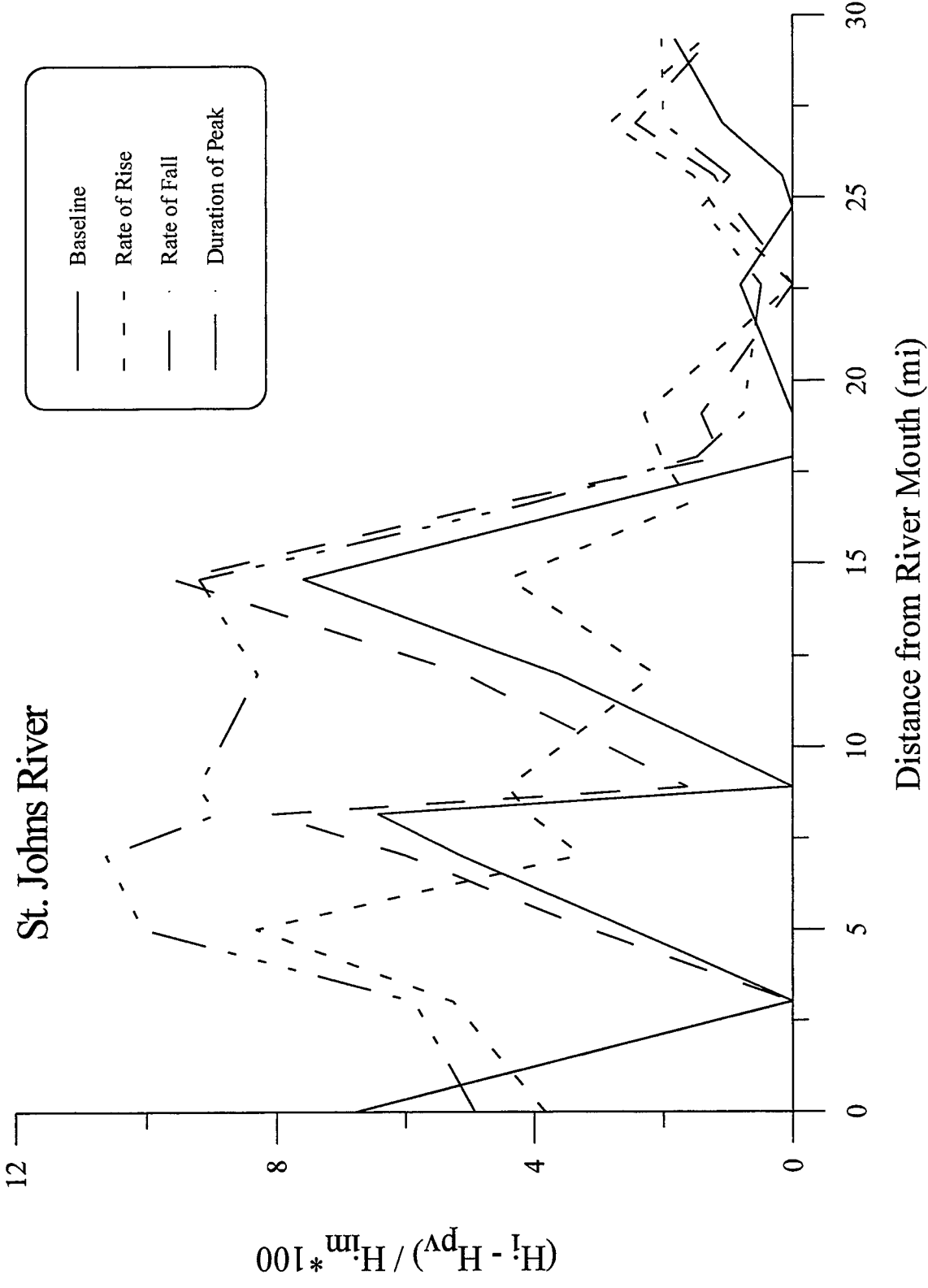


Figure 40. Maximum water elevation and elevation at maximum velocity magnitude comparisons – St. Johns River.

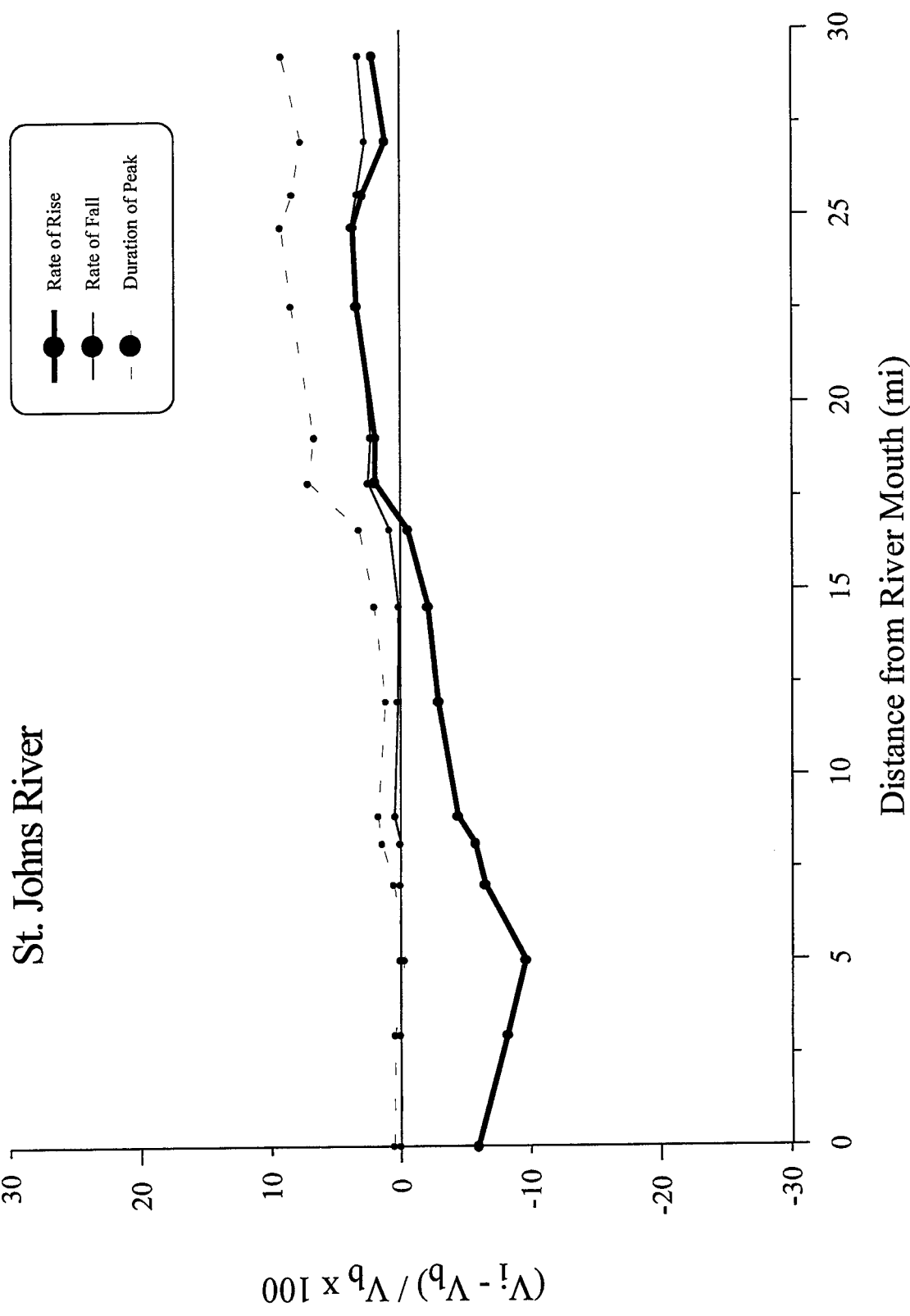


Figure 41. Maximum velocity magnitude comparisons – St. Johns River.

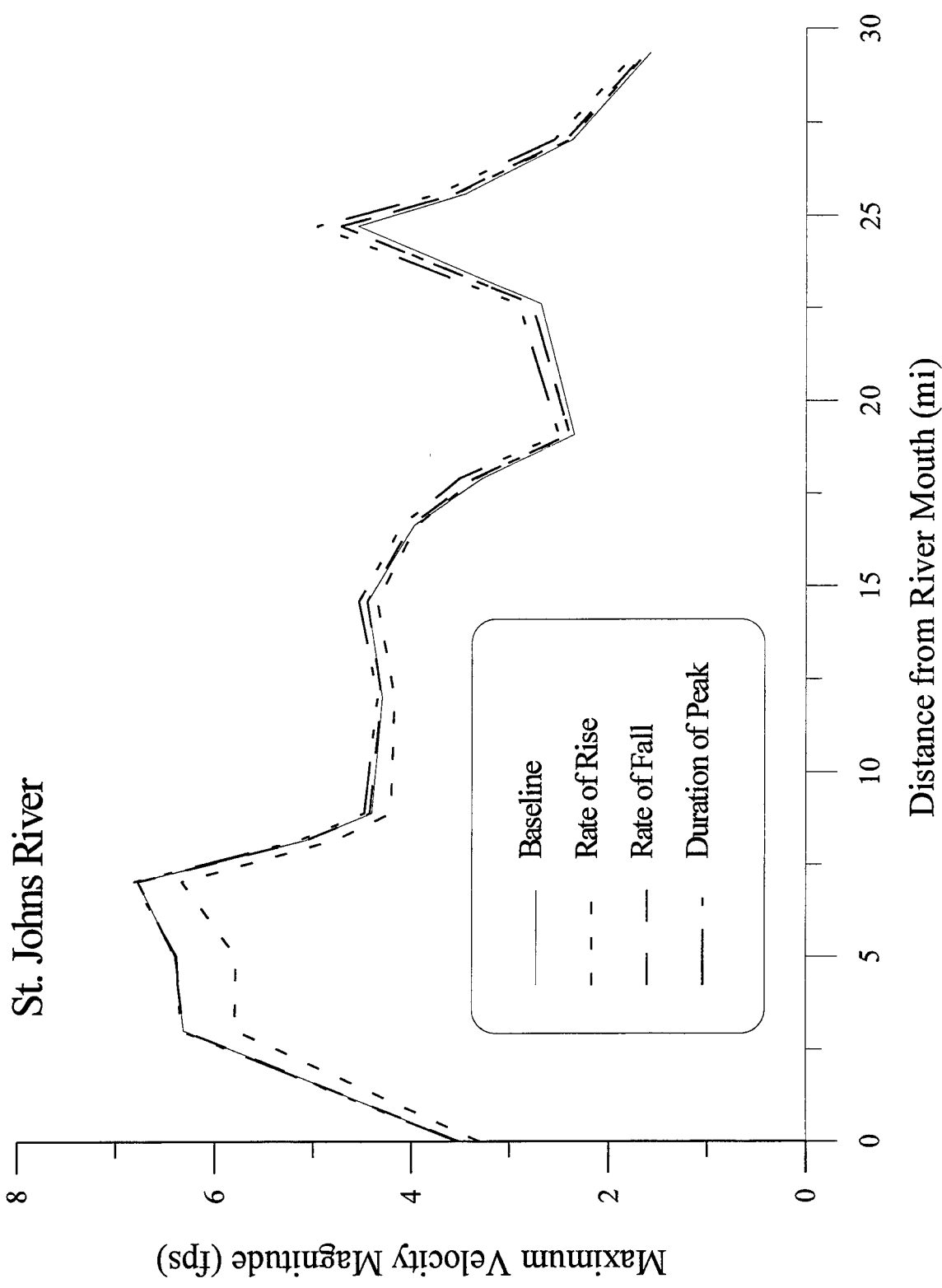


Figure 42. Maximum velocity magnitude vs. distance – St. Johns River.

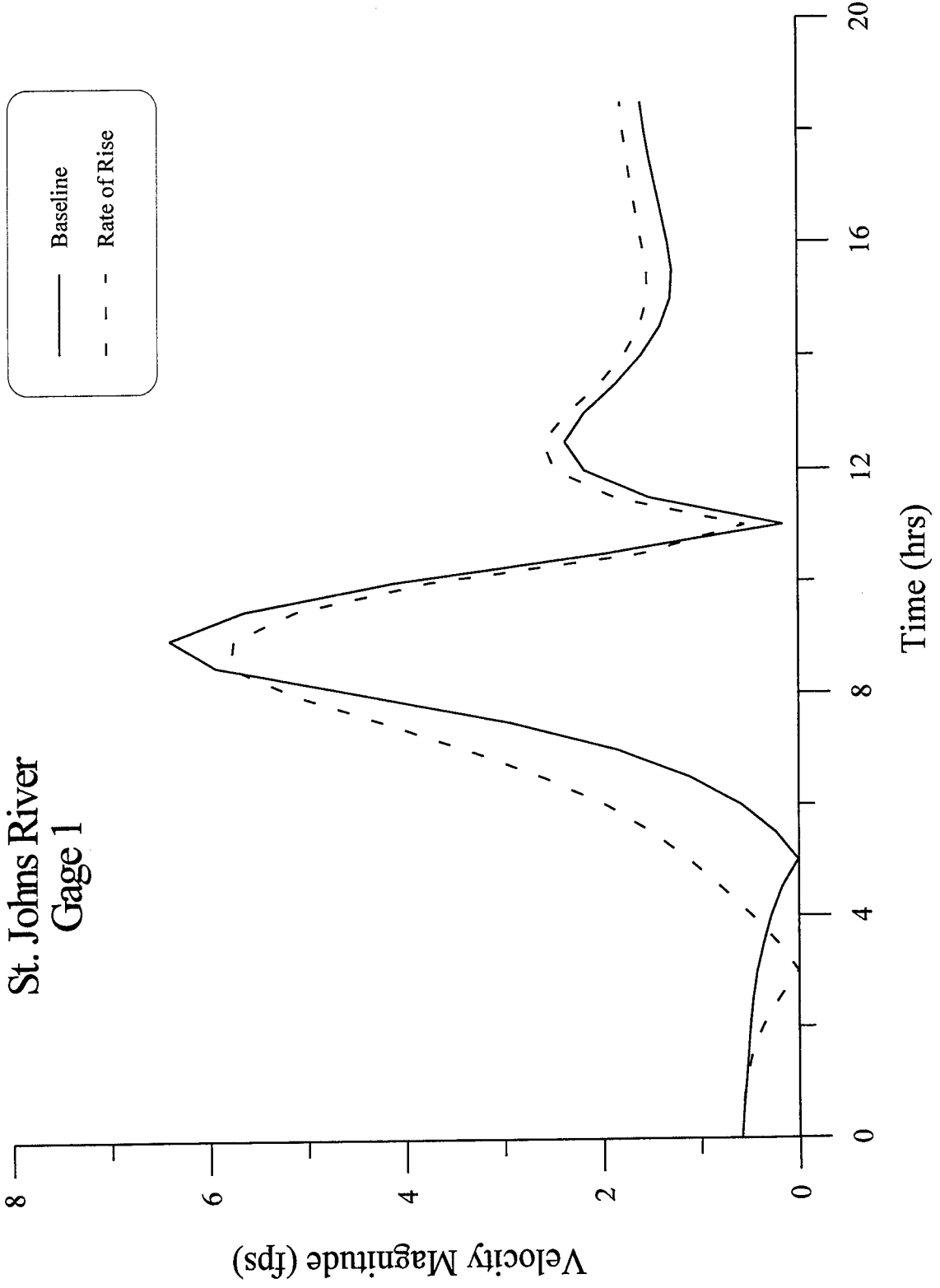


Figure 43. Velocity magnitude vs. time at Gage 1 -- rate of rise variation -- St. Johns River.

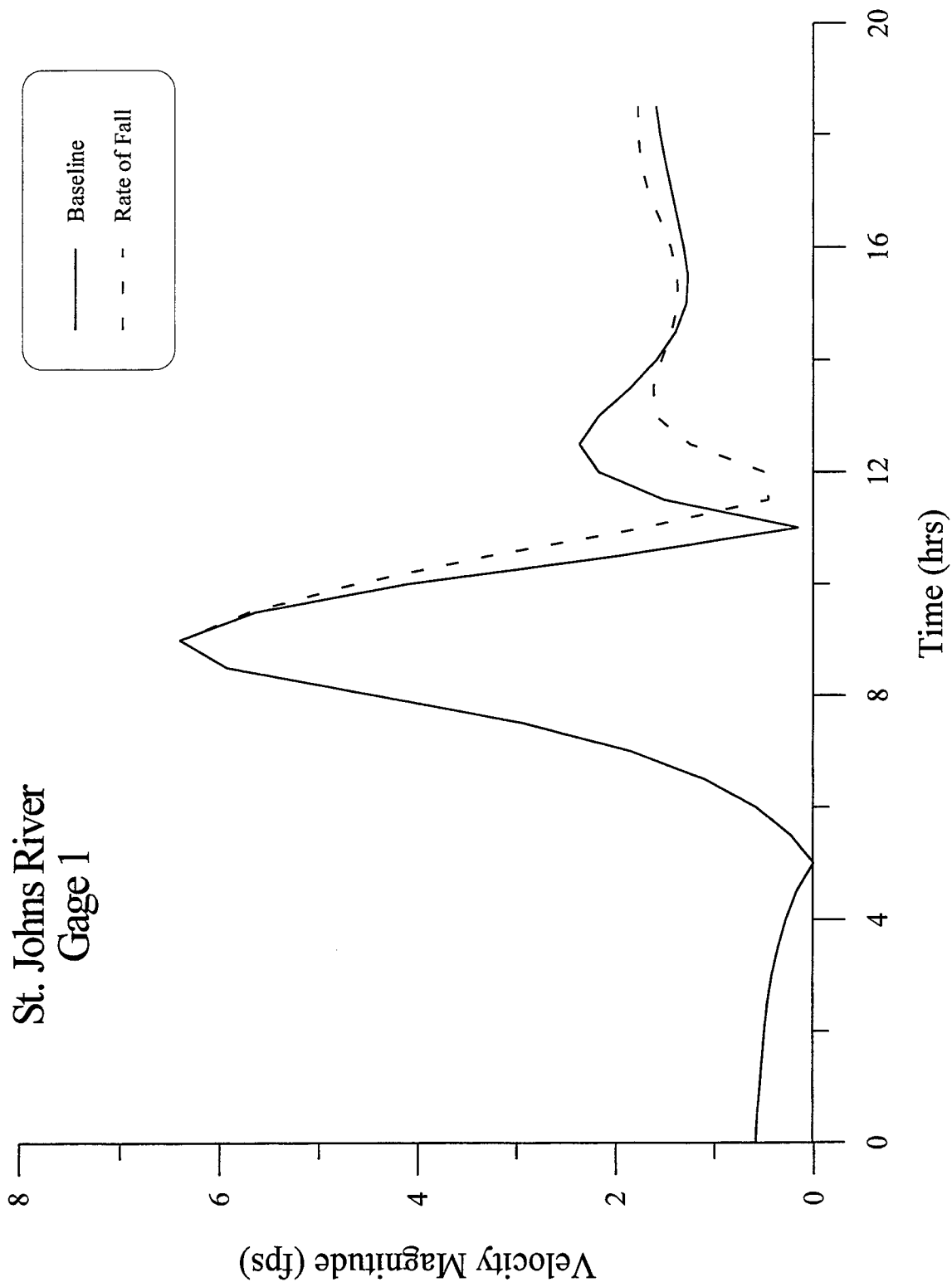


Figure 44. Velocity magnitude vs. time at Gage 1 – rate of fall variation – St. Johns River.

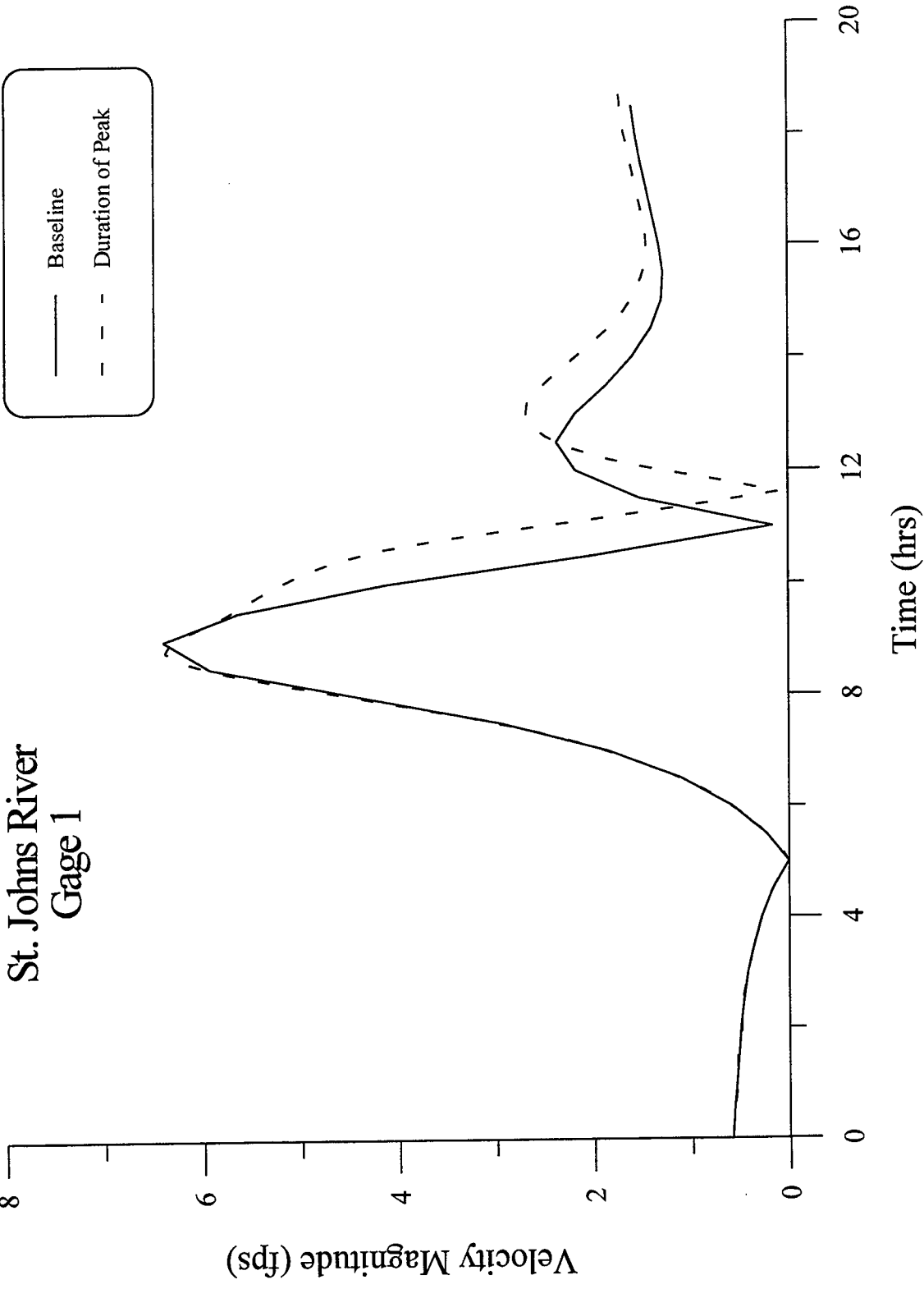


Figure 45. Velocity magnitude vs. time at Gage 1 – duration of peak variation – St. Johns River.

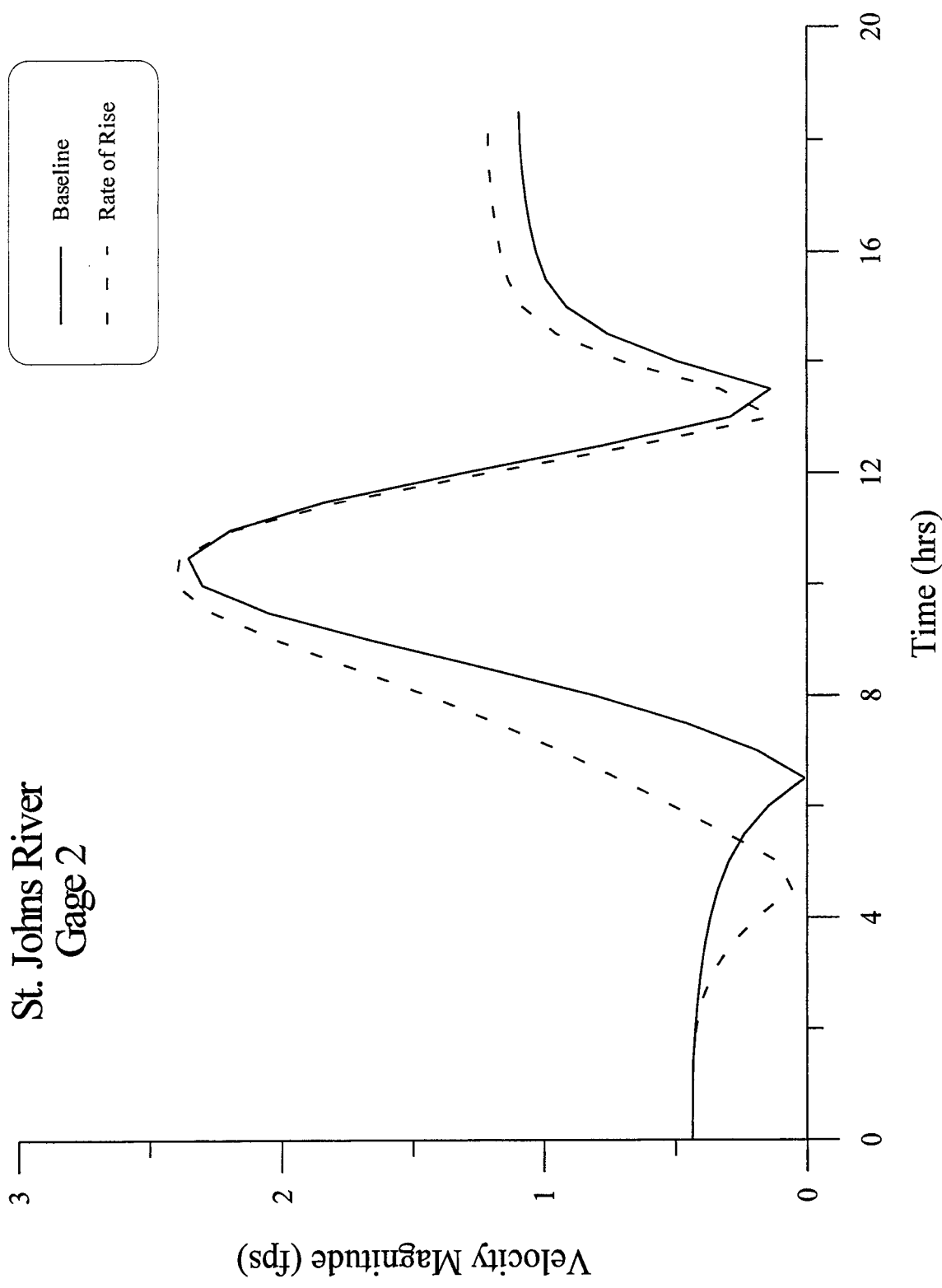


Figure 46. Velocity magnitude vs. time at Gage 2 – rate of rise variation – St. Johns River.

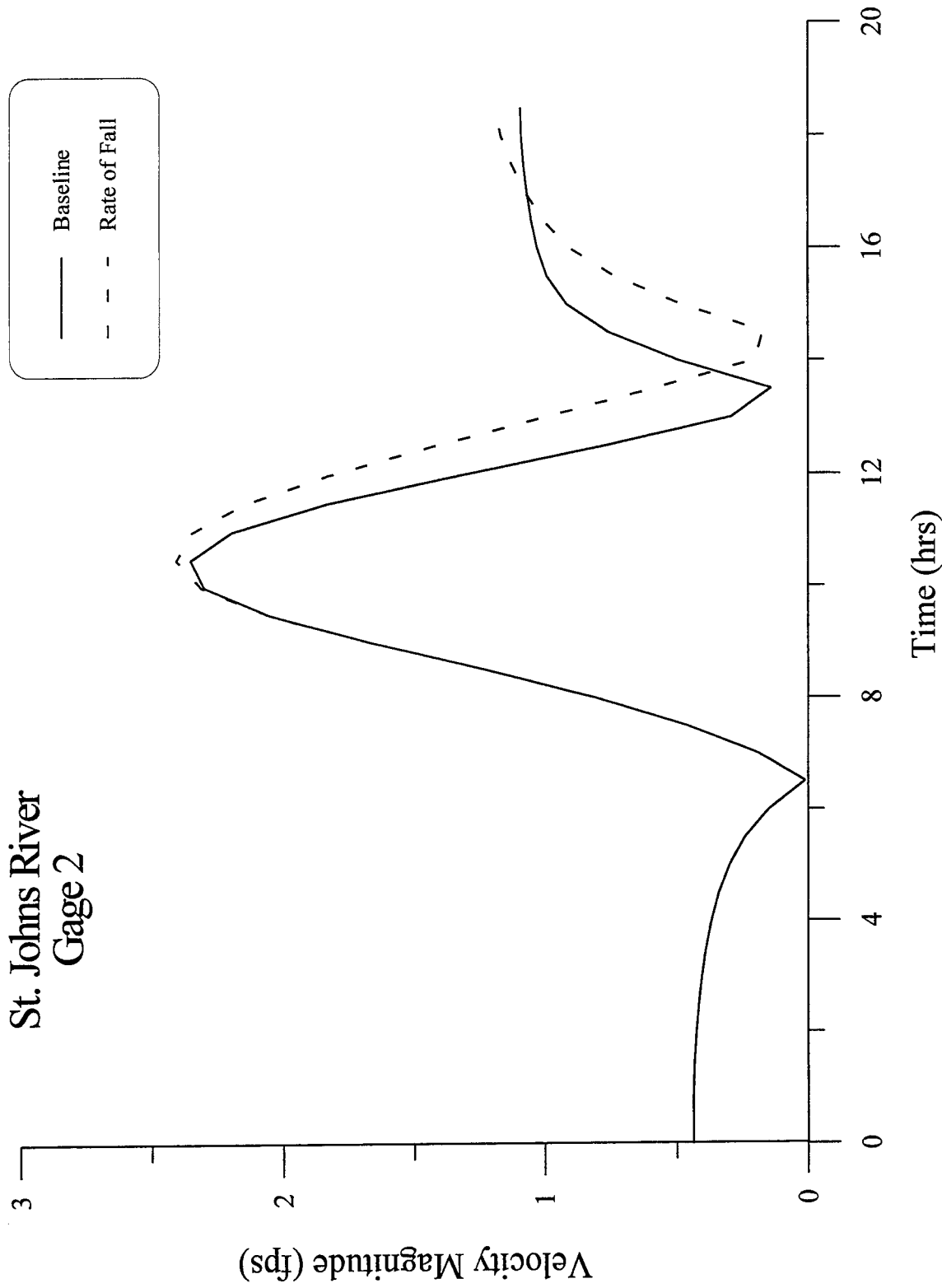


Figure 47. Velocity magnitude vs. time at Gage 2 – rate of fall variation – St. Johns River.

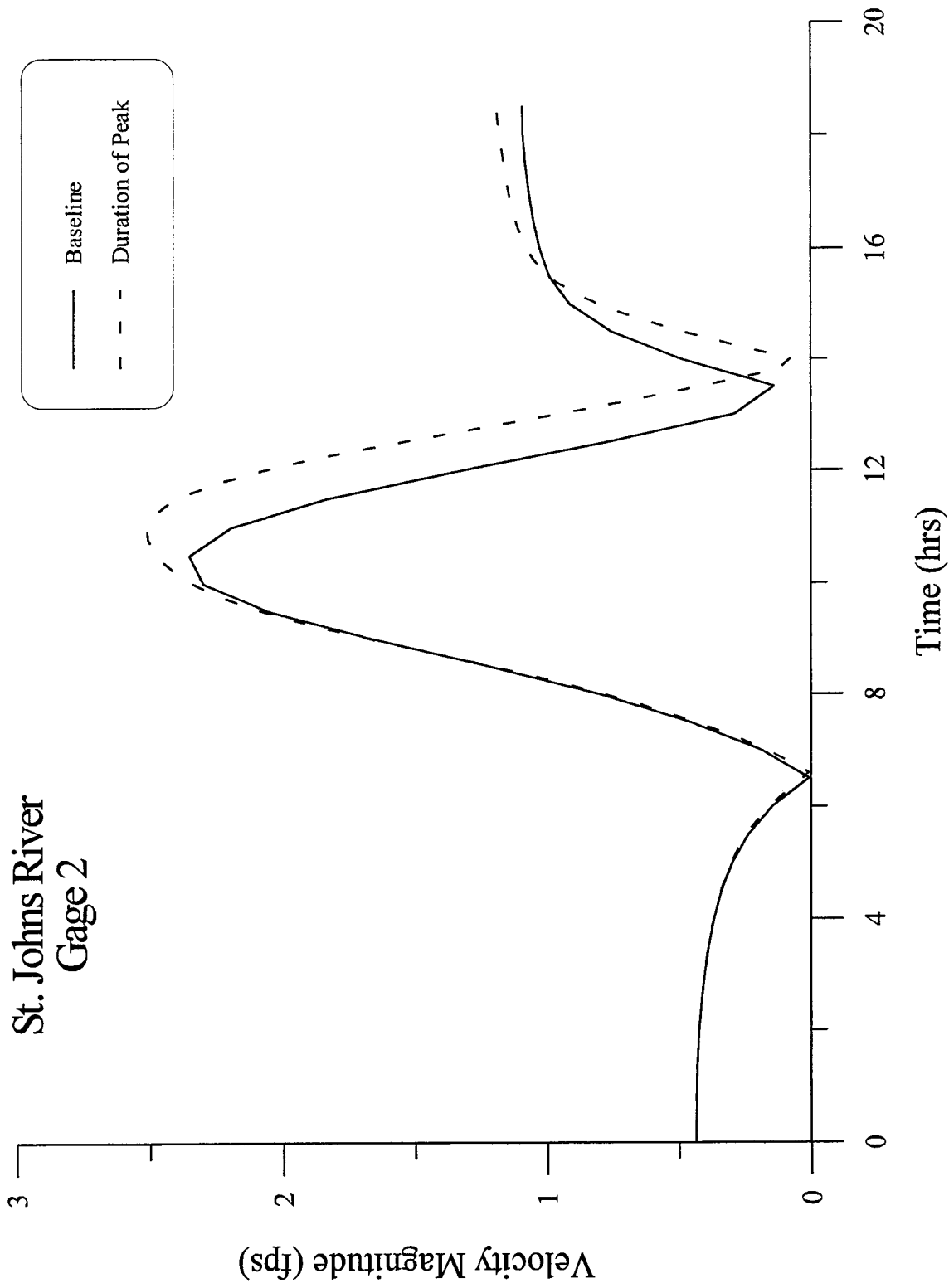


Figure 48. Velocity magnitude vs. time at Gage 2 – duration of peak variation – St. Johns River.

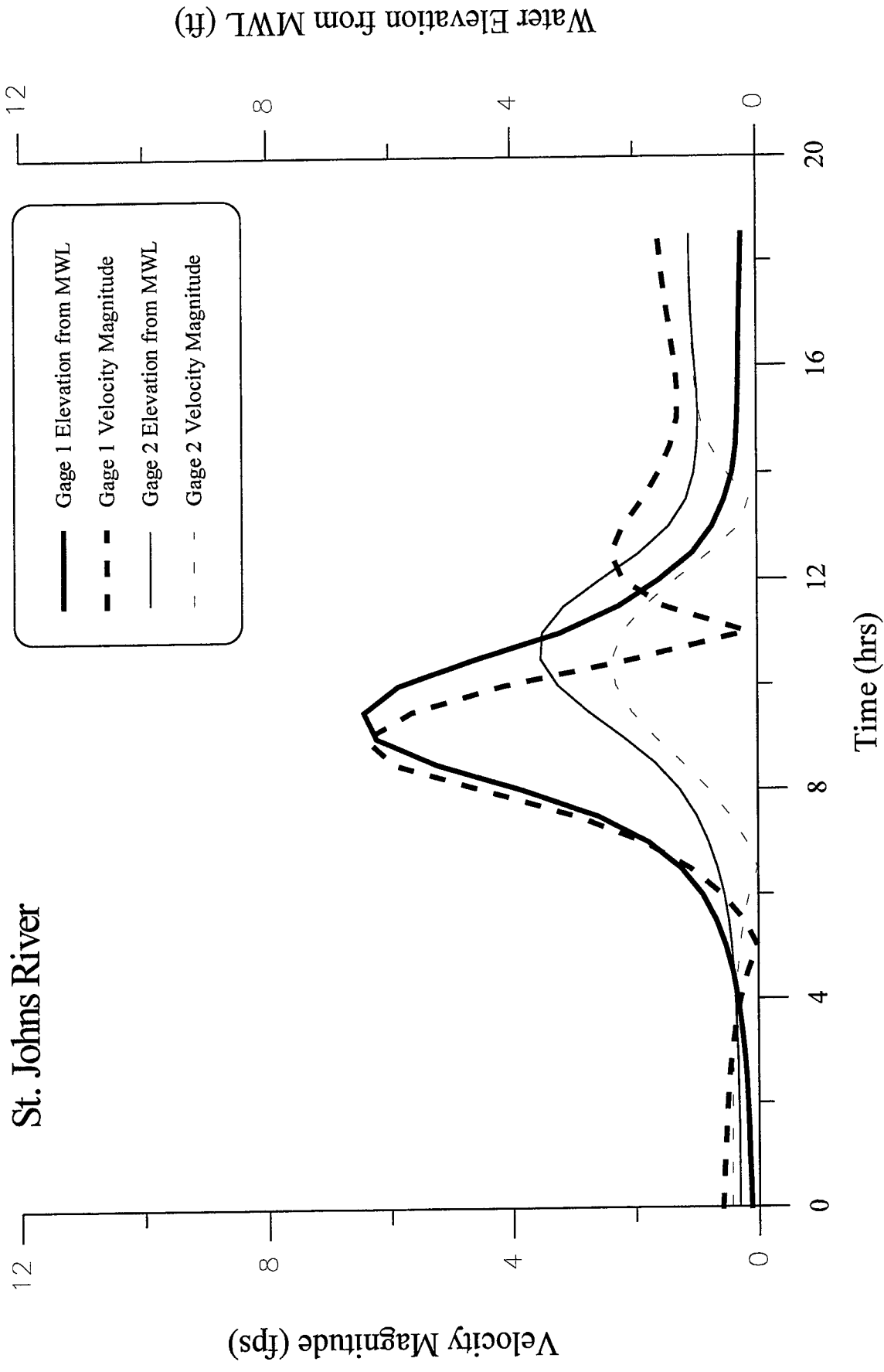


Figure 49. Velocity magnitude and baseline elevation vs. time – St. Johns River.

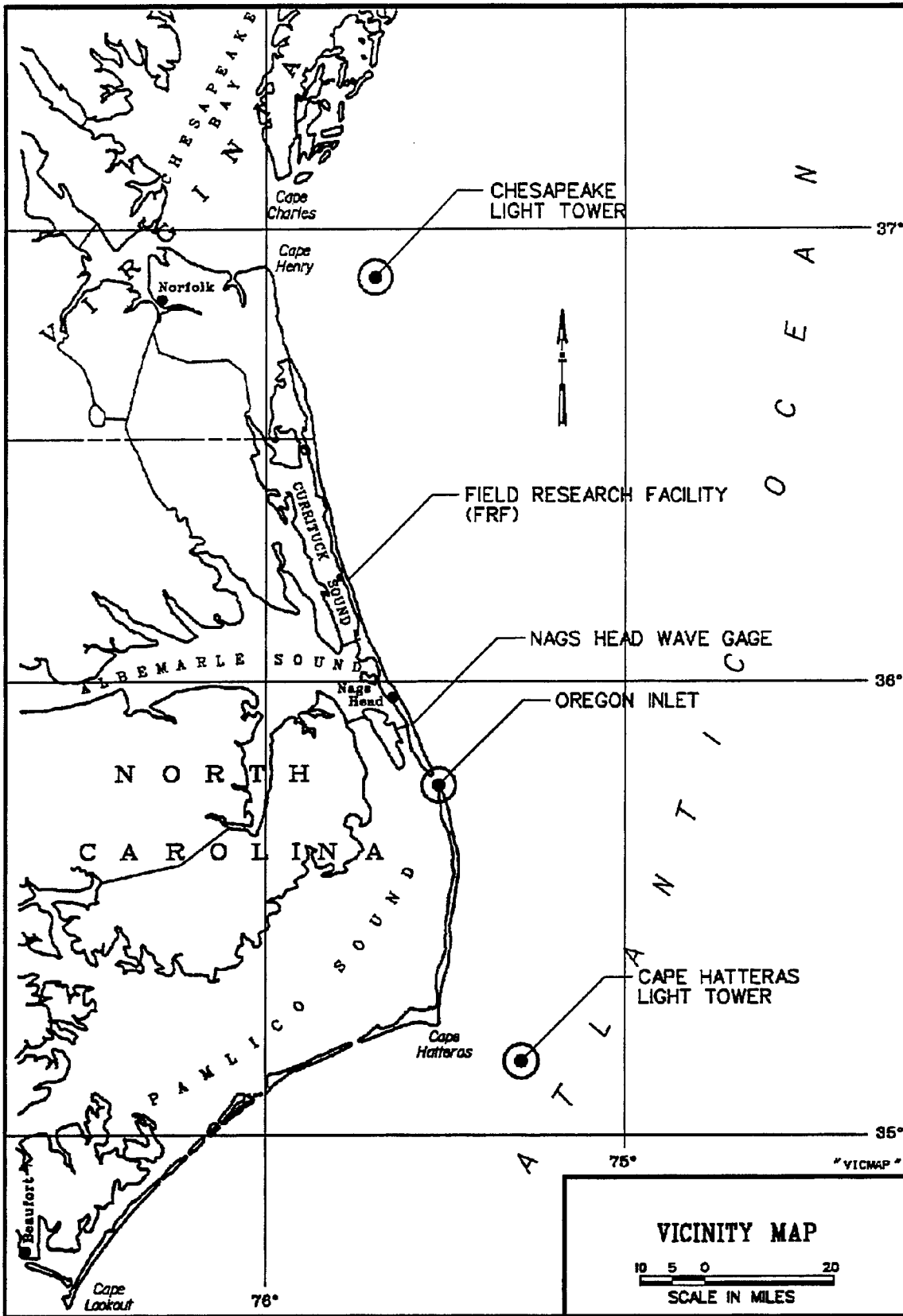


Figure 50. Vicinity map for Oregon Inlet.

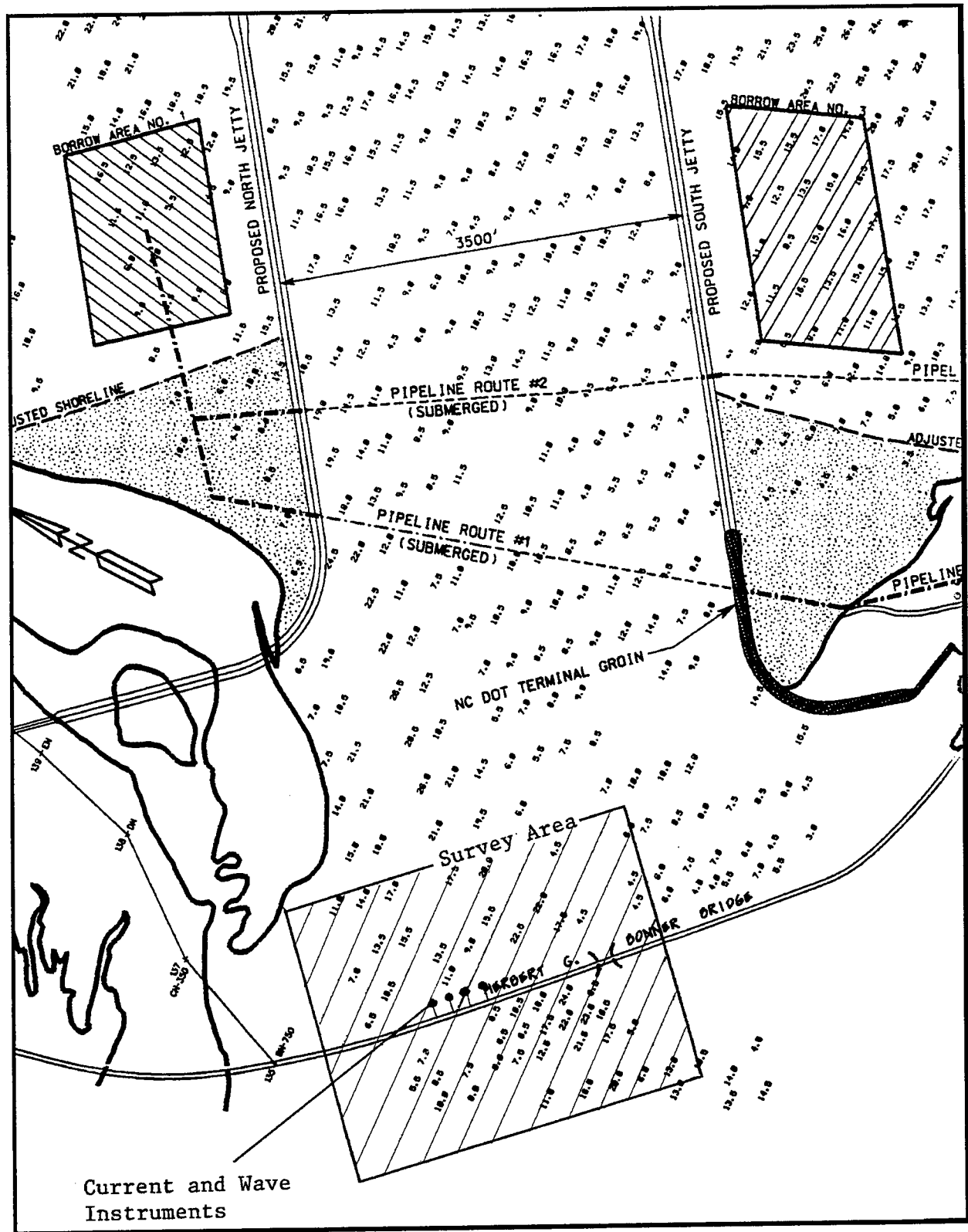


Figure 51. Drawing of Herbert C. Bonner Bridge over Oregon Inlet.

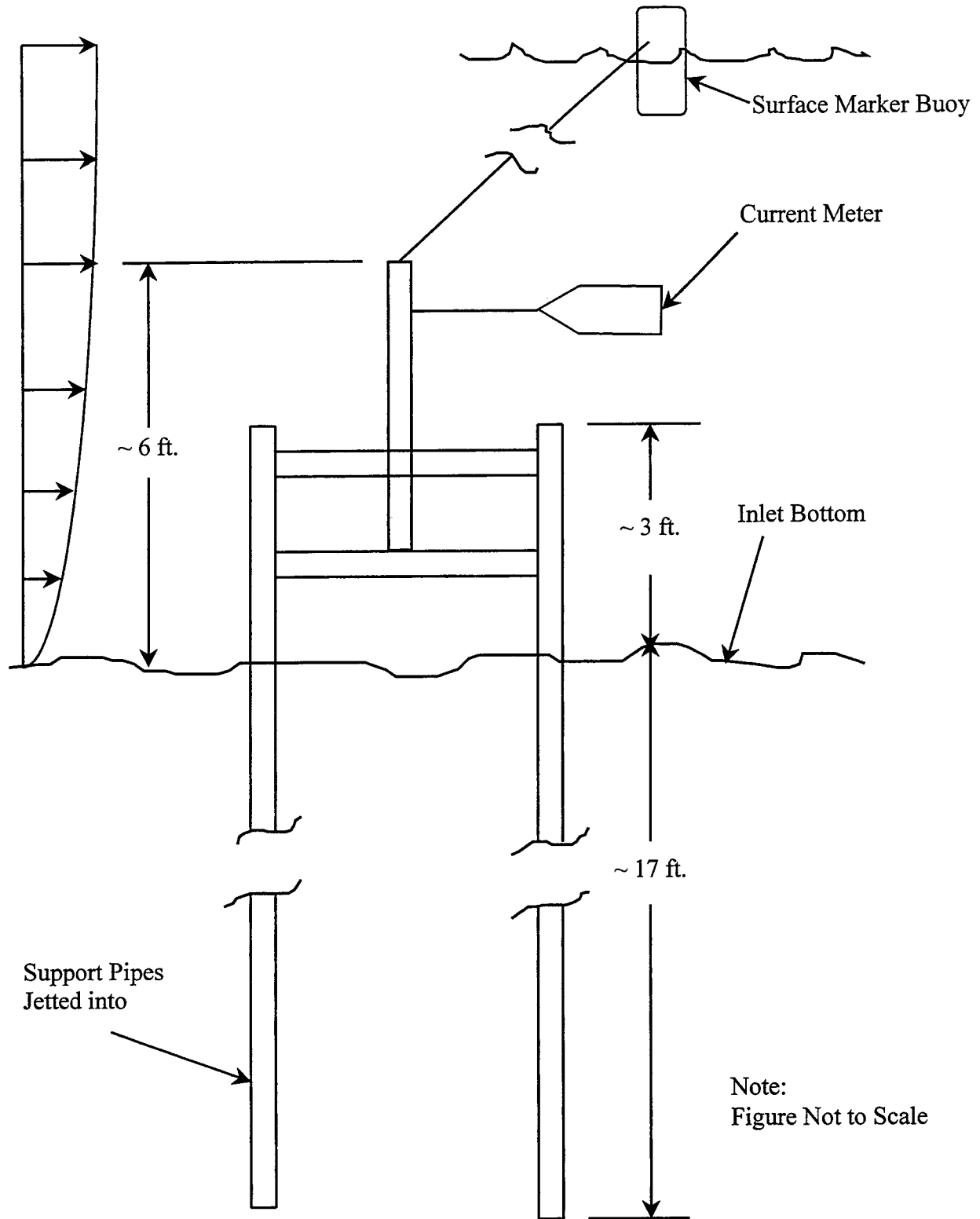


Figure 52. Tethered current meter installation.

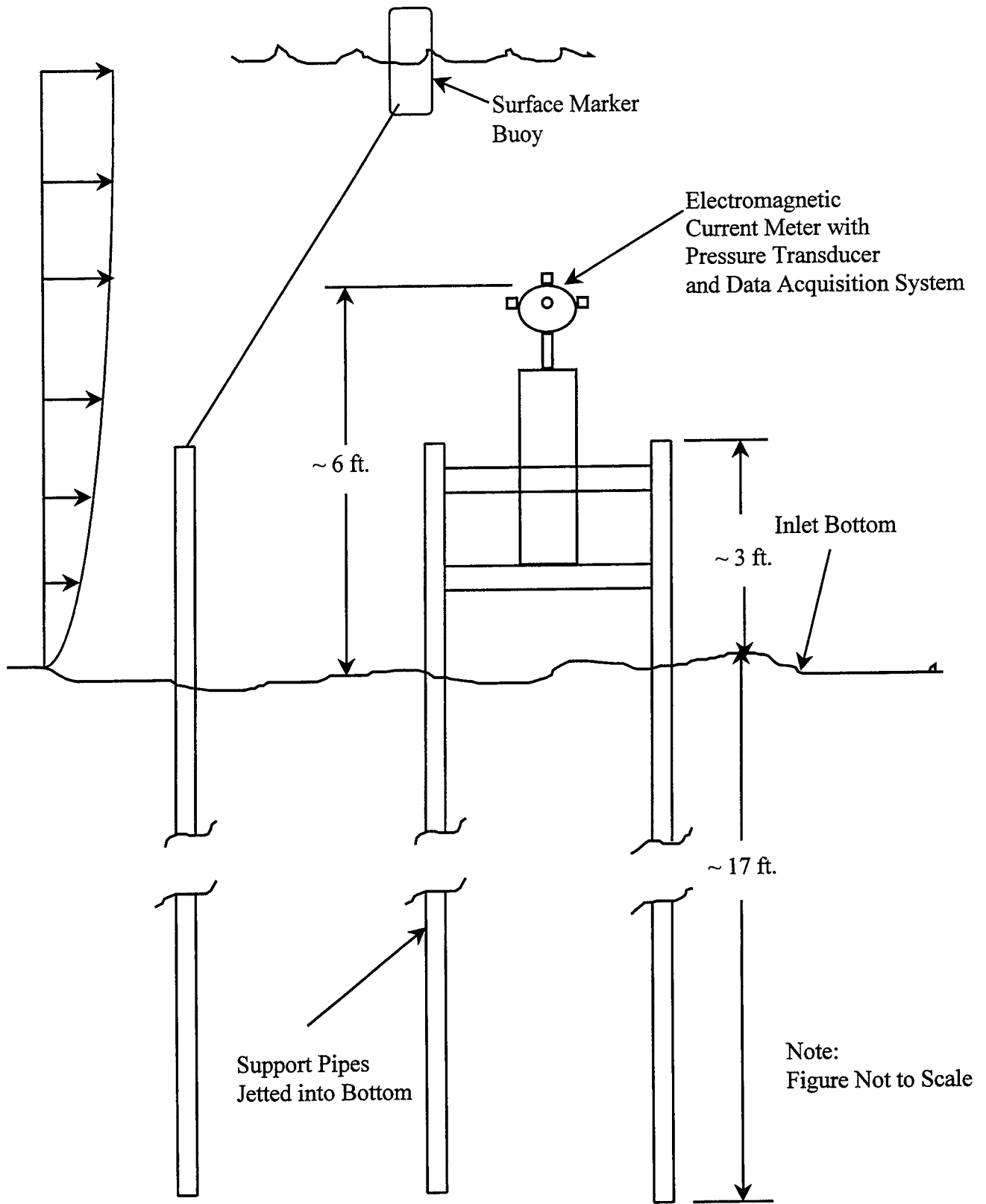


Figure 53. Electromagnetic current meter, pressure transducer, data acquisition (puv) installation.

Appendix A

ASCE Conference on
Water Resources Engineering
San Antonio TX, August 14-18, 1995

Sensitivity of Bridge Scour Producing Currents to Storm Surge Parameters

Christopher W. Reed¹, Susan Harr² and D. Max Sheppard³, M. ASCE

Abstract

A study has been conducted to determine the sensitivity of storm surge induced currents in a tidal system to variations in the storm surge parameters. Numerous storm surge hydrographs have been developed which are representative of surges predicted for the southeast coast of Florida. A depth averaged, finite-element hydrodynamic model (RMA2) has been used to calculate the velocities within a shallow water estuary system for systematic variations in the surge hydrograph. Results indicate significant sensitivity to surge parameters such as the peak surge elevation, duration, and rate-of-rise for the tidal system studied.

Introduction

Design scour computations in tidal inlets, bays, estuaries and rivers use one in one-hundred and one in five-hundred year return interval storm conditions. Storm surge hydrographs, predicted at the coastline for each storm, are used as the basis for calculating the associated surge velocities in the inlets and adjacent tidal waters. Comparisons of predicted and measured storm surges on the open coast indicate that the predicted peak water elevations are relatively close to the measured value, but other features of the hydrograph, such as the rate of rise or fall, can differ greatly. The propagation of meteorological tides (storm surges) through a tidal inlet or river mouth into a bay-estuary-river system can be extremely complex. The complexity is enhanced when there is flooding of barrier islands and other low lying subaerial lands. It is by no means obvious how the "errors" in the predicted coastal hydrograph influence the currents and water elevations at various locations in the bay-estuary-river system. Variations in design currents and water elevation can have a major impact on design scour depth predictions and therefore it is important to

¹ Post Doctoral Fellow in the Coastal and Oceanographic Engineering Department, University of Florida, Gainesville, FL 32611.

² Graduate Assistant in the Coastal and Oceanographic Engineering Department, University of Florida, Gainesville FL 32611.

³ Professor of Coastal and Oceanographic Engineering, University of Florida, Gainesville FL 32611.

know how sensitive these quantities are to variations in the storm surge parameters. In order to address these issues, a study has been conducted to determine the sensitivity of design scour producing currents in a tidal system to variations in the storm surge parameters. A calibrated depth averaged, two-dimensional, finite-element hydrodynamic model has been used to provide the velocity predictions for each variation in the surge hydrographs.

It should be noted that surge models, such as SLOSH (Jarvinen and Gebert, 1987), were developed primarily for obtaining peak elevations for use in flood evacuation planning for severe storms events. To this end the models have been relatively successful. For instance, a comparison of SLOSH predicted surge elevations with measured water elevation data for Hurricane Gloria's landfall over Long Island (Jarvinen and Gebert, 1987) and for Hurricane Hugo's landfall near Charleston, South Carolina (Garcia et al., 1990) show generally good agreement. In these cases, the variations between the predicted and measured hydrographs may be insignificant since the peak water elevations are usually well predicted. However, for the purposes of design scour calculations, it is necessary to accurately predict the storm driven currents as well as water elevations. The effects of hydrograph variations on storm currents is not well documented. Furthermore, many of the other hydrograph features, such as rate of rise and fall, duration of the peak, etc., are not well predicted. Since hydrographs are typically used in design storm velocity predictions, it is important to quantify the sensitivity of the predictions to velocity uncertainties in the hydrographs.

Sensitivity Analysis

The approach for determining the sensitivities is based on the application of a two-dimensional, depth averaged hydrodynamic model to a southern Florida tidal system, namely the St. Lucie Estuary and portions of the Indian River Lagoon. The hydrodynamic model used is RMA2 (Norton and McAnally, 1973; Thomas and McAnally, 1991) with the FASTTABS pre and post processor (Fasttabs, 1992).

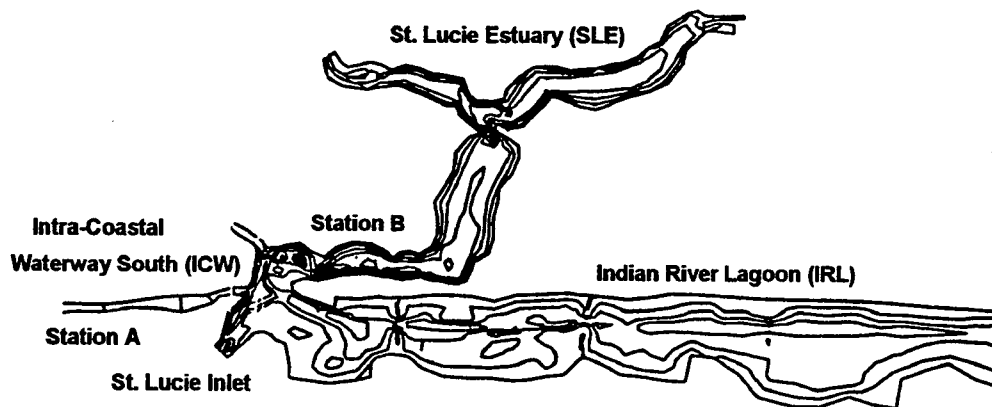


Figure 1. Contour and Station Map of Estuary System

RMA2 is a depth averaged two-dimensional model employing finite-element solution methods to solve the shallow water wave equations. The tidal system is characterized by relatively shallow water, generally 2 to 6 ft deep at MLW, throughout most of the system with maximum depths of 10 ft in narrow maintained channels. A portion of the modeled area is shown in Figure 1 which shows bathymetric contours on 2.5 ft intervals. The Intracoastal Waterway extends southward to Jupiter Inlet. A section of the Indian River Lagoon is represented, including Fort Pierce Inlet and portions of the lagoon to the north.

Calibration of the model to normal tidal conditions was completed prior to beginning the sensitivity analysis. A number of modeling studies have been conducted for portions of the estuary system, (Williams, 1985; Morris, 1987; Sheng et al., 1990; Smith, 1990) and were used to investigate estuary hydrodynamics, salinity transport and water quality. Data obtained for these studies as well as information from the NOAA Tide Tables was used for calibration of the St. Lucie Estuary model.

The sensitivity analysis was conducted for the tidal system by driving the flows at the inlets with a typical surge hydrograph superimposed on a normal tide. The surge parameters such as amplitude, duration and shape were varied and then the calculated flows for each surge within the tidal system were compared. In each case the surge parameter variations were scaled such that each of the surges had the same energy. This was necessary to eliminate effects of the surge size on the results, and focus only on the effects due to "shape" parameters. The energy associated with each surge was calculated by considering the surge as a solitary wave propagating with speed \sqrt{gh} where g is gravity and h is the water depth. This definition allows one to transform the surge hydrograph (i.e. time series) into a wave profile, from which the total kinetic and potential energy could be calculated. Typical perturbations used are

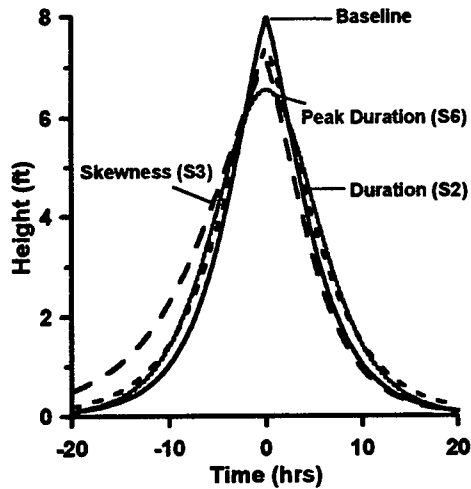


Figure 2. Surge Variations

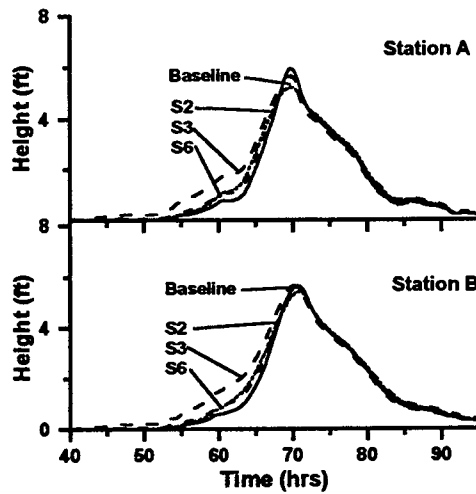


Figure 3. Computed Hydrographs

shown in Figure 2, representing changes in height and duration, rate-of-rise, skewness and peak duration. The variations in height and duration of these surges averaged about 15% of the baseline surge values.

Results

The water elevation time series plots shown in Figure 3 (corresponding to points A and B in Figure 1), are representative of results from the hydrodynamic model. Note that the tidal influence associated with the astronomical tide has been removed from the curves. Comparison of the three curves representing perturbations to the baseline indicate that the variations in the surge height and width are of similar magnitude (averaging 15%) to those of the input hydrographs. The discharge time series corresponding to the water elevation plots in Figure 3 are shown in Figure 4. The differences in the maximum discharge (and subsequently the maximum velocity) at these stations vary greatly with the type of surge perturbation and can exceed 50%. Using changes in maximum discharge as an indicator of sensitivity, plots of the sensitivity for points along the St. Lucie Estuary, Intracoastal Waterway (South) and the Indian River Lagoon can be developed. These plots are shown in Figure 5. The results indicate that the highest sensitivity and largest range of sensitivities are in the Intracoastal Waterway (South), and the least occur in the Indian River Lagoon. Note that the Intracoastal Waterway and the Indian River Lagoon represent the smallest and largest water volume respectively within the system.

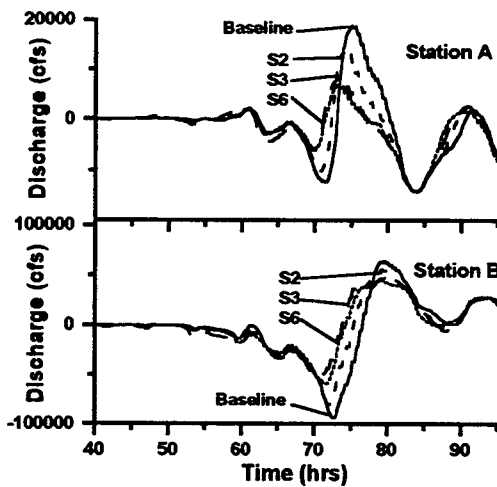


Figure 4. Computed Discharges

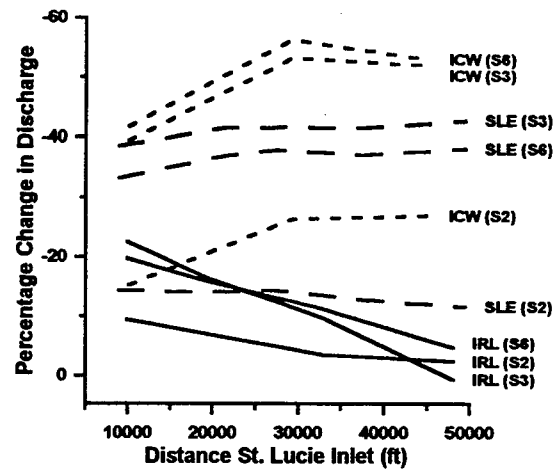


Figure 5. Sensitivities of Discharge

Conclusions

Equilibrium sediment scour depths and the rates at which these depths are reached depend on, among other quantities, the local depth average velocity. Just how dependent scour is on velocity again depends on several quantities, including the magnitude of the velocity, but under certain circumstances it can be sensitive to changes in velocity. Thus, the relatively large dependence of velocity on the storm

surge parameters found in this study can translate into an even greater dependence of scour on these parameters. The results of this study provide some guidelines for determining the locations within a tidal system and the conditions under which the currents are most sensitive to variations in storm surge parameters. Improvements in storm surge predictions are needed. Meanwhile, for points of interest within the tidal system that are in sensitive areas, a range of the critical design storm surge hydrograph parameters (around the predicted values) should be investigated.

Acknowledgments

The authors would like to thank the Florida Department of Transportation for supporting this research. The authors also acknowledge the valuable technical contributions to this work made by Shawn McLemore and Luis Maldonado of FDOT in Tallahassee.

References

- Fasttabs User's Manual (1992) Boss Corporation and Brigham Young University.
- Garcia, A.W., B.R. Jarvinen and R.E. Schuck-Kolben (1990) "Storm Surge Observations and Model Hindcast Comparison for Hurricane Hugo," in *Shore and Beach*, October, Vol.58-59, p.15.
- Jarvinen, B.R. and J. Gebert (1987) "Observed Versus SLOSH Model Storm Surge for Connecticut, New York and Upper New Jersey in Hurricane Gloria, September 1985," NOAA Technical Memorandum, NWS NHC 36, August.
- Morris, F.W. (1987) "Modeling of Hydrodynamics and Salinity in the St. Lucie Estuary," SFWMD Technical Publication 87-1, January.
- NOAA Tide Tables, Department of Commerce.
- Norton, W.A. and W.H. McAnally (1973) "A Finite Element Model for Lower Granite Reservoir," Water Resources Engineers, Inc., Walnut Creek California.
- Sheng, Y.P., S. Peene and Y.M. Liu (1990) "Numerical Modeling of Tidal Hydrodynamics and Salinity Transport in the Indian River Lagoon," *Florida Scientist*, Vol.53, No.3, p.147.
- Smith, N.P. (1990) "Longitudinal Transport in a Coastal Lagoon," *Estuarine, Coastal and Shelf Science*, Vol.31, pp.835-849.
- Thomas, W.A. and W.H. McAnally (1991) "User's Manual for the Generalized Computer Program System: Open-Channel Flow and Sedimentation, TABS-2," US Army Engineer Waterways Experiment Station, Vicksburg, Mississippi.
- Williams, J.L. (1985) "Computer Simulation of the Hydrodynamics of the Indian River Lagoon," M.S. Thesis, Florida Institute of Technology, Melbourne.

Appendix B

results from the monitoring system are presented. Although the scour-depth monitoring system was installed in September 1992, most of the discussion is limited to data collected in November 1993, the period for which there are concurrent scour-depth and other hydrographic data.

FIELD PERFORMANCE OF AN ACOUSTIC SCOUR-DEPTH MONITORING SYSTEM

By Robert R. Mason, Jr.¹, Member ASCE, and D. Max Sheppard²

Abstract

The Herbert C. Bonner Bridge over Oregon Inlet serves as the only land link between Bodie and Hatteras Islands, part of the Outer Banks of North Carolina. Periodic soundings over the past 30 years have documented channel migration, local scour, and deposition at several pilings that support the bridge. In September 1992, a data-collection system was installed to permit the off-site monitoring of scour at 16 bridge pilings. The system records channel-bed elevations at 15-minute intervals and transmits the data to a satellite receiver. A cellular phone connection also permits downloading and reviewing of the data as they are being collected. A digitally recording, acoustic fathometer is the main component of the system. In November 1993, current velocity, water-surface elevation, wave characteristics, and water temperature measuring instruments were also deployed at the site. Several performance problems relating to the equipment and to the harsh marine environment have not been resolved, but the system has collected and transmitted reliable scour-depth and water-level data.

Introduction

Scour processes at bridges are very difficult to predict as they are dependent on the physical properties of the bridge and many environmental factors, such as sediment transport rates. Some bridges are known to be scour-critical and may need to be continuously monitored pending remedial repair or replacement (Johnson and Jones, 1993). A variety of scour-depth monitoring systems have been proposed for this task ranging from simple mechanical devices to elaborate bottom-penetrating sonar and radar systems (Jarrett and Boyle, 1986; Skinner, 1986; Gorin and Haeni, 1989; Butch, 1991). The most efficient and cost-effective way to monitor scour depends on the type and location of the structure, hydraulic and environmental conditions, and sediment characteristics and concentrations (Fenner, 1993).

This paper describes the acoustic scour-depth monitoring system used at the Herbert C. Bonner Bridge, Oregon Inlet, North Carolina, including its design, its performance, and the conditions under which the system has operated. Instruments used to collect ancillary hydrographic data also are described, and some preliminary

¹ Hydrologist, U.S. Geological Survey, 3916 Sunset Ridge Road, Raleigh, NC 27607.

² Professor, Coastal and Oceanographic Engineering Department, University of Florida, Gainesville, FL 32611.

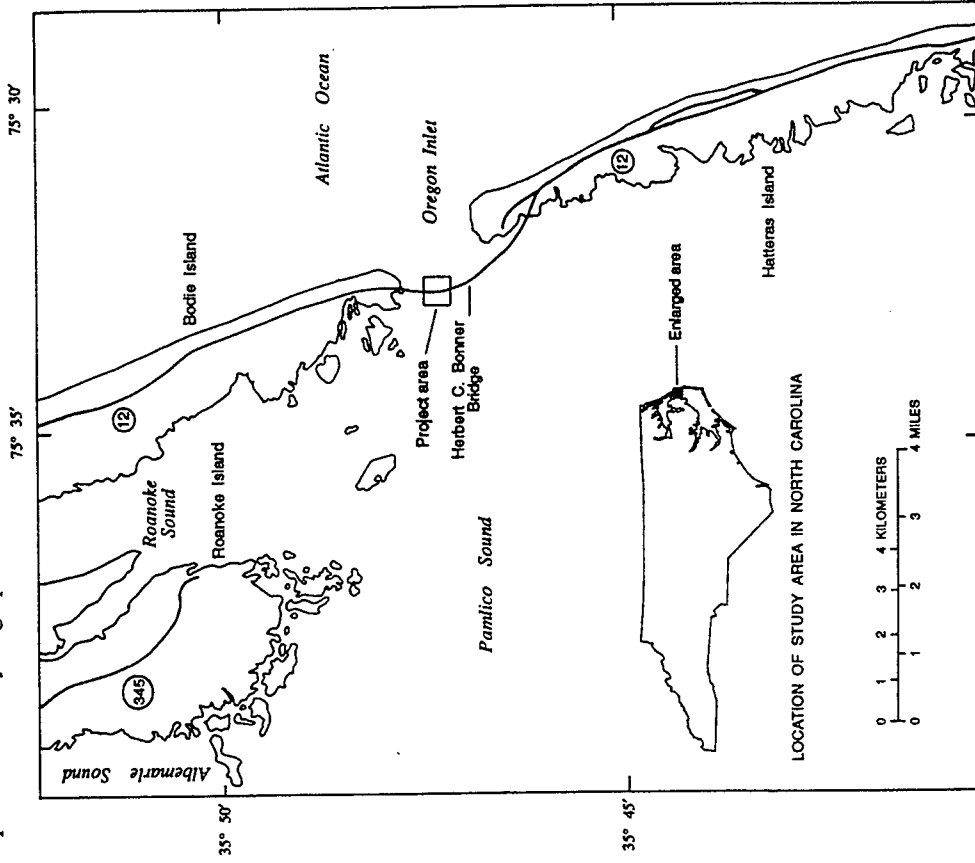


Figure 1. Location of Herbert C. Bonner Bridge and Oregon Inlet, North Carolina.

Background

Oregon Inlet is a narrow, shallow, and dynamic waterway connecting Albemarle and Pamlico Sounds to the Atlantic Ocean and separating Bodie and Hatteras Islands, two in a chain of barrier islands commonly referred to as North Carolina's Outer Banks (fig. 1). Since its formation by a severe Atlantic storm in 1846,

the inlet has frequently shifted in depth, width, and location as a result of persistent southward migration of Bodie and Hatteras Islands; local scour produced by tide and wind-driven currents and waves; deposition due to long-shore sediment transport; and transport of sand from shoals in the sound during periods of strong easterly currents (Dolan and Lins, 1986). The rate of southward migration of the inlet varies greatly but has averaged 21 meters (m) per year from 1846 to 1993 (U.S. Department of Transportation, 1993). Currently (January 1994), the inlet is approximately 1.6 kilometers (km) wide and ranges from 2 to 3 m deep, except for the navigation channel, which is maintained at about 12 m deep. The channel bed is composed of thick deposits of coarse sand with little to no vegetative cover.

Oregon Inlet is spanned by the Herbert C. Bonner Bridge. Built in 1962 and located 1,200 m inland of the Atlantic Ocean and partly within the surf zone, the bridge is 4 km long, 11 m wide, and crests 20 m over the mean low-water level of Oregon Inlet. The Bonner Bridge is supported by 240 pile bents each capping clusters of 8-12 driven piles, which penetrate 1.5-27 m into the channel sediments. The bridge is the main component of the only land link from the mainland to Hatteras Island and carries an average daily traffic load of 6,900 vehicles during the summer months.

Since completion of Bonner Bridge in 1962, the North Carolina Department of Transportation (NC-DOT) has made periodic soundings of Oregon Inlet to monitor channel migration, deposition, and local scour. These data indicate that some sections of Oregon Inlet have scoured and filled through an 11-m range (fig. 2). In 1978, NC-DOT discovered that, as a result of scour, several pilings were penetrating only 2.1 m

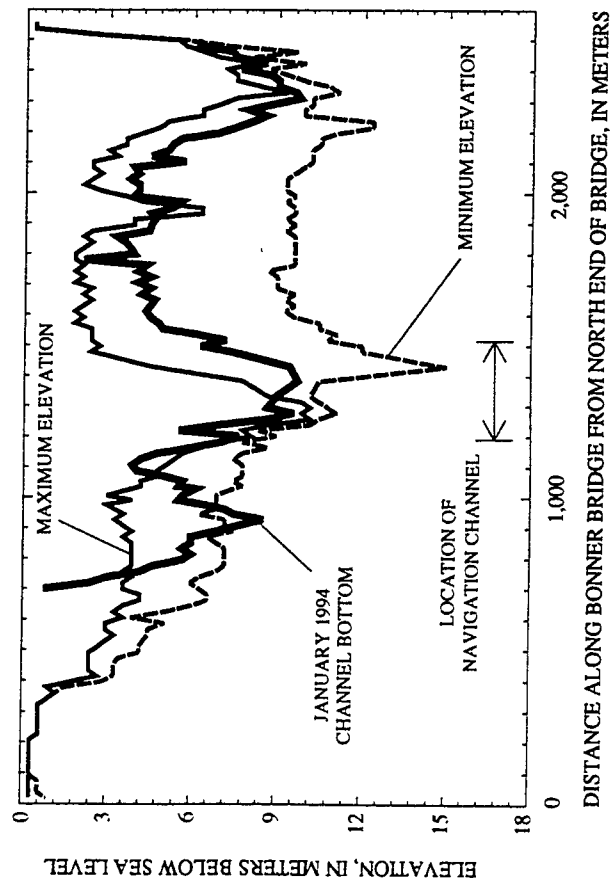


Figure 2. Cross section of Oregon Inlet at Bonner Bridge showing maximum and minimum channel-bottom elevations and January 1994 channel-bottom elevation.

into the channel bottom. From that year to 1992, scour-preventive and remedial actions to protect the bridge have cost over \$9 million. In response to this history of channel instability, the U.S. Geological Survey (USGS) and the NC-DOT joined in a cooperative effort to develop and install a data-collection system to permit continuous remote monitoring of scour depth at 16 bridge pilings. The system was installed in September 1992.

A second data-collection program began in November 1993 and ended in January 1994. This effort consisted of deployment and operation of three instruments that measure and record current magnitude and direction, wave frequency and direction, water-surface elevation, and water temperature near the Bonner Bridge. This program was a cooperative effort between the Florida Department of Transportation (F-DOT), the University of Florida, Coastal and Oceanographic Engineering Department (UFCOE), the NC-DOT, and the USGS. In conjunction with the scour-depth data, the resulting hydrographic data can enable evaluation of theoretical scour-depth predictive equations.

Scour-Depth Monitoring System

The main component of the Bonner Bridge scour-depth monitoring system is a Datasonics PSA 902a digitally-recording, acoustic fathometer operating 16 transducers, each generating a 200-kHz acoustic beam with a conical 10-degree spread. At the time of deployment in 1992, each transducer was mounted at least 1.5 m above the channel bottom and between 1.8 and 4 m below the water surface. These depths were chosen to minimize interference from entrained air, surface turbulence (waves), suspended sediment, and debris. Transducers are secured to the inside of 7-degree battered pilings on both ends of eight consecutive pile bents (fig. 3).

The fathometer is configured as two separate channels, each controlling eight transducers. A time-varying gain circuit, one for each channel, can be adjusted to calibrate the transducers on that channel to an overall (group) optimal setting. However, the transducers cannot be calibrated individually.

The distances between the transducers and the channel bottom (scour depths) are recorded at 15-minute intervals and are output through a standard RS-232 port to a Vitel VX1004 programmable electronic datalogger and then transmitted to a Geostationary Earth Orbiting Satellite (GOES) receiver. The data logger is also equipped with a Mitsubishi CDL 100 cellular phone and computer modem for downloading of data and for changing software attributes remotely.

On November 4, 1993, three additional hydrographic instruments were installed near the Bonner Bridge in the project area (fig. 1). Two of these instruments were Endeco current meters (type 174SSM) that measure and record water temperature as well as current magnitude and direction. The third instrument was a Seadata wave-tide recorder that measures and records current magnitude and direction, wave frequency and direction, and water-surface elevation. The current-meter instruments were located in line with three consecutive piers and approximately 30 m east (ocean side) of the bridge.

^aAny use of trade, product, or firm names is for descriptive purposes only and does not imply endorsement by the U.S. Government.

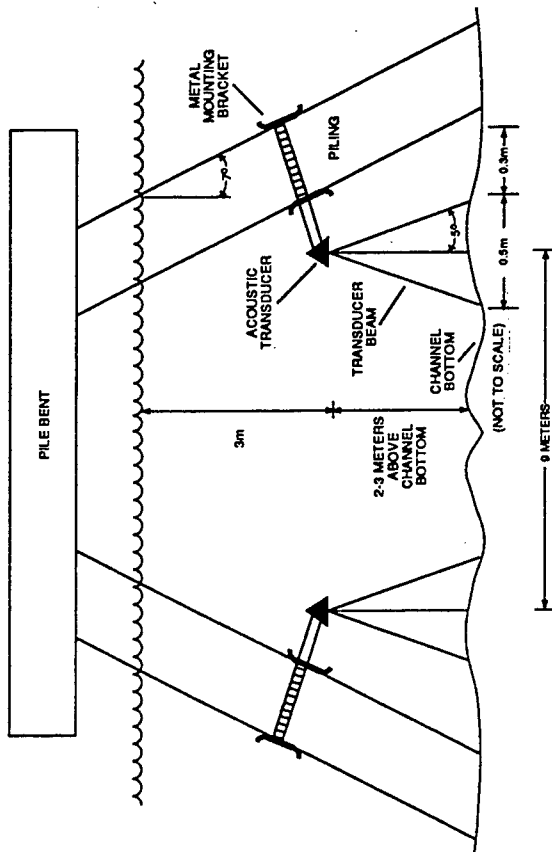


Figure 3. Transducer mounting on Bonner Bridge.

Monitoring System Performance

The performance of an acoustic scour-depth monitoring system is influenced by its design, its mounting, and by the environment in which it operates. Mounting considerations include the rigidity of the mounting and the location of the transducer relative to the piling, the channel bottom, and the water surface. Environmental factors, which can influence system performance, include suspended debris, suspended sediment, entrained air, biological growth, varying bed-slopes and bed-forms, and possibly, electronic interference from radios, radars, power lines, and other sources.

Four calibration checks were made during the period from November 17, 1992, to May 25, 1993. In each case the distances from the transducers to the channel bottom (scour depths) were physically measured by NC-DOT scuba divers. Some transducers were mounted closer to the channel bottom than were others. This difference and likely differences in bed-form and local bed-slope beneath each transducer probably resulted in slightly different acoustic-signal properties and rates of attenuation. Thus, the resulting operational settings were not necessarily optimum for each individual transducer. Some transducers, therefore, could be expected to perform more reliably than others. Overall, however, the correlation between the physically measured and acoustically sensed data is very good. The results of the calibration checks for transducer 10 are typical of the overall correlations (fig. 4).

Fathometer records for transducer 13 typify the variability of scour and fill during the data-collection period from August to November 1993 (fig. 5). On August 30, the channel bed beneath transducer 13 was 2 m below the transducer. This depth

increased to 2.6 m due to erosion from currents associated with Hurricane Emily (August 31 to September 1, 1993). Following the passage of the hurricane through September 12, there was a net deposition of approximately 0.5 m of sediment as indicated by a sustained reduction in scour depth. From October 12 to November 14, there was a net erosion of approximately 1 m of sediment. Periods of significant fill occurred on September 18 (0.4 m), November 15 (0.9 m), and November 27 (0.2 m), 1993. In addition to scour associated with Hurricane Emily, scour also occurred on October 12 and November 28. On November 30, the channel bed was 2.0 m below the transducer, having traversed a minimum to maximum change in depth of 1.2 m.

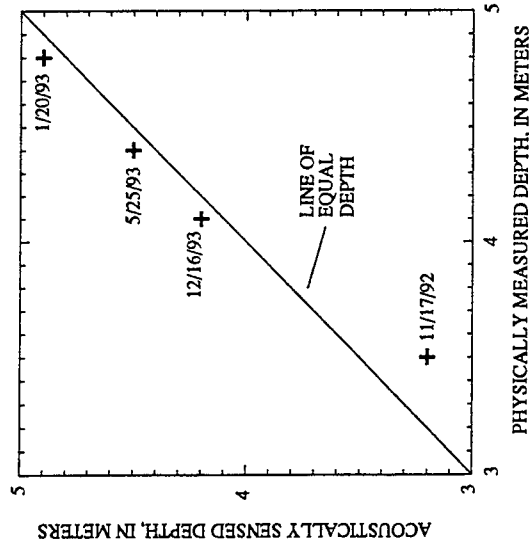


Figure 4. A typical result of transducer-calibration checks.

For the purposes of this paper, the reliability of the Bonner Bridge scour-depth monitoring system during November 1993 was evaluated using two performance characteristics: (1) the percentage of transmitted acoustic signals that were not recorded by the datalogger (failed signal return) and (2) the consistency of computed distances from one reading to the next (table 1). For the 16 transducers, the percentage of failed signals during November ranged from about 6 percent for transducers 13 and 14 to nearly 100 percent for transducer 7 (table 1). Failed signals are shown in the record for transducer 13 as lines extending to the top of the graphs (fig. 5).

The cause of the failed signals is unknown. Attempts to correlate signal dropouts or no returns with hydraulic phenomena such as tidal current magnitude and direction have been unsuccessful. However, strong daily cycles are evident in the frequency of failure of transducers 1 and 8. In both instances the highest frequency of failure occurs from 700 hours to 1700 hours, when the solar panel battery-chargers are in operation. Intermittent current surges resulting from battery recharging operations during daylight could be the source of the problem with these transducers. Modifications to the system to remedy this problem are planned. Failures of the

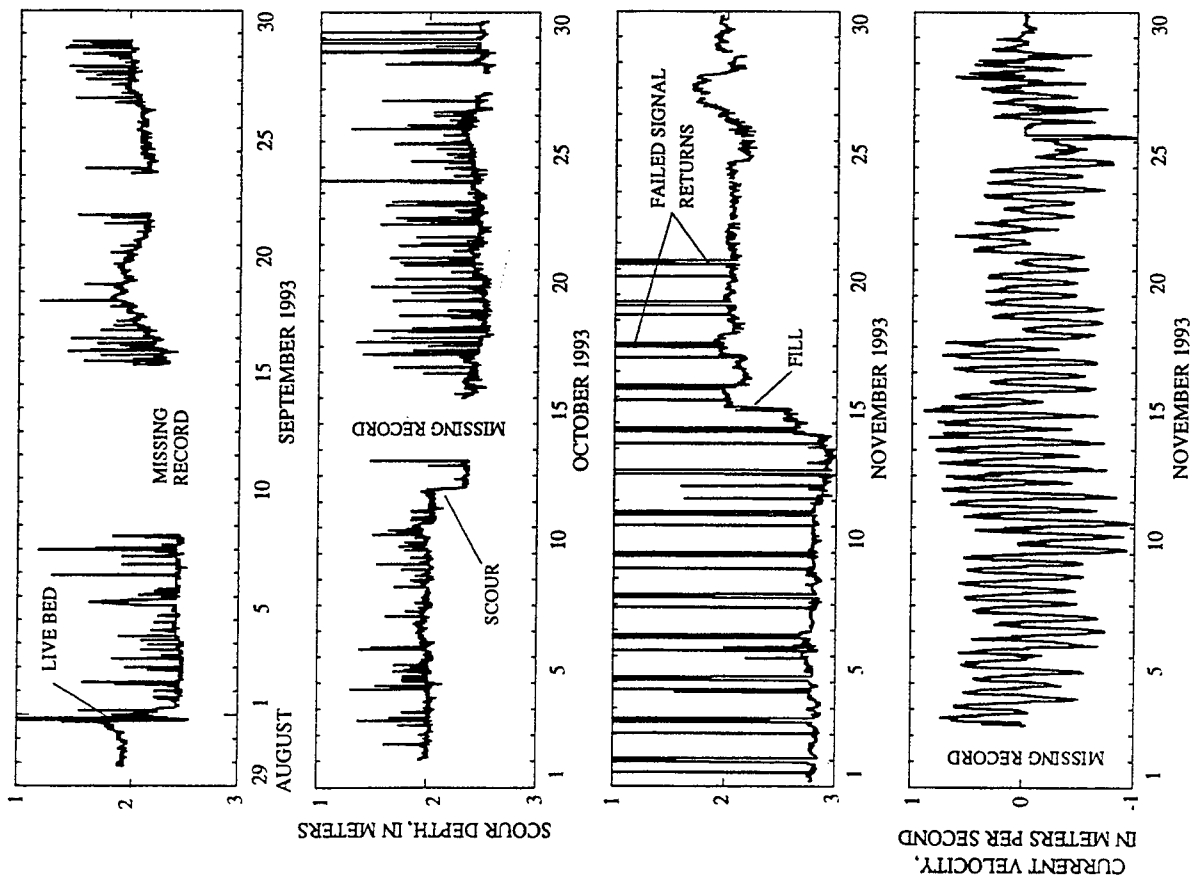


Figure 5. Scour depth at transducer 13 for September-November 1993 and tidal current velocity for November 1993.

remaining transducers appear to be random in a temporal sense, but are highly correlated to one another. When a failure occurs on a normally reliable transducer, transducer 2 for instance, the remaining transducers usually also fail. This correlation is probably the result of communication anomalies between system components.

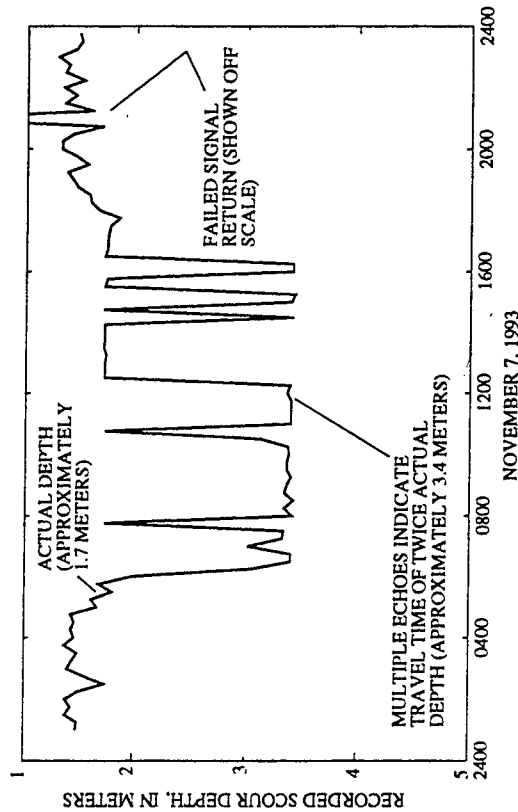
Table 1.--Percentage of failed signal returns and consecutive readings differing by selected ranges for each transducer, November 1993 [m, meter]

Transducer no.	Failed signal returns (percent)	Percent of consecutive readings differing by indicated ranges		Mean distance to channel bottom (m)
		0.25-0.49 (m)	0.50-0.99 (m)	
1	81.9	14.5	37.3	28.6
2	8.8	4.2	17.6	10.0
3	8.8	4.1	8.8	4.4
4	8.8	7.0	25.1	13.6
5	8.8	2.9	12.9	8.4
6	8.8	8.8	3.9	1.5
7	99.6	0	81.8	81.8
8	32.1	19.2	27.6	27.6
9	55.7	1.8	1.0	.1
10	14.4	2.4	4.6	6.3
11	12.8	2.1	6.3	2.0
12	9.1	1.3	7.7	4.8
13	6.4	.10	.30	.20
14	6.4	.20	.30	.50
15	68.6	0	.1	3.7
16	66.0	.2	.6	3.9

Movement of sediment after episodes of scour or fill is detected by the fathometer as a change in scour depth. Although changes are expected, they are usually small (<0.25 m) for consecutive 15-minute readings. To evaluate measurement consistency, the differences between consecutive scour-depth measurements were computed, and the percentage of these differences exceeding selected thresholds (0.25 m, 0.5 m, 1.0 m, and 1.5 m) were summarized for each transducer (table 1). The magnitude and frequency of differences between consecutive readings were examined for correlations with current magnitude and direction and temporal patterns, but none were detected.

Large differences between consecutive readings also can be caused by multiple echoes of the same transducer signal. Multiple echoes occur when a transducer return signal is emitted from the transducer, bounces off the channel bottom, then off the transducer, and back off the channel bottom for a second time before it is detected by

the fathometer. Multiple echoes result in computed depths that are twice the actual depth to the channel bottom (fig. 6).



6. Depth to channel bottom for transducer 3 showing effects of multiple echoes.

Large differences in depth readings also can be the result of suspended debris. An object could enter the signal path and cause abnormal readings. A similar condition could also result from high concentrations of suspended sediment as during live-bed conditions. Such conditions were not noted during the period when the current meters were deployed (November 1993); however, a live-bed condition could have developed during the passage of Hurricane Emily (fig. 5). As the hurricane currents abated, some of the suspended sediment was transported, leaving the channel bed approximately 0.6 m below its previous elevation.

The performance of the other hydrographic instruments was likely hampered by the movement of suspended and bed-load sediment. Prior to deployment of the current meters and wave-tide recorder on November 3, 1993, a bathymetric survey of an area approximately 300 m by 300 m on either side of the bridge was conducted. On January 25, 1994, 83 days after the instruments were deployed, an attempt was made to retrieve the instruments and download the data. While making a second bathymetric survey of the same area, it became evident that a significant quantity (2 to 3 m) of sand had been deposited in the study area since November. The dive to recover the instruments verified this fact. The Seadata meter was completely buried, and the two Endeco meters were just above the channel bottom. Tethers on the Endeco meters allowed them to move up and remain above the deposited sediment. The meters did, however, suffer some damage. The impellers on both instruments were missing. The top of the Seadata meter that was originally 2 m above the channel bottom is believed to be buried under 0.5 m of sediment and is yet to be recovered. Current velocity data

for November, downloaded from one of the Endeco meters, are shown in figure 5. There is little, if any, apparent correlation between these velocities and changes in scour depths for the same period.

Conclusions

Remote collection of acoustically sensed scour-depth data in a dynamic tidal environment such as Oregon Inlet is possible. Even though there is considerable unexplained variation within the Bonner Bridge scour-depth data, they do demonstrate the overall trends of scour and deposition. However, the Bonner Bridge data-collection system deployed is susceptible to errors arising from failed signal returns, multiple echoes, live-bed conditions, and suspended objects. Modifications of the data-collection system hardware and software are underway to improve the reliability and accuracy of the data. In addition, deployment of current meters and other hydrographic sensors are expected to yield more information about the effect of the Oregon Inlet environment on system performance. Assuming the Seadata velocity meter can be recovered and that it functioned properly during November 1993, the complete data set will include scour depth, wave frequency and direction, water-surface elevation, and water temperature.

References

- Butch, G.K., 1991, Measurement of bridge scour at selected sites in New York, excluding Long Island: U.S. Geological Survey Water-Resources Investigations Report 91-4083, 17 p.
- Dolan, Robert, and Lins, Harry, 1986, The Outer Banks of North Carolina: U.S. Geological Survey Professional Paper 1177-B, 46 p.
- Fenner, T.J., 1993, Scoping out scour: Civil Engineering, v. 63, no. 3, p. 75-77.
- Gorin, S.R., and Haeni, F.P., 1989, Use of surface-geophysical methods to assess riverbed scour at bridge piers: U.S. Geological Survey Water-Resources Investigations Report 88-4212, 33 p.
- Jarrett, R.D., and Boyle, J.M., 1986, Pilot study for collection of bridge-scour data: U.S. Geological Survey Water-Resources Investigations Report 86-4030, 89 p.
- Johnson, P.A., and Jones, J.S., 1993, Merging laboratory and field data in bridge scour: Journal of Hydraulic Engineering, v. 119, no. 10, p. 1176-1181.
- Skinner, J.V., 1986, Measurement of scour-depth near bridge piers: U.S. Geological Survey Water Resources Investigations Report 85-4106, 33 p.
- U.S. Department of Transportation, Federal Highway Administration, and North Carolina Department of Transportation, 1993, Administrative action, draft environmental impact statement and draft section 4(F) evaluation: Federal Highway Administration FHWA-NC-EIS-93-01-D, p. 3.1, 3.30-3.38.

NTIS does not permit return of items for credit or refund. A replacement will be provided if an error is made in filling your order, if the item was received in damaged condition, or if the item is defective.

Reproduced by NTIS

National Technical Information Service
Springfield, VA 22161

*This report was printed specifically for your order
from nearly 3 million titles available in our collection.*

For economy and efficiency, NTIS does not maintain stock of its vast collection of technical reports. Rather, most documents are printed for each order. Documents that are not in electronic format are reproduced from master archival copies and are the best possible reproductions available. If you have any questions concerning this document or any order you have placed with NTIS, please call our Customer Service Department at (703) 605-6050.

About NTIS

NTIS collects scientific, technical, engineering, and business related information — then organizes, maintains, and disseminates that information in a variety of formats — from microfiche to online services. The NTIS collection of nearly 3 million titles includes reports describing research conducted or sponsored by federal agencies and their contractors; statistical and business information; U.S. military publications; multimedia/training products; computer software and electronic databases developed by federal agencies; training tools; and technical reports prepared by research organizations worldwide. Approximately 100,000 *new* titles are added and indexed into the NTIS collection annually.

For more information about NTIS products and services, call NTIS at 1-800-553-NTIS (6847) or (703) 605-6000 and request the free *NTIS Products Catalog*, PR-827LPG, or visit the NTIS Web site <http://www.ntis.gov>.

NTIS

***Your indispensable resource for government-sponsored
information—U.S. and worldwide***



U.S. DEPARTMENT OF COMMERCE
Technology Administration
National Technical Information Service
Springfield, VA 22161 (703) 605-6000
